Crystalline liquids: the blue phases

David C. Wright* and N. David Mermin

Laboratory of Atomic and Solid State Physics, Cornell University, Ithaca, New York 14853-2501

The blue phases of cholesteric liquid crystals are liquids that exhibit orientational order characterized by crystallographic space-group symmetries. We present here a pedagogical introduction to the current understanding of the equilibrium structure of these phases accompanied by a general overview of major experimental results. Using the Ginzburg-Landau free energy appropriate to the system, we first discuss in detail the character and stability of the usual helical phase of cholesterics, showing that for certain parameter ranges the helical phase is unstable to the appearance of one or more blue phases. The two principal models for the blue phases are two limiting cases of the Ginzburg-Landau theory. We explore each limit and conclude with some general considerations of defects in both models and an exact minimization of the free energy in a curved three-dimensional space.

CONTENTS

I. INTRODUCTION: CRYSTALLINE LIQUIDS

They are totally useless, I think, except for one important intellectual use, that of providing tangible examples of topological oddities, and so helping to bring topology into the public domain of science, from being the private preserve of a few abstract mathematicians and particle theorists.

F. C. Frank (1983)

One of the great lessons of condensed matter physics is that nature is more fertile than the human imagination in devising ways for matter to organize itself into coherent structures. Yet, given the initial clue from nature, the

*Present address: Center for Science and International Affairs, Kennedy School of Government, Harvard University, Cambridge, MA 02138.

human imagination has proved remarkably adept at eventually inventing simple theoretical models that display and illuminate strange new kinds of behavior.

Blue phases are a wonderful example of this process. They have been known observationally for a hundred years and have finally begun to be understood theoretically within the last dozen. Unlike some of the more celebrated examples (e.g., superconductivity) they are not yet of any technological interest. Indeed, the puzzle they present is not widely known, and the apparent solution to that puzzle has been found in a more thoughtful application of existing theories, rather than through the introduction of radically new ideas. They nevertheless deserve to be brought to the attention of a wider community of physicists for several reasons.

The phenomenon is both beautiful and extraordinary. A blue phase can look like a stained glass window: an intricate mosaic of bright colors. Photographs have served as Christmas cards. The colors are produced by a collection of crystallographic domains that selectively Bragg-reflect visible light. The blue phases are naturally occurring crystals whose periodicity is on a scale of thousands of angstroms, affording crystallographers an opportunity to practice their art not in the x-ray, but in the optical domain.

The existence of blue phases, however, requires a redefinition, or at least a refinement, of the word "crystal." If the crystalline state is defined to be one with discrete translational symmetry in three independent directions, then the blue phases are indeed crystalline. But conventional crystals are solid, and the discrete group of translations is associated with the mean equilibrium positions of the constituent molecules, atoms, or ions. Blue phases are liquid. The molecules are positionally disordered and have no fixed mean positions. The discrete group of translations is associated with the spatial pattern of molecular orientations.

Blue phases are liquid crystals. They can be poured from one vessel to another. But unlike other liquid crystals, which display a variety of translational and rotational symmetries peculiar to the liquid crystal state, blue phases have symmetry groups that are simply conventional crystallographic space groups (in all cases reported to date, members of the cubic crystal system in the absence of fields). They are therefore the only truly crystalline liquid crystals. In recognition of this, Frank (1983) has proposed that they should be regarded as a fourth class of liquid crystals, beyond Friedel's standard classification into nematics, cholesterics, and smectics. The term "crystalline liquids" might serve to make this distinction and is certainly more accurate than "blue phases," since they can, in fact, show a whole rainbow of colors.

Beyond their beauty and extraordinary structure, however, these crystalline liquids—the blue phases—also have a powerful conceptual appeal. There is a simple Ginzburg-Landau free energy that appears to be rich enough to encompass the phenomena in all their intricacy. Since the relevant transitions are first order, the mean-field minimization of that free energy may well give an accurate enough picture of the blue phases without the complications of fluctuation effects that dominate the behavior at second-order transitions. On the other hand, the problem of minimizing that simple mean-field free energy has proved surprisingly resistant to theoretical analysis. Structures favored by the bulk free energy do not take full advantage of the possibilities for minimizing the gradient free energy, and vice versa, with the result that no exact blue-phase solutions have yet been found even in this simple model.

This has resulted in two lines of attack that might at first appear so different as to be viewed as competing theories. One of our major aims in this review is to give a single unified presentation of both approaches, to emphasize that they are simply different computational schemes, appropriate in different limiting cases.[1]

The first approach to be developed began with work by Brazovskii and co-workers, and was subsequently refined and developed by Hornreich, Shtrikman, and their collaborators (Brazovskii and Dmitriev, 1975; Brazovskii and Filev, 1978; Hornreich and Shtrikman, 1979, 1980a, 1980b, 1981b, 1981c; Alexander, 1981; Alexander *et al.*, 1981; Kleinert and Maki, 1981; Hornreich, Kugler, and Shtrikman, 1982; Grebel, Hornreich, and Shtrikman, 1983a, 1984; Wright and Mermin, 1985). It can be carried out systematically when the gradient free energy dominates (characterized, for reasons that will emerge below, as the "high-chirality limit"). Blue phases are built out of a highly degenerate set of forms favored by the gradient energies, with the bulk free energy treated as a small perturbation that splits the degeneracy of these forms, building them into a variety of crystallographic structures.

The other approach, put forth by Meiboom *et al.*, arises naturally when the bulk free energy is dominant (which we shall characterize as the "low-chirality limit") (Meiboom, Sethna, Anderson, and Brinkman, 1981; Meiboom, Sammon, and Berreman, 1983; Meiboom, Sammon, and Brinkman, 1983). Blue phases are built from structures that locally minimize the bulk free energy, and the way in which these are put together from point to point is determined by the weaker gradient free energy. In this limit the system is characterized by geometrical frustration: structures that are favored locally by the gradient free energy cannot be extended throughout all of space, leading to intricate compromise structures, the most favorable of which, again, appear to have crystallographic symmetries.

The latter situation, in which local ordering is incompatible with global ordering, has recently received con-

[1]The connection between these limits has also been noted by Meiboom, Sammon, and Brinkman (1983), Grebel, Hornreich, and Shtrikman (1984), and Belyakov and Dmitrienko (1985).

siderable attention in various realms of condensed matter physics (Frank, 1952; Frank and Kasper, 1958, 1959; Kleman and Sadoc, 1979; Sadoc, 1980; Kleman, 1981, 1982, 1983, 1985; Steinhardt, Nelson, and Ronchetti, 1981, 1983; Nelson, 1982, 1983a, 1983b; Sadoc and Mosseri, 1982, 1984; Sethna, 1983, 1985, 1987; Renn and Lubensky, 1988). From a conceptual point of view, one of the most interesting things about the blue phases is that in the low-chirality limit they provide an extremely simple example of a real system that unambiguously illustrates the physics and mathematics of geometrical frustration.

In both cases singular line defects play an important role, though they are interestingly disguised in the high-chirality limit. A second reason for the intellectual interest of blue phases (as noted above by Frank) lies in the concrete illustration they offer of some of the more subtle concepts arising in the topological theory of defects.

Our aim in this paper is to provide an elementary introduction to our current understanding of the equilibrium structure of these phenomenologically and conceptually intriguing substances. In recent years there have been several reviews of various aspects of theory and experiment (Stegemeyer and Bergmann, 1980; Crooker, 1983; Barbet-Massin *et al.*, 1984a; Belyakov and Dmitrienko, 1985; Stegemeyer, Blümel, Hiltrop, Onusseit, and Porsch, 1986; Cladis, 1987; Sethna, 1987; Hornreich and Shtrikman, 1988a; Crooker, 1989). We therefore view our task as primarily pedagogical. On the theoretical side we have tried to gather into a simple, accessible, and unified presentation the many diverse strands that make up our basic understanding of the blue phases. Our discussion of experimental studies is intended primarily to provide a brief historical survey and to give a persuasive selection from the compelling evidence establishing those aspects of the phenomena central to our current understanding. It is not our aim to give a systematic survey of either theory or experiment, and the references we give are intended primarily to acquaint readers with some of the major works in the field, for the benefit of those wishing to explore the subject more thoroughly.

We begin our introduction to blue phases in Sec. II, with a brief review of the elementary concepts of liquid-crystal physics essential to their description. We then survey in Sec. III the major experimental facts with which a model of blue phases must contend. In Sec. IV we describe the simple Ginzburg-Landau theory in terms of which both theoretical models of blue phases can be viewed as different limiting cases. In Sec. V we apply the model of Sec. IV to a detailed discussion of the helical phase, indicating when its conventional description as a uniaxial "cholesteric" is valid and when this picture is significantly modified by biaxiality. In Sec. VI we describe the instability of the helical phase at high chirality and survey the resulting blue phase models that emerge in the high-chirality limit. In Sec. VII we turn to the rather different approach to blue phases, based on "double twist" and line defects in a uniaxial liquid, appropriate when the chirality is not high. In Sec. VIII we point out several features common to both the high- and low-chirality descriptions, to emphasize that they are not competing theories, but descriptions of the same phenomenon in two different limiting cases. We end by describing an exact minimization of the free energy in a curved three-dimensional space.

II. ANISOTROPIC LIQUIDS

In this section we provide a brief introduction to the relevant concepts and nomenclature of liquid-crystal physics (for a general review, see for example, de Gennes, 1974; Stephen and Straley, 1974; Chandrasekhar, 1977). Conventional nomenclature is not always well suited to a discussion of blue phases. To avoid ambiguity we have taken pains to use a precise, if slightly unconventional, set of terms. Even readers conversant with liquid-crystal terminology should therefore skim through the remarks that follow.

A. Nematics, cholesterics, and blue phases

All of the phenomena we shall be describing take place in liquids in which the mean molecular orientations are able to acquire order, although the mean molecular positions are disordered. In the conventional liquid-crystal classification scheme such anisotropic liquids are divided into two categories: nematics and cholesterics. (There is a third category, smectics, which will not concern us here, in which there is also ordering in the mean molecular positions.)

A liquid crystal is *nematic* if the constituent molecules have inversion symmetry, or if chiral molecules are present but equally distributed among the two handednesses (a "racemic mixture"), so the fluid as a whole is inversion symmetric. If the constituent molecules are chiral and the two handednesses are not equally represented, the liquid crystal is *cholesteric.* Blue phases occur in the cholesteric class. Cholesterics are sometimes called *chiral nematics.* Nematics may then be called *ordinary nematics* if one wishes to emphasize their nonchiral character.

Unfortunately the term "cholesteric" is also widely used with a more narrow meaning to denote the particular phase, which we shall refer to as the *helical phase,* that chiral liquid crystals enter at temperatures more than a degree or so below the transition from isotropic to anisotropic liquid. This usage leads to no confusion when the helical phase is the only ordered phase under consideration. Many such chiral liquid crystals, however, display additional phases—the *blue phases*—at temperatures immediately below the transition from the isotropic liquid. Blue phases can be viewed as phenomena taking place in cholesteric liquid crystals only if the term "cholesteric" is taken in its broader sense of "chiral an-

	Our Nomenclature		
MATERIAL:	*NEMATIC*	*CHIRAL NEMATIC*	
ORDERED PHASES:	*Nematic*	*Helical*	*Blue*
	Conventional Nomenclature		
MATERIAL:	*NEMATIC*	*CHOLESTERIC*	
ORDERED PHASES:	*Nematic*	*Cholesteric*	*Blue*

isotropic liquid."

To avoid the confusion that a failure to distinguish between the broad and narrow meanings of "cholesteric" can bring to a discussion of blue phases, we shall avoid using the term "cholesteric" at all, except in contexts where no possible ambiguity can result. We shall call the nonchiral liquids "nematics"(or "ordinary nematics") and shall call the chiral liquids "chiral nematics".[2] In this scheme, the two types of phases found in chiral nematics are helical phases and blue phases.

Our nomenclature is summarized and contrasted with the more conventional nomenclature in Table I.

B. Homogeneous versus inhomogeneous nematics

The state of an anisotropic liquid is said to be *homogeneous* if the local anisotropy is identical throughout the liquid in all respects, including orientation. The unstrained equilibrium state of ordinary nematics is homogeneous. As we shall see, even in unstressed thermodynamic equilibrium chiral nematics are inhomogeneous.

C. Uniaxial versus biaxial anisotropy

Nematics (ordinary or chiral) are characterized as *uniaxial* or *biaxial,* according to whether the anisotropy of the ordered liquid has a rodlike (cylindrical) or bricklike symmetry. (In inhomogeneous nematics the characterization is based on the rotational symmetry of the local configuration.) No nematics are known with arrowlike symmetry, in which one direction along the rod differs from the other. (This, of course, is the symmetry one would find in a ferromagnetically ordered liquid, and in Sec. VIII we shall find it interesting to contrast the behavior of the rodlike uniaxial nematics to hypothetical arrowlike liquid ferromagnets.)

Almost all nonchiral homogeneous nematics are uniaxial, though they have recently been synthesized with biaxial symmetry (Yu and Saupe, 1980; Bartolino *et al.*, 1982). The helical phases of chiral nematics are generally treated as uniaxial although, as we shall see, their inhomogeneous equilibrium structure induces a slight and generally unimportant degree of biaxiality (Wulf, 1973; Priest and Lubensky, 1974; Schröder, 1980; Yaniv *et al.*, 1981; Chidichimo *et al.*, 1982; Yaniv, Chidichimo, and Doane, 1983; Yaniv, Neubert, and Doane, 1983; Hornreich and Shtrikman, 1984). Biaxiality does, however, play an important role in one limiting case of the general theory of the blue phases of chiral nematics (what we shall call the "high-chirality limit"), and an understanding of how biaxiality arises is important for understanding the essential unity of all currently proposed models of blue phase ordering.

The symmetry of the ordered phase need not directly reflect the symmetry of the individual constituent molecules. Molecules with arrowlike symmetry, for example, can form a uniaxial liquid with only rodlike symmetry if the arrows are randomly oriented both parallel and antiparallel to the preferred direction. Similarly, molecules with bricklike or even lower symmetry will form a uniaxial liquid if the *distribution* of molecular orientations has uniaxial symmetry. For example, a fluid of bricks would have uniaxial symmetry if the long axes of the bricks were aligned with one another while the orientations of the bricks about that direction were random. In both of these examples the symmetry of the liquid is higher than the symmetry of the individual molecules.

On the other hand, as we shall see in some detail, even molecules with ideal rodlike symmetry can give rise to locally biaxial liquids if the distribution of molecular directions has a lower than rodlike symmetry (as is generally the case for the local distribution in inhomogeneous configurations).

D. The helical phase of chiral nematics: Preliminary remarks

Although we shall subsequently characterize it in more detail, it is useful to have at hand a preliminary description of the equilibrium structure assumed by chiral nematics in the helical phase. This structure is inhomogeneous and locally uniaxial (except for a small degree of biaxiality, often ignored, which we shall examine in Sec. V). A uniaxial structure is characterized at each point by a single preferred axis, which we shall denote by a unit vector $\mathbf{n}(\mathbf{r})$, known as the *director.* Because the local structure is unchanged by a mirroring in the plane perpendicular to $\mathbf{n}$, the vectors $\mathbf{n}$ and $-\mathbf{n}$ describe the same configuration, and $\mathbf{n}$ should be regarded as a "headless arrow." This is a fact of central importance. If $\mathbf{n}$ had a sense associated with it, for example, the line singularities (see Sec. II.F below) would have a very different character and, at least in one rather general model, there would be no blue phases (see Sec. VIII).

The equilibrium state of an ordinary nematic is homogeneous: the director $\mathbf{n}$ does not vary with position (Fig. 1). The equilibrium helical phase of a chiral nematic is inhomogeneous: $\mathbf{n}$ is everywhere perpendicular to a fixed direction, the *pitch axis* $\hat{\ell}$, and is uniform in planes per-

[2]The term "chiral nematic" is sometimes used to refer to biphenyl compounds to distinguish them from derivatives of cholesteryl esters, which were the original "cholesterics." We would propose calling both types of materials "chiral nematics" and using the terms "biphenyl chiral nematics" and "cholesteric chiral nematics" to make the chemical distinction.

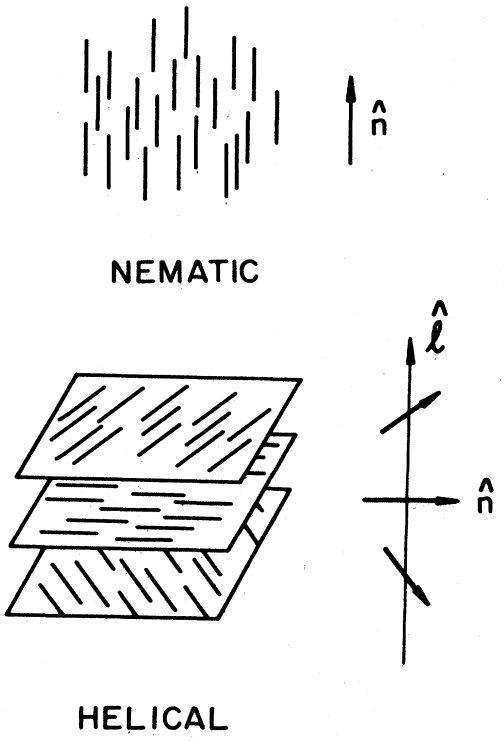

FIG. 1. The director field in the nematic and helical phases. The director **n** is uniform in the nematic phase, while in the helical phase **n** twists along the pitch axis ℓ and is constant in directions perpendicular to ℓ.

pendicular to ℓ (Fig. 1). As one moves along ℓ, however, the direction of **n** twists uniformly about ℓ with a repeat distance p_0 for **n** returning to **n** (which is therefore twice the physical repeat distance, since **n** and $-\mathbf{n}$ represent the same configuration). The distance p_0 is called the *pitch* of the helical phase (or the "cholesteric pitch"). While the constituent molecules of chiral nematics are 10–50 Å in length, the pitch is typically thousands of angstroms.

If the z axis is taken along the direction ℓ, then the analytic form for the director in the equilibrium helical phase is

$$\mathbf{n}(\mathbf{r})=\mathbf{x}\cos q_0 z+\mathbf{y}\sin q_0 z\ , \tag{2.1}$$

where the pitch p_0 is given by

$$p_0=2\pi/q_0\ . \tag{2.2}$$

The quantity q_0 is a measure of the "chirality" of the nematic—a term we shall define more precisely in Sec. IV. Ordinary nematics can be viewed as the limiting case $q_0=0$.

E. The blue phases of chiral nematics: Preliminary remarks

The structures of blue phases are considerably more intricate and less well understood than that of the simple helical phase; their detailed description will emerge in the sections that follow. Not all chiral nematics have blue phases. When they do occur, they are only found within a degree or so of the transition from isotropic to anisotropic liquid. At lower temperatures chiral nematics have the helical phase as a stable equilibrium structure.

Because all chiral nematics with blue phases also have helical phases at lower temperatures, the blue phases of a chiral nematic are sometimes characterized by properties that are in fact only possessed by the helical phase of that chiral nematic at lower temperatures. In particular, the pitch of the helical phase, though it varies with temperature, does not vary significantly on a scale comparable to the range of temperatures through which the blue phases are stable (Fergason *et al.*, 1966). One often associates a pitch with a blue phase, by which one means either the pitch that would have been assumed by the helical phase of the same material, were it stable in that temperature range, or, what amounts to the same thing, the pitch assumed by the helical phase at the temperature at which it first becomes stable with respect to the blue phase.

On a more theoretical level, the pitch can also be formally identified with a parameter appearing in the free-energy function characterizing a chiral nematic, independently of whether that free energy favors helical or blue phase ordering. Should the helical phase be favored, that parameter is indeed its pitch. Should a blue phase be favored, the parameter continues to be an important characteristic of the material, though its geometrical manifestation can be rather less direct.

F. Line defects: General features

Structures containing singular lines play a central role in one limiting case of the general theory of blue phases (low chirality), and the ghostlike residues of such line defects can be identified in the other limiting case (high chirality). A major basis for the conceptual appeal of blue phases is that they provide a simple case study of some of the more subtle aspects of the topological theory of defects (see, for example, Mermin, 1979). A line defect

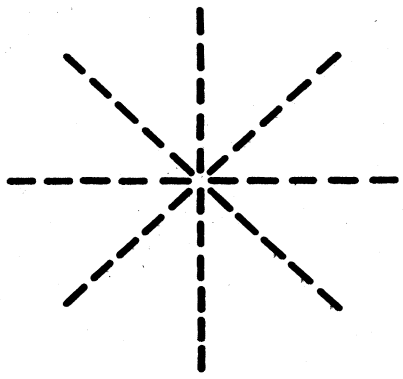

FIG. 2. The director field in the neighborhood of a 2π disclination.

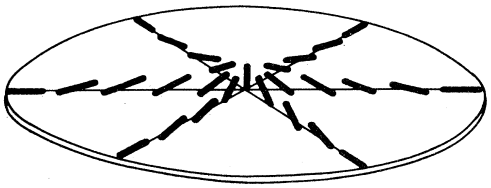

FIG. 3. "Escape in the third dimension": by allowing the director field to tilt out of the plane, the disclination of Fig. 2 can deform into a nonsingular configuration. The director at the center of Fig. 3 is now aligned perpendicular to the plane.

is said to be *unstable* (or "topologically unstable") if the liquid can continuously relax into a nonsingular configuration that differs from its original one only in the immediate neighborhood of the formerly singular line. Figure 2 shows an example of such an unstable singularity in a uniaxial nematic, the 2π disclination (or "$s=1$ disclination"). The "2π" indicates that the director rotates through a full 360° as the singular line is encircled; "disclination" is analogous to the term "dislocation" in crystals, but emphasizes that here the ordering that becomes singular is orientational rather than positional. The deformation of the 2π disclination into a nonsingular configuration is shown in Fig. 3. The process by which the core is thus rendered nonsingular is called "escape in the third dimension."

A stable singularity of a uniaxial nematic—the π disclination (or "$s=\frac{1}{2}$ disclination")—is pictured in Fig. 4(a). Because the local preferred direction turns only through 180° as the line is encircled, escape in the third dimension is no longer possible. Note that such a line defect is only possible because of the identification of $\mathbf{n}$ and $-\mathbf{n}$; if the order parameter were not a director but a vector, the line singularity of Fig. 4(a) would be the boundary of an entire singular sheet, across which $\mathbf{n}$ turned through 180°.

It can be shown that any stable line singularity in a uniaxial nematic is equivalent to the π disclination, in that it can continuously relax into a structure that has the form of the π disclination in the neighborhood of the singular line, without appreciably altering the configuration far from the line. Figure 4(b) shows a superficially distinct $-\pi$ disclination. This configuration can be transformed continuously into the π disclination of Fig. 4(a) by rotating the director at each point $\mathbf{r}$ by 180° about an axis passing through $\mathbf{r}$ and parallel to the direction shown in the figure. To perform this transformation only in the neighborhood of the singularity, the director must be rotated by an angle $\theta(r)$, where θ approaches 180° as r goes to zero, and vanishes as r goes to infinity.

Whether a given singularity is regarded as stable or not (or whether or not two singularities are regarded as equivalent) can depend on how one views the physical system in which the singularities appear. By restricting the set of configurations the system is allowed to assume, one can stabilize unstable singularities; conversely, by expanding the set, one can make stable ones unstable.

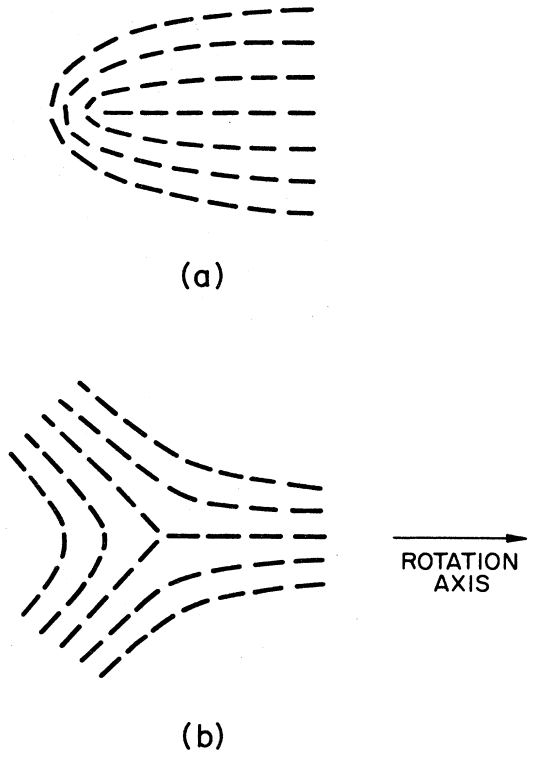

FIG. 4. (a) The director field in the neighborhood of a π disclination; (b) the director field in the neighborhood of a $-\pi$ disclination. This pattern can be continuously deformed into that of (a) by rotating the director at each point $\mathbf{r}$ by 180° about an axis passing through $\mathbf{r}$ and parallel to the axis shown. (During the rotation the director will point out of the plane.)

Consider, for example, the 2π disclination in the uniaxial nematic. If this structure appeared in a hypothetical "x-y nematic"—one in which the director were required to lie in a single plane (by boundary conditions or applied fields)—then escape in the third dimension could not take place and the singularity would become stable. On the other hand, as we shall see in Sec. VIII, in a nematic capable of assuming not only uniaxial but also general biaxial anisotropy the π disclination is no longer a stable singularity, for it can acquire a nonsingular core by passing through biaxial forms, thereby "escaping into biaxiality."[3]

[3]This absence of stable line defects when biaxiality is allowed might appear to contradict the esoteric fact that in "biaxial nematics" there are four classes of stable line defects, including three distinct classes of stable π disclinations. There is no contradiction, because these four classes are only stable in "hard" biaxial nematics, which *must* have bricklike symmetry everywhere and are not allowed to be anywhere uniaxial. The biaxiality we shall consider is always "soft"—the ration of the eigenvalues of the tensor order parameter (see Sec. IV) are not fixed.

The only line singularities we shall be considering below are the stable line singularities of uniaxial nematics, i.e., the π disclinations. When we refer to line singularities without qualification or elaboration, these are the ones we have in mind.

G. Line defects: A cautionary note

It is often a pedagogical error to draw attention to a wrong way of looking at things, and the reader is therefore urged to ignore this subsection if its point is not immediately evident.

The relative character of the stability or equivalence of defects can give rise to considerable confusion in describing defects in the helical phase of chiral nematics, and this confusion can turn into a major muddle if the blue phases are incorrectly regarded, not as an independent class of chiral nematics, but as a variant of the "cholesteric" (in the narrow sense of "helical phase") class, an error induced by a careless identification of the broad and narrow meanings of "cholesteric" (see Table I.)

Helical phases can be viewed as nematics with a very special kind of inhomogeneity in the directional ordering. If one required the director field locally to resemble the helical structure, then the director field would be restricted to a subclass of all possible uniaxial nematic configurations, with the result that the set of helical phase defects would include many more types of stable and distinct line singularities than would be the case if the local configurations were unrestricted. (This is analogous to restricting the director field to lie in a plane, which gives rise to additional stable singularities compared to an unrestricted nematic.) Among the stable helical phase defects are several kinds of inequivalent disclinations, as well as what are known as focal conic singularities. When viewed as singularities in a (chiral) nematic, however, every one of these helical phase defects is either unstable—i.e., not a defect at all—or equivalent to the unique stable π disclination.

In a similar way defects in the blue phase can either be regarded as nematic defects or be classified by a scheme based on the special inhomogeneity that blue-phase ordering imposes on the more general nematic anisotropy. In neither case, however, is the special classification scheme for the helical phase ("cholesteric defects") relevant to the description of blue-phase defects.

We shall use only the simple classification scheme for line defects in a nematic (which has only one type of stable defect) whether we are dealing with ordinary or chiral nematics, and whether the chiral nematics are in the helical or the blue phases. We do this not only to avoid ambiguity, but also because we shall be concerned only with helical and blue phases in their unstressed equilibrium configurations. We shall therefore have no need for the complexities of the special helical or blue-phase classification schemes.

We shall, however, allow ourselves both the uniaxial and biaxial point of view in characterizing nematic singularities. Since no stable line singularities survive when the uniaxial class is expanded to allow for possible biaxiality, this flexibility will not be the occasion for confusion. When line singularities are mentioned at all they must be uniaxial nematic singularities, and these come in only one variety: the π disclination.

III. EXPERIMENTAL OVERVIEW

A. Introduction

Observations of the blue phase date back to the earliest days of liquid-crystal research. Stegemeyer and Bergmann (1980) note that Reinitzer, in his pioneering work on liquid crystals, described seeing bright blue-violet reflections on cooling liquid cholesteryl benzoate (Reinitzer, 1888), an effect now known to be characteristic of the blue phase of this compound (see also Gray, 1956; Gray and Winsor, 1974). Both Lehmann (1906) and Stumpf (1911) observed similar phenomena in several cholesteric compounds and proposed that this indicated a new, thermodynamically stable phase at temperatures between the isotropic liquid and the helical phase. After 1911 interest in the phenomenon waned; Friedel described it only in passing in his important 1922 review (Friedel, 1922). The suggestion that the blue phase is stable has been verified only within the past decade and a half; until then the lack of experimental evidence for a distinct, stable phase (e.g., latent heats or volume discontinuities at the transition) led people to believe that they were merely observing a metastable "modification" of the helical phase, similar to the focal conic structure (for early observations in recent times, see Gray, 1956, 1962; Elser, 1966; Chistyakov and Gusakova, 1969; Saupe, 1969; Prince and Wendorf, 1971, 1972; Coates and Grey, 1973, 1975; Coates, Harrison, and Grey, 1973; Elser, Pohlmann, and Boyd, 1973).

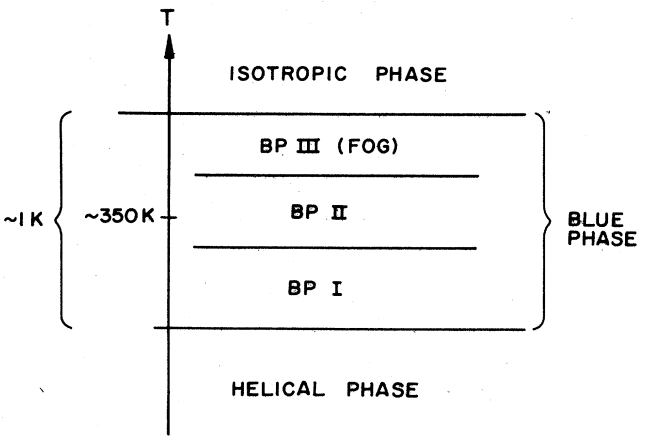

FIG. 5. A schematic phase diagram showing the blue phases in relation to the helical and isotropic phases as a function of temperature. Not all three blue phases occur in every material.

Up to three distinct blue phases appear in a great variety of chiral nematic compounds (see, for example Coates and Gray, 1973; Coates, Harrison, and Grey, 1973; Elser *et al.*, 1973; Johnson *et al.*, 1980; Meiboom and Sammon, 1980; Marcus and Goodby, 1982; Nicastro and Keyes, 1983; Tanimoto *et al.*, 1985; Chanishvili *et al.*, 1986; Keyes, 1987; Yang and Crooker, 1987, 1988), and the appearance of one or more blue phases seems to be a general property of such systems when the pitch is sufficiently short (typically less than 5000 Å). The two lower-temperature phases, called blue phase I and blue phase II (BP I and BP II), appear to have cubic structures in all samples studied, while the highest-temperature phase, known as BP III (or historically as the "blue fog"), appears to be amorphous (Fig. 5). These phases exist only in a very small temperature range between the high-temperature isotropic phase and the low-temperature helical phase. The width of the entire blue phase-region is typically only about one degree, though typical transition temperatures are several hundred.[4]

The most striking feature of the blue phases is the mosaic of bright colors they can display, in contrast to the relatively featureless helical phase and isotropic liquid (Chistyakov and Gusakova, 1969; Price and Wendorf, 1971; Coates, Harrison, and Gray, 1973; Elser *et al.*, 1973; Marcus, 1981). The mosaic consists of brightly colored wrinkled flakes, or *platelets,* typically 100 μm in size, that appear throughout the temperature range of blue phases I and II, and which were originally incorrect believed to be small randomly oriented domains of the helical structure (Coates and Gray, 1973, 1975). The colors are often blues or violets, thus the name, but a wide variety of colors can be seen, sometimes varying considerably through the sample or shifting with temperature (for color plates, see Elser *et al.*, 1973; Stegemeyer and Bergmann, 1980; Brinkman and Cladis, 1982; Stegemeyer *et al.*, 1986).

A second general feature of blue phases that any theory of structure must explain is their effect on polarized light. Like the helical phase, the blue phases are optically active and therefore rotate the direction of polarization of linearly polarized light, although with rotatory powers that are orders of magnitude less than those of the helical phase (Bergmann and Stegemeyer, 1978; Brog and Collings, 1980; Bensimon *et al.*, 1983). However, unlike the helical phase, they are optically isotropic and are not birefringent (Saupe, 1969; Pelzl and Sackmann, 1973; Bergmann and Stegemeyer, 1978; Demus *et al.*, 1978).

A number of experimental techniques, some of which we discuss in detail below, have been used to explore the blue phases in the effort to determine their structures. We give here a brief overview of the major experimental results on the blue phases. For more detailed reviews, see for example, Bergmann and Stegemeyer (1978), Belyakov and Dmitrienko (1985), Stegemeyer *et al.* (1986) and Crooker (1989).

B. Stability of the blue phases

For many years the blue-phase region was believed to consist of a single phase and was not regarded as thermodynamically distinct, but merely as a metastable form of the helical phase. The metastability argument was persuasive because the blue phase can supercool into the helical phase by several degrees, an amount often larger than its entire range of stability, and within the supercooled range stirring can indeed induce a transition to the helical state. [Supercooling of two to five degrees is typical (see, for example, Collings and McColl, 1978; Johnson *et al.*, 1980), although supercooling of as much as ten degrees has been observed (Chanishvili *et al.*, 1986).] Price and Wendorf (1971), however, found that near the high-temperature end of its range of existence the blue phase could not be induced to make such a transition, indicating that it was indeed stable at these temperatures.[5]

The blue phase finally became generally regarded as a distinct stable phase when Armitage and Price (1975, 1977) detected both a latent heat and a density change at the blue-helical transition in several chiral nematics. They measured a latent heat of the order of 0.01 cal/g, a value only 3–10 % of the value at the isotropic-blue transition, which is more typical of liquid-crystal transitions.[6] In addition, they found volume changes at the helical-blue transition that were extremely small but observable: roughtly 0.01% (Armitage and Price, 1975, 1976). These two results show that the helical-blue transition is (weakly) first order, consistent with the supercooling effects seen at this transition.

Bergmann and Stegemeyer (1979a) later confirmed the observations of Armitage and Price, and also discovered a second specific-heat anomaly nearer to the transition to the isotropic phase, indicating that the blue phase region consisted of at least two distinct phases, BP I at lower temperatures, and BP II at higher. They estimated the latent heat at the BP I–BP II transition to be very close

[4]Recently, a blue phase stable over a two-to-five-degree temperature range has been reported (Chanishvili *et al.*, 1986).

[5]Somewhat earlier, in 1967, Barrall *et al.* measured the specific heat and optical activity of cholesteryl myristate near the helical-to-isotropic transition and reported observing a new cholesteric phase, but did not identify it as the blue phase (see also Arnold and Roedinger, 1968).

[6]Transitions between different liquid-crystal phases typically have latent heats of 0.1 cal/gm and are much more weakly first order than liquid-crystal–solid transitions, where latent heats and volume changes are 50–100 times larger (Armitage and Price, 1977).

to the helical–BP I value. Unlike BP I, BP II does not appear to supercool (Johnson *et al.*, 1980; Tanimoto and Crooker, 1984).

Evidence for a third stable blue phase (BP III) was noted soon afterwards by Stegemeyer and Bergmann (1980), and by Marcus (1981), who called it the "blue fog" for its featureless, blue-gray appearance (although in many materials it is transparent). Meiboom and Sammon (1981) also detected this phase and found it to be much more elusive than the other blue phases, appearing in very few of their samples. It is found only in systems with very short pitches, and typically exists over a range of less than 0.05 K. Like BP I and II, BP III shows no birefringence and exhibits selective reflection of circularly polarized light and strong optical activity, suggesting a local chiral structure with correlations over distances of the pitch (Demikhov and Dolganov, 1983; Collings, 1984b; Kizel' and Prokhorov, 1984; Demikhov *et al.*, 1985; Yang and Crooker, 1988). However, unlike BP I and II, this phase appears to be amorphous and does not exhibit Bragg scattering or platelets.

Optical measurements and direct observations of the phase suggested that BP III was a distinct, stable blue phase (Marcus, 1981; Meiboom and Sammon, 1981; Demikhov and Dolganov, 1983; Hornreich and Shtrikman, 1983; Collings, 1984b). The stability became generally accepted following experiments by Collings (1984b), who measured optical rotatory dispersion in the phase, and by Kleiman *et al.* (1984), who measured heat capacity, shear elasticity, and viscosity throughout the blue phase region. While the helical–BP I, BP I–BP II, and BP II–BP III transitions have been known for a number of years to be first order, the nature of the BP III–isotropic transition has only recently been resolved. Thoen (1988), using his high-resolution calorimetry results (Fig. 6), was able to separate the latent heat at this transition from pretransitional effects and show that the transition is weakly first order. As is evident from Fig. 6, most of the latent heat evolved in going from the isotropic phase to the helical phase is released at the BP III–isotropic transition (see also Taborek, Goodby, and Cladis, 1989).

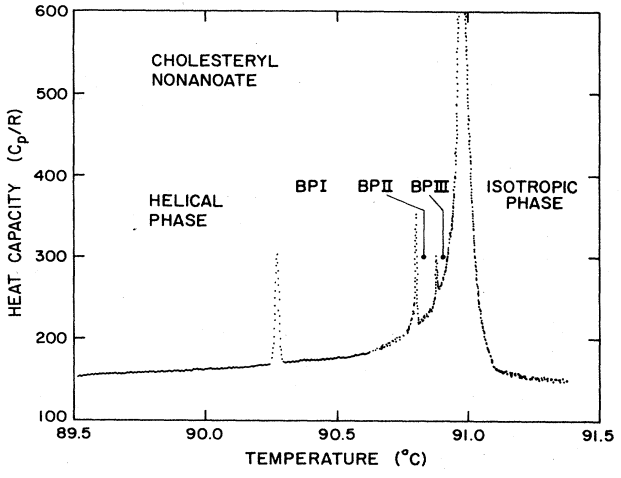

FIG. 6. High-resolution heat-capacity measurements for the blue-phase region of cholesteryl nonanoate (from Thoen, 1988). The latent heats measured at the transitions shown are 18±1 J/mol at helical–BP I, 5.8±0.5 at BP I–BP II, 1.9±0.5 at BP II–BP III, and 170±15 at BP III–isotropic. Nearly 87% of the latent heat is at the BP III–isotropic transition. The other latent heats are atypically small for liquid-crystal transitions. (Here R is the gas constant.)

C. Pitch dependence of the blue phases

Considerable experimental work has been done to understand the effect of pitch on the blue phases (Bergmann and Stegemeyer, 1978; Finn and Cladis, 1981, 1982; Keyes and Nicastro, 1981; Keyes, Nicastro, and McKinnon, 1981; Flack and Crooker, 1981b; Her *et al.*, 1981; Marcus and Goodby, 1982; Onusseit and Stegemeyer, 1982, 1983a; Nicastro and Keyes, 1983; Flack *et al.*, 1984; Blümel and Stegemeyer, 1984b; Tanimoto, Crooker, and Koch, 1985; Blümel, Collings, Onusseit, and Stegemeyer, 1985; Collings, 1986; Miller *et al.*, 1987; Yang and Crooker, 1987). Drawing conclusions from such experiments can be difficult since the usual methods of varying the pitch, i.e., varying chemical composition or considering a series of compounds with closely related molecular structures ("homologs"), can also change properties of the system other than the pitch (e.g., the transition temperature to the isotropic phase can vary considerably with the pitch in these systems). Some recent studies, however, have varied the pitch by using a series of mixtures of right- and left-handed versions of the same material ("chiral-racemic mixtures"), which should leave other properties largely unaffected (Marcus and Goodby, 1982; Tanimoto *et al.*, 1985; Collings, 1986; Tius *et al.*, 1987; Yang and Crooker, 1987).

Blue phases are found to appear only in systems with

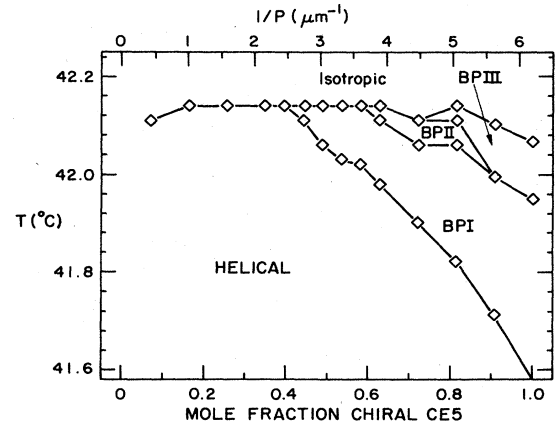

FIG. 7. A phase diagram of the blue phases as a function of inverse pitch for chiral-racemic mixtures of the compound CE5 (from Yang and Crooker, 1987).

short pitch, typically less than 5000 Å. As the pitch is decreased, the temperature range over which the blue phases are stable generally increases. A phase diagram as a function of pitch in a series of chiral-racemic mixtures of the compound CE5 is shown in Fig. 7. The disappearance of BP II for large inverse pitch is observed in a number of compounds homologous to CE5 (Yang and Crooker, 1987); whether this is a general feature of blue phases remains an open question.

D. Optical Bragg scattering

Many of the early experiments on the blue phases were versions of experiments traditionally done on the helical phase. In many cases, these experiments give results similar to those found for the helical phase, indicating that the local structure of the two is similar. These include, for example, measurements of the selective reflection of circularly polarized light (Bergmann and Stegemeyer, 1978, 1979b; Bergmann, Pollman, Scherer, and Stegemeyer, 1979; Pollman and Scherer, 1979, 1980; Stegemeyer and Bergmann, 1980; Tanimoto and Crooker, 1984; Blümel *et al.*, 1985; Demikhov *et al.*, 1985), the angular dependence of selective reflections (Flack and Crooker, 1981a; Marcus, 1982c; Kuczynski, 1985a; Heppke *et al.*, 1987; Keyes, 1987; Yang, Crooker, and Tanimoto, 1988), rotatory power (Bergmann and Stegemeyer, 1978; Beevers *et al.*, 1982; Demikhov and Dolganov, 1983; Collings, 1984a, 1984b; Blümel *et al.*, 1985), NMR spectra (Collings and McColl, 1978; Samulski and Luz, 1980; Shivaprakash and Prasad, 1982; Grebel *et al.*, 1983b; Yaniv *et al.*, 1983), and observation of Grandjean-Cano lines (Kuczynski and Stegemeyer, 1980; Stegemeyer and Bergmann, 1980; Feldman, Crooker, and Goh, 1987; Blümel and Stegemeyer, 1988). Additional probes of these phases have included measurements of thermal fluctuations (Marcus, 1984, 1985), index of refraction (Pelzl and Sackman, 1973; Bergmann and Stegemeyer, 1978), kinetics of the helical–blue phase interface (Würz *et al.*, 1979), and optical measurements of the order parameter (Marcus, 1982c; Barbet-Massin and Pieranski, 1984, 1985).

Optical measurements, which have traditionally been an important tool for studying liquid crystals, become more informative with the possibility of optical Bragg scattering off the crystalline blue phases BP I and II. Because the pitch of these systems is typically several thousands of angstroms, they Bragg-scatter visible light just as crystals scatter x rays, and many of the techniques used in x-ray crystallography to determine crystal structures can be applied here.

Such scattering reveals three-dimensional periodic structures with cubic lattices having lattice spacings on the order of the helical phase pitch (see Sec. III.F). The platelets that always appear in blue phases I and II are interpreted as domains of blue phase ordering, their differing colors arising from their different orientations to the observer, which leads to Bragg reflection for different wavelengths.

Marcus (1981) has given a detailed explanation of the striking appearance of the blue phases I and II in terms of their ability to Bragg-scatter visible light. To remove background light and increase contrast, samples are typically placed between crossed linear polarizers; without polarizers the fluid appears largely transparent. Viewed in reflected light, BP I and II appear as a collection of platelets suspended in a dark liquid. The platelets that appear in these phases look like bright flakes of metallic foil of various colors that nonetheless appear transparent, allowing platelets below them to show through undiminished. Regions between the platelets that appear dark in reflected light are found also to consist of platelets that are visible in transmission.

The platelets are interpreted as randomly oriented domains of crystalline blue phase ordering, and their bright colors arise from the Bragg scattering into the direction of the observer of those wavelengths that satisfy the Bragg condition. Platelets with different orientations reflect different colors, and those that cannot satisfy the Bragg condition at all will instead pass the incident light and appear dark in reflection.

When these phases are viewed in transmitted light, the situation is somewhat different. Since the system is between polarizers, the light reaching a platelet is linearly polarized and can be considered to be the sum of equal amounts of right and left circular polarizations. The only light passing the second polarizer will be at those wavelengths that have one component of circular polarization Bragg scattered out of the incident direction.[7] The transmitted light will therefore be those wavelengths that satisfy the Bragg condition, and thus the color will again depend on the orientation of the platelet.

Note that in reflection, if more than one set of Bragg planes in a platelet satisfies the Bragg condition, different colors will be scattered in different directions, but in transmission they will be superimposed, giving a multicolored appearance. Notice also that if one platelet overlaps another, but the two scatter at different wavelengths, then neither will affect the light scattered by the other, and thus they will appear transparent. The platelets probably appear as thin flakes in reflection because of the strength of the Bragg scattering, which causes most of the light to be scattered by a thin surface layer of the domain.

E. Other properties of the blue phases

1. Nonzero elastic shear modulus

One of the hallmarks of a solid in contrast to a liquid is its ability to resist static shears, i.e., the existence of a nonzero elastic shear modulus. Since two of the blue

[7]Rotation of the plane of polarization of the light at wavelengths that are not scattered is at most a few degrees over the thickness of the samples (0.2 mm) (Brog and Collings, 1980).

phases have three-dimensional periodicity like crystals, but nonetheless pour like liquids, one might ask what elastic measurements would show for these phases. Measurements of the response of the blue phase in a torsional oscillator confirm the existence of a nonzero elastic shear modulus, although with a magnitude on the order of 10^3 dyn/cm^2, roughly a million times smaller than that of conventional solids (Cladis *et al.*, 1984; Clark *et al.*, 1984; Kleiman *et al.*, 1984). This value agrees with estimates that follow from dimensional considerations (Clark *et al.*, 1984). One would expect an elastic modulus to be on the order of Kq_0^2 where K is an elastic constant from the free energy describing distortions of the director field, and q_0^{-1} is roughly a typical lattice constant for the blue phases. For typical values of K and q_0, Kq_0^2 is on the order of 10^3-10^4 dyn/cm^2.

2. Anomalous viscosity

Measurements in chiral nematics of anomalously large bulk viscosities in a narrow temperature range near the helical-isotropic transition have existed since the 1930s (for references, see Stegemeyer and Pollman, 1982; see also Yamada and Fukada, 1973; Keyes and Ajgaonkar, 1977). Stegemeyer and Pollman (1982) measured the bulk viscosity as a function of temperature near the transition to the isotropic phase in two chiral mixtures by studying flow through millimeter-sized capillaries. By varying the composition of these mixtures, and thus the pitch, they could produce closely related materials that differed in whether or not they exhibited blue phases. They found that in those mixtures with blue phases, the viscosity is anomalously large in the blue phase region, climbing sharply to a factor of up to 10^6 times its value in the helical phase as the temperature is raised, and dropping back in the isotropic phase. Since peaks were only observed in mixtures exhibiting blue phases, they concluded that the increase in viscosity was due to the presence of the blue phase ordering.

3. Electric field effects

Several groups have studied the effects of electric fields on the blue phases (for a review of work up to 1986, see Stegemeyer *et al.*, 1986), including field-induced transitions (Armitage and Cox, 1980; Finn and Cladis, 1982; Heppke *et al.*, 1983, Stegemeyer and Porsch, 1984; Ziolo *et al.*, 1986; Porsch and Stegemeyer, 1987; Stegemeyer and Spier, 1987; Yang and Crooker, 1988), field-induced optical birefringence and other effects on optical properties (Beevers *et al.*, 1982; Heppke *et al.*, 1983, 1985a, 1985b, 1987; Porsch *et al.*, 1984; Gerber, 1985; Pieranski and Cladis, 1986; Porsch and Stegemeyer, 1986), the faceting and orienting of single crystals in a field (Pieranski, Cladis, and Barbet-Massin, 1986; Pieranski, Cladis, Garel, and Barbet-Massin, 1986), and the effects of time-varying fields (Gleeson *et al.*, 1985). Lubin and Hornreich (1987) have recently studied the effects of fields theoretically using Landau theory.

One of the most interesting aspects of work in this area is the appearance of new phases in the presence of an electric field. In 1985, Hornreich, Kugler, and Shtrikman (1985a, 1985b) predicted a field-induced blue phase with a two-dimensional hexagonal structure. Pieranski, Cladis, and Barbet-Massin (1985) observed field-induced transitions to a three-dimensional hexagonal structure containing a screw axis, as well as a phase of tetrahedral symmetry. Subsequent work has detected a number of additional field-induced phases (Cladis *et al.*, 1986; Pieranski and Cladis, 1987; Porsch and Stegemeyer, 1987; Yang and Crooker, 1988).

4. Direct smectic A–blue phase transition

In at least one material, a transition has been observed directly between BP I and a smectic A phase, without an intermediate helical phase, as usually occurs (Onusseit and Stegemeyer, 1984; Stegemeyer *et al.*, 1986). This was found by mixing cholesteryl myristate with a material that has only a smectic phase. At low concentration of the smectic material, the sample showed a transition from the blue phase to a helical phase and finally to a smectic A phase as the temperature was decreased. As the concentration of the smectic material was increased, the temperature range over which the helical phase appeared decreased and finally disappeared altogether. This observation strengthens Frank's proposal (1983) that the blue phase be considered as a new class of liquid crystals, distinct from nematics, cholesterics, and smectics.

F. Experimental determinations of structures

Determining the structures of the blue phases has been a major focus of both experimental and theoretical work. Since the energy differences are small between the various structures emerging from the theory, one might expect that different structures would be seen depending on details of the chemical composition of the system or the method of preparation of the sample. Experiments have been conducted on a large variety of materials exhibiting blue phases, however, and most if not all of these systems seem to indicate a single space group describing BP I and a second describing BP II. There are currently no compelling theoretical grounds for this uniformity. We outline below the techniques that have been used to explore the structures, noting at the end the conclusions of these studies as well as some of the evidence contradicting these assignments.

Several models have been proposed for BP III (see Sec. VI and VII), but little is known about its structure except that it appears to be amorphous, lacking long-range translational symmetry, and that locally it has a chiral structure, as evidenced by selective reflection of circular-

ly polarized light and optical activity (Demikhov and Dolganov, 1983; Kizel' and Prokhorov, 1984; Collings, 1984b; Demikhov *et al.*, 1985; Yang and Crooker, 1988). Estimates of the extent of long-range order in this phase from optical rotatory dispersion spectra (Collings, 1984b) and the width of selective reflection peaks (Demikhov *et al.*, 1985; Yang and Crooker, 1988; Yang, Crooker, and Tanimoto, 1988) gives values of a few pitch lengths. A considerable amount of the ordering within the blue phase region must take place at the isotropic–BP III transition since nearly 90% of the latent heat of the series of blue phase transitions between the helical phase and the isotropic phase is given off at this transition (see Fig. 6). Freeze-fracture electron micrographs of BP III in the material CE4 appear to show a disordered packing of filamentary objects (Zasadzinski *et al.*, 1986). While it is tempting to interpret these images as evidence that this phase consists of a tangle of low-energy cylinders of ordered material (the "double-twist cylinders" of Sec. VII), one expects such cylinders to have diameters not much less than a quarter pitch (Hornreich, Kugler, and Shtrikman, 1982), which is considerably larger than the structures seen in the micrographs. The correct interpretation of these data is thus unclear.

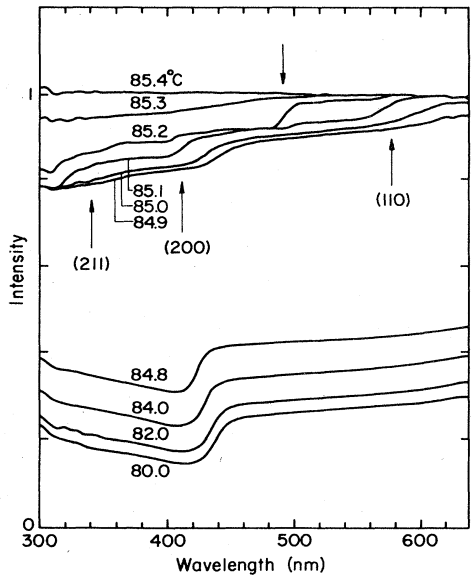

FIG. 8. Bragg scattering in the blue phases (from Meiboom and Sammon, 1980). The traces (made at successively higher temperatures, as marked) show the intensity of the light transmitted through a "powder" of randomly oriented platelets in a mixture of cholesteryl nonanoate and cholesteryl chloride, normalized to transmission in the isotropic phase. As expected for a powder sample, Bragg scattering leads to steps rather than peaks in the transmitted intensity. The single step in traces below 84.8 °C indicates the helical phase. Three steps resulting from BP I are visible in the trace at 85.1 °C (marked by the upward-pointing arrows and indexed to a bcc lattice), while a single step from BP II appears in the trace at 85.26 °C (marked by the downward-pointing arrow).

Measurements of selective reflection (Bergmann and Stegemeyer, 1978, 1979b; Bergmann, Pollman, Scherer, and Stegemeyer, 1979; Pollman and Scherer, 1979, 1980; Stegemeyer and Bergmann, 1980; Demikhov *et al.*, 1985; Blümel *et al.*, 1985) and rotatory power (Bergmann and Stegemeyer, 1978; Beevers *et al.*, 1982; Demikhov and Dolganov, 1983; Collings, 1984a) show that the two lower-temperature blue phases (BP I and BP II), which exhibit three-dimensional periodicity, also have local chiral structures with pitches on the order of the pitch of the helical phase that appears at lower temperatures. By studying the wavelength and angle dependence of Bragg scattering, Marcus (1982c) was able to infer that BP I and BP II exhibit long-range order extending over distances of at least 50 lattice spacings. As early as 1969, Saupe (1969) pointed out that the lack of birefringence observed in these phases suggests an underlying cubic structure and proposed a possible structure having body-centered-cubic translational symmetry and a lattice constant on the order of the helical pitch.

The translational symmetry of the blue phases was first probed by optical Bragg scattering by Meiboom and Sammon (1980, 1981), who recorded steps in the intensity of light transmitted through a sample composed of a "powder" of randomly oriented platelets in a mixture of cholesteryl nonanoate and cholesteryl chloride (Fig. 8), and by Johnson, Flack, and Crooker[8] (1980) who studied Bragg reflections in mixtures of biphenyls CB15 and E9 (Fig. 9). These experiments showed that both BP I and BP II in these systems had either simple cubic (sc) or body-centered-cubic (bcc) translational symmetry, and gave a lattice constant of roughly the helical phase pitch for a bcc lattice, or half the pitch for sc.[9] However, because the Bragg powder patterns of sc and bcc match up to seven reflections—more than have been observed—other techniques must be used to distinguish them.

Several groups have borrowed techniques from conventional crystallography to determine the lattices. Onusseit and Stegemeyer (1981, 1983b) (in cholesteryl nonanoate) and Marcus (1982b) (in two mixtures of cholesteryl compounds with nematic E7) grew large defect-free platelets of BP I and BP II and were able to infer the translational symmetry from the morphology. Onusseit and Stegemeyer found strong evidence for sc symmetry for BP II of their material, while Marcus was able to show that BP I in his sample was bcc and BP II was sc (see also Nicastro and Keyes, 1982; Blümel and Stegemeyer, 1985; Stegemeyer *et al.*, 1986; Yang and

[8]Evidence presented in this paper and in Her *et al.* (1981) for the existence of two BP II phases is now believed to be due to compositional separation of the mixtures used (Marcus, 1982a).

[9]Recall that the pitch, as defined in Eq. (2.2) for the helical phase, is actually twice the physical repeat distance of the helical phase, since $\mathbf{n}$ and $-\mathbf{n}$ are equivalent configurations of the director field.

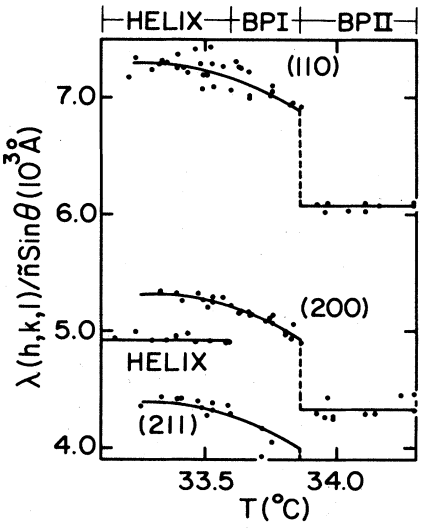

FIG. 9. The wavelength of Bragg peaks in a mixture of CB15 and E9 in which the platelets have been aligned by the sample preparation (from Johnson, Flack, and Crooker, 1980). (Here θ is the Bragg angle and n is the index of refraction; all data were measured for $\theta=\pi/2$.) The single line at low temperature arises from the helical phase. The three lines at higher temperatures indicate BP I (note the supercooling of the BP I below the helical–BP I transition at 33.6 °C) and are marked by the indexing to a bcc lattice. At higher temperatures, a discontinuous jump in wavelength is observed at the transition to BP II, in which two Bragg peaks were observed.

Crooker, 1987). Recent electron micrographs of freeze-fractured samples of BP I in an E9-CB15 mixture show periodic features that have been interpreted as evidence of bcc symmetry (Costello *et al.*, 1984; Berreman *et al.*, 1986). Kuczynski (1985a) measured the angles between the Bragg planes in BP II of MMBC and deduced that it has a single cubic lattice.

Since BP I and BP II have cubic symmetry and are chiral, the possible space groups they can have are restricted to six with sc translational symmetry[10] [T^1 ($P23$), $T^4(P2_13)$, $O^1(P432)$, $O^2(P4_232)$, $O^6(P4_332)$, $O^7(P4_132)$] and four with bcc translational symmetry [$T^3(I23)$, $T^5(I2_13)$, $O^5(I432)$, $O^8(I4_132)$]. In order to determine which of these groups actually describe the observed phases, a number of properties of BP I and BP II have been examined. These include measurements of the Mueller matrix, which describes light scattering (Hornreich and Shtrikman, 1981a, 1983; Flack, Crooker, and Svoboda, 1982; Gorman and Crooker, 1985); circular dichroism (Kizel' and Prokhorov, 1983, 1984); Kossel diagrams (Cladis *et al.*, 1986; Pieranski and Cladis, 1987; Jerome *et al.*, 1988); electric field effects (Lubin and Hornreich, 1987); intensities of Bragg reflections (Meiboom, Sammon, and Berreman, 1983; Berreman, 1984; Grebel *et al.*, 1984); and the ratio of the blue phase lattice constant to the helical-phase pitch (Hornreich and Shtrikman, 1980a; Grebel *et al.*, 1984; Belyakov and Dmitrienko, 1985). These results indicate that in the materials studied, BP I has a bcc $O^8(I4_132)$ structure, and BP II has a sc $O^2(P4_232)$ structure (for detailed discussions of the considerations leading to these conclusions, see Meiboom, Sammon, and Berreman, 1983; Grebel *et al.*, 1984; Belyakov and Dmitrienko, 1985; Stegemeyer *et al.*, 1986; Crooker, 1989).

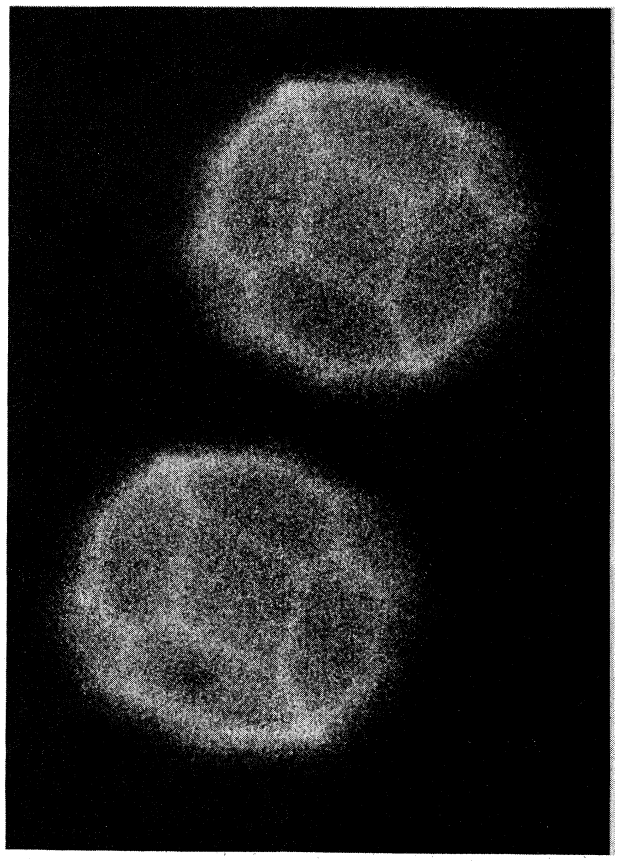

FIG. 10. Single crystals of BP I, showing well-defined facets (cf. Fig. 11) (from Cladis, Pieranski, and Joanicot, 1984). Single crystals up to 0.1–0.2 mm have been grown.

[10]We label space groups by both their Schönflies and their International labels (Sands, 1969; Hahn and Vos, 1987; Burzlaff and Zimmerman, 1987). The Schönflies notation is X^n, where X is a letter (possibly subscripted) denoting the point group, and n is a number assigned by Schönflies that labels the various space groups with point group X. Here T denotes tetrahedral symmetry, and O denotes cubic (octahedral) symmetry. The International notation is $Yjkl$ where Y gives the translation symmetry of the system (P=sc, I=bcc, F=fcc) and the integers j, k, and l denote rotational symmetry axes of $2\pi/j$, etc. A j-fold axis with inversion is written $\bar{j}$, and a screw axis consisting of a rotation by $2\pi/j$ followed by a translation through a fraction p/j of a lattice vector along the rotation axis, is written j_p. The easiest way to understand a space group is to see an object having the symmetries described by the group. Figures 19–22 illustrate the space groups O^2 and O^8.

One of the most striking of the experimental results has been the observation of three-dimensional single crystals of BP I and II showing well-defined facets (Cladis *et al.*, 1984; Barbet-Massin *et al.*, 1984a, 1984b); Blümel and Stegemeyer, 1984a; Pieranski, Barbet-Massin, and Cladis, 1985; Pieranski, Cladis, Garel, and Barbet-Massin, 1986; Stegemeyer *et al.*, 1986, 1988; Pieranski and Cladis, 1988) (Figs. 10 and 11). Single crystals of BP I have been grown up to 0.1–0.2 mm in size, and their morphology in conjunction with light scattering results has been interpreted by these groups as strong evidence for assigning the space group O^8 to this structure. The faceting in BP II indicates cubic symmetry but does not specify the space group.

The other experimental technique that has been important in determining the blue phase structures has been optical Bragg scattering of polarized light. Such scattering can give a considerable amount of structural information, since optical wavelengths, which are on the order of the blue phase lattice constant, are much larger than the size of the constituent molecules and can therefore probe macroscopic properties of the system, such as the polarizability. As a result, these techniques are sensitive to the tensor nature of the order parameter. This is in contrast to x-ray scattering, in which the scattering essentially occurs from single electrons, and which is therefore not sensitive to properties of the system as a whole. Such scattering can therefore only probe scalar quantities, such as the mean density.

Extinctions in the scattering of the polarized light can provide distinct signatures of the space groups of these structures. The selection rules for such scattering have been calculated for the appropriate space groups (Hornreich and Shtrikman, 1981a; Belyakov *et al.*, 1982; Grebel *et al.*, 1983a; Belyakov and Dmitrienko, 1985) and have been used by a number of people to help identify the space groups of the blue phase structures (Hornreich and Shtrikman, 1981a, 1981c; Flack and Crooker, 1981b; Belyakov *et al.*, 1982; Nicastro and Keyes, 1982; Grebel *et al.*, 1983a, 1984; Kizel' and Prokhorov, 1983, 1984; Meiboom, Sammon, and Berreman, 1983; Tanimoto and Crooker, 1984; Kuczynski, 1985a, 1985b; Yang and Crooker, 1987; Keyes, 1987). Even when such scattering does not uniquely specify the full space group, it can still sometimes be used to distinguish sc and bcc lattice symmetry.

The results of Bragg scattering of polarized light for BP I have supported the evidence from morphology and other experiments that this phase has bcc $O^8(I4_132)$ symmetry. The situation for BP II, however, is more puzzling. A simple cubic lattice is indicated for BP II by morphology (Onusseit and Stegemeyer, 1981; Marcus, 1982b; Stegemeyer *et al.*, 1986, 1988; Yang and Crooker, 1987; Pieranski and Cladis, 1988) as well as a variety of other results (Kizel' and Prokhorov, 1983, 1984; Meiboom, Sammon, and Berreman, 1983; Grebel *et al.*, 1984; Kuczynski, 1985a; Blümel and Stegemeyer, 1988; Jerome *et al.*, 1988). The results of scattering studies with polarized light, however, are inconsistent with the selection rules of a simple cubic lattice (Hornreich and Shtrikman, 1981a, 1981c; Belyakov *et al.*, 1982; Tanimoto and Crooker, 1984; Kuczynski, 1985a, 1985b; Yang and Crooker, 1987; Keyes, 1987), and the question has been raised whether there may be difficulties in applying the selection rules. The effects of multiple scattering (Crooker, 1985) and local biaxiality (Belyakov *et al.*, 1982) appear not to account for the differences, and this discrepancy remains an open question.

We stress that while in many materials BP I and BP II appear to have space groups O^8 and O^2, there are currently no compelling theoretical grounds for excluding the appearance of different structures in other materi-

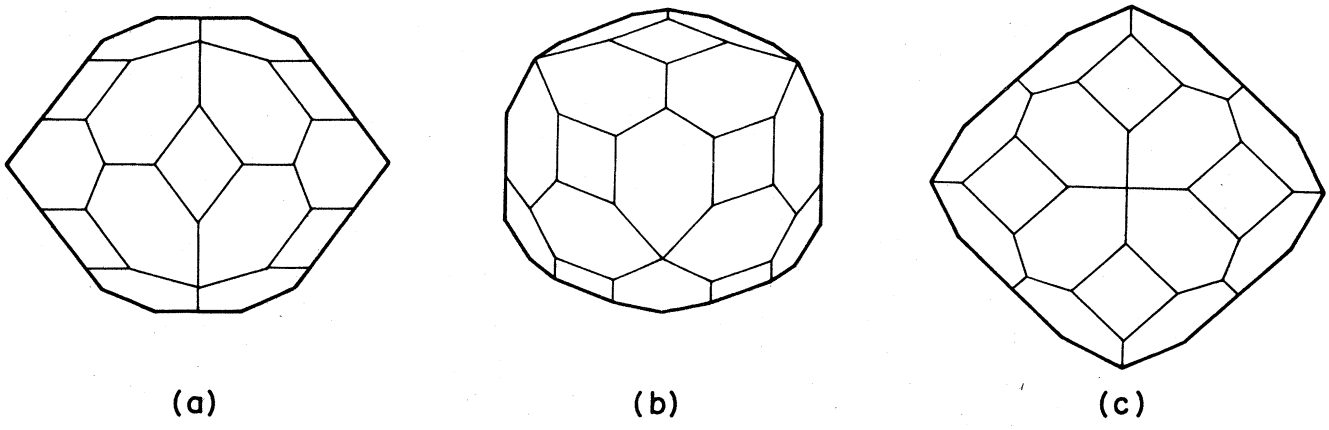

FIG. 11. The shape, proposed by Blümel and Stegemeyer (1984a) and by Barbet-Massin, Cladis, and Pieranski (1984b), for the BP I single crystals, showing the two-, three-, and fourfold symmetry axes (cf. Fig. 10). These groups argue that such a crystal shape indicates a structure with $O^8(I4_132)$ symmetry. From Barbet-Massin *et al.*, 1984b.

als.

In Secs. VI and VII we shall discuss forms of the order parameter that may describe the real space structures of the blue phases.

IV. ORDER PARAMETER AND FREE ENERGY

A. Dielectric anisotropy and the order parameter

Unlike ferromagnetic ordering, which is characterized by a vector property (the spontaneous magnetization), the directional ordering in nematic liquid crystals, whether ordinary or chiral, is characterized by a tensor. In the special case of *uniaxial* nematics the tensorial character of the order is distinguished from vector ordering only by the (very important) fact that $\mathbf{n}$ and $-\mathbf{n}$ represent identical configurations. In order not to prejudice the possible forms of anisotropy, however, one should formulate the problem in terms of a general tensor order parameter, which may or may not assume a uniaxial form in the equilibrium state.

At the transition from isotropic to anisotropic liquid, the form of the local dielectric constant changes. In isotropic liquids the tensor dielectric constant reduces to a scalar:

$$\varepsilon_{ij}=\tfrac{1}{3}\mathrm{tr}(\varepsilon)\delta_{ij}. \tag{4.1}$$

In anisotropic liquids, however, we have

$$\varepsilon_{ij}-\tfrac{1}{3}\mathrm{tr}(\varepsilon)\delta_{ij}\equiv Q_{ij}\neq 0\ . \tag{4.2}$$

The ordering in an anisotropic liquid is thus accompanied by the appearance of a symmetric (since ε_{ij} is symmetric), traceless [as an immediate consequence of the definition (4.2)] tensor $\mathbf{Q}$.

The tensor $\mathbf{Q}$ is generally taken as the order parameter characterizing nematic ordering. Any other tensor exhibiting the anisotropy would do as well, and another common choice is the anisotropic part of the magnetic susceptibility. The dielectric anisotropy is a particularly natural choice, since it is directly related to the light scattering experiments.

In homogeneous anisotropic liquids the dielectric tensor (and hence $\mathbf{Q}$) is independent of position. Although the helical and blue phases of chiral nematics are inhomogeneous, the length scale of the inhomogeneities is large compared with atomic lengths. As a result, the relation between the electric field $\mathbf{E}$ and the electric displacement $\mathbf{D}$ is local, and one can therefore define a position-dependent dielectric constant and dielectric anisotropy, $\varepsilon_{ij}(\mathbf{r})$ and $Q_{ij}(\mathbf{r})$.

The anisotropy at $\mathbf{r}$ is uniaxial if $\mathbf{Q}(\mathbf{r})$ has two degenerate eigenvalues, and biaxial if all three eigenvalues are distinct. If $\mathbf{n}(\mathbf{r})$ is the local preferred direction in a uniaxial liquid, then the tensor $\mathbf{Q}(\mathbf{r})$ has the form

$$Q_{ij}=\gamma(n_i n_j-\tfrac{1}{3}\delta_{ij}). \tag{4.3}$$

Thus the order parameter is indeed determined by a vector $\mathbf{n}$, but is independent of its sign. The uniaxial anisotropy is said to be prolate or oblate according to whether γ is positive or negative.

In the helical phase with the pitch axis along $\mathbf{z}$, the director $\mathbf{n}(\mathbf{r})$ has the form (2.1), which gives for the dielectric anisotropy [Eq. (4.3)]

$$\mathbf{Q}^{\mathrm{uh}}=\gamma\begin{pmatrix}\frac{1}{6}&0&0\\0&\frac{1}{6}&0\\0&0&-\frac{1}{3}\end{pmatrix}+\tfrac{1}{2}\gamma\begin{pmatrix}\cos 2q_0z&\sin 2q_0z&0\\\sin 2q_0z&-\cos 2q_0z&0\\0&0&0\end{pmatrix}. \tag{4.4}$$

(The superscript stands for "uniaxial helix.")

The first term in Eq. (4.4) gives the $k=0$ Fourier component of the anisotropic part of the dielectric constant and therefore governs the direct transmission of light through the liquid. It describes birefringence with the optic axis along the pitch axis $\mathbf{z}$. The second term is responsible for Bragg reflection with a change of wave vector of magnitude $2q_0$ along the pitch axis.

B. Ginzburg-Landau theory

Equilibrium structure is determined by minimizing the free energy. In a Ginzburg-Landau theory of nematics (ordinary or chiral) this free energy is the volume integral of a free-energy density that is a simple local function of the tensor order parameter $\mathbf{Q}$ and its derivatives. Two sets of terms in the free-energy density are distinguished: terms containing derivatives of the order parameter make up the *gradient* free-energy density, while terms that do not, make up the *bulk* free-energy density.

Both sets of terms are expanded in powers of the order parameter $\mathbf{Q}$. The expansion is usually taken far enough to ensure thermodynamic stability, but no farther. To achieve stability against unbounded growth in the amplitude of the order parameter it is necessary to retain terms through the fourth order in the bulk free energy. Stability against unbounded gradients is achieved by retaining terms through the second order in gradients, and these gradient energies are taken only to quadratic order in $\mathbf{Q}$.

Because, as we shall see, the transition to the anisotropic state is first order, we shall describe the ordering with a simple mean-field theory without worrying about fluctuation corrections.[11] On the other hand, because of this first-order character, one must keep in mind the possibility that terms beyond leading order in $\mathbf{Q}$ may play a significant role (see Appendix F). In spite of this, most of the analysis we describe below will be based on minimizing the very simple Ginzburg-Landau free energy de-

[11] A description that does take into account fluctuations has been given by Brazovskii and co-workers (Brazovskii, 1975; Brazovskii and Dmitriev, 1975; Brazovskii and Filev, 1978). For a brief summary of this approach, see Crooker (1983).

scribed above, since the structures it reveals almost certainly have a wider validity, and even that problem turns out to be quite difficult for chiral nematics.[12]

The source of this difficulty is that the bulk and gradient free energies of a chiral nematic are separately minimized by different forms of the order parameter. The bulk free energy favors a uniaxial $\mathbf{Q}$, while the gradient free energy is minimized by a strongly biaxial form. Far below the transition temperature the bulk free energy dominates and the uniaxial helical phase is favored, but nearer to the transition the competition between bulk and gradient energies can lead to some rather intricate compromise structures. These are the blue phases.

C. The bulk free-energy

The only rotational invariants of a traceless three-dimensional tensor are $\mathrm{tr}(\mathbf{Q}^2)$, $\mathrm{tr}(\mathbf{Q}^3)$, or functions of these two. Through fourth order the general form of the bulk free-energy density is therefore[13]

$$f_{\text{bulk}}=c\,\mathrm{tr}(\mathbf{Q}^2)-\sqrt{6}b\,\mathrm{tr}(\mathbf{Q}^3)+a[\mathrm{tr}(\mathbf{Q}^2)]^2\ . \tag{4.5}$$

We define the coefficient of the cubic term with the explicit factor of $\sqrt{6}$ to simplify subsequent expressions [because of relations such as (4.7) below that hold for traceless matrices]. The quartic term can also be written as $2a\,\mathrm{tr}(\mathbf{Q}^4)$, since any traceless 3×3 matrix satisfies $\mathrm{tr}(\mathbf{Q}^4)=\frac{1}{2}\mathrm{tr}(\mathbf{Q}^2)^2$ (see Appendix B).

Stability requires the coefficient a to be positive. Since the term in b is the only term in the bulk or gradient free energies that is odd in $\mathbf{Q}$, changing the sign of b simply changes the sign of the order parameter $\mathbf{Q}$ that minimizes the full free energy. In studying the minimization problem it therefore suffices to consider non-negative b with the understanding that, depending on the actual sign of b, either $\mathbf{Q}$ or $-\mathbf{Q}$ is to be interpreted as the dielectric anisotropy. The sign of $\mathbf{Q}$ is such as to make $\mathrm{tr}(Q^3)$ positive or negative, depending on whether b is positive or negative. The parameter c can have either sign. In the limit of a second-order transition ($b=0$), f_{bulk} starts to favor a nonzero $\mathbf{Q}$ when c changes from positive to negative.

When we need to consider the temperature dependence of the free-energy parameters, we shall assume that the only significant variation can be taken to be that associated with the change in sign of c. We shall thus take c to drop linearly with decreasing temperature through a range that includes the value 0, while regarding b and a as temperature independent. Much of what we have to say, however, will be independent of how c, b, and a vary with temperature.

A nonvanishing cubic coefficient b leads to a bulk free-energy density that is minimized at any point by a uniaxial tensor—i.e., the minimizing traceless symmetric matrix $\mathbf{Q}$ has a pair of degenerate eigenvalues. To see this let the eigenvalues of the general traceless symmetric $\mathbf{Q}$ be $-s$, $-t$, and $s+t$. If we define λ (non-negative) and θ by (Freiser, 1970)

$$\lambda\cos\theta=\sqrt{3/2}(s+t),\quad \lambda\sin\theta=\sqrt{1/2}(s-t)\ , \tag{4.6}$$

then we have simply

$$\mathrm{tr}(\mathbf{Q}^2)=\lambda^2\ ,\quad \mathrm{tr}(\mathbf{Q}^3)=(\lambda^3/\sqrt{6})\cos3\theta\ . \tag{4.7}$$

Since θ appears only in the cubic term, which is proportional to $-\cos3\theta$, for any value of λ the minimum is achieved by taking $\cos3\theta$ to be 1. The choice $\theta=0$ clearly gives two degenerate eigenvalues, and one easily verifies that the other two choices simply give permutations of these same three eigenvalues.

With $\cos3\theta$ equal to 1, f_{bulk} depends only on λ:

$$f_{\text{bulk}}=c\lambda^2-b\lambda^3+a\lambda^4, \tag{4.8}$$

or, equivalently,

$$f_{\text{bulk}}=a\lambda^2[(\lambda-b/2a)^2+c/a-b^2/4a^2]\ . \tag{4.9}$$

Since the zero of free energy is defined to be that of the isotropic liquid ($\lambda=0$), the bulk free energy will favor ordering when it can be negative for some nonzero λ. It is evident from Eq. (4.9) that as c drops (i.e., as the temperature drops) this can first happen when c is less than a critical value

$$c_0=b^2/4a\ , \tag{4.10a}$$

at which point λ can acquire the nonzero value

$$\lambda_0=b/2a=\sqrt{c_0/a}\ . \tag{4.10b}$$

If b were zero, the bulk free energy would favor ordering when c became negative, the order parameter would grow continuously from zero, and the transition would be second order. Because b is in general nonzero, ordering occurs for positive c (i.e., at a higher temperature) and with an order parameter that jumps discontinuously to a nonzero value. Thus when ordering is driven entirely by the bulk free energy (which is the case in ordinary nematics, as noted below) then the nonvanishing of the coefficient b of the cubic term is responsible for the transition's being first order.

Note that if f_{bulk} were a more general function $g(\mathrm{tr}(\mathbf{Q}^2),\mathrm{tr}(\mathbf{Q}^3))$ of the two independent invariants, as would be the case for a strongly first-order transition, then the above argument would still favor a uniaxial order parameter, unless $g(x,y)$ had its minimum in the in-

[12]There is some evidence (Poggi, Atten, and Filippini, 1976; Poggi, Filippini, and Aleonard, 1976) that the quartic bulk free energy fits the properties of an ordinary nematic quite well in a temperature range of more than a degree below the transition, i.e., throughout the temperature range in which chiral nematics can have blue phases.

[13]For the relation between the free-energy parameters used here and those of Grebel, Hornreich, and Shtrikman (1983a), see Appendix A.

terior of the range of allowed values, $|y| \leq x^{3/2}/\sqrt{6}$ determined by Eq. (4.7).

D. The gradient free-energy

To second order in gradients and second order in the symmetric traceless tensor $\mathbf{Q}$, there are just four rotationally invariant quantities:

$$\begin{aligned} &(\nabla_i Q_{jk})(\nabla_i Q_{jk}) , \\ &(\nabla_i Q_{ik})(\nabla_j Q_{jk}) , \\ &(\nabla_i Q_{jk})(\nabla_j Q_{ik}) , \\ &\varepsilon_{ijk}(\nabla_i Q_{js}) Q_{ks} . \end{aligned} \tag{4.11}$$

We employ the usual convention of summing on repeated indices.

With the understanding that indices appearing only once within a squared quantity are also to be summed on after the squaring has been done, we can simplify the first line of Eq. (4.11) to

$$(\nabla_i Q_{jk})^2 . \tag{4.12}$$

With the additional understanding that indices appearing twice within a squared quantity are to be summed on before the squaring is done, we can also simplify the second line of Eq. (4.11) to

$$(\nabla_i Q_{ij})^2 . \tag{4.13}$$

The third line of Eq. (4.11) differs from the second by a total derivative and therefore, when integrated, gives a contribution to the total free energy differing only by a surface term. Since we shall be concerned only with the limit in which surface energies are negligible compared with bulk effects, this term need not be separately considered.

The final line in Eq. (4.11) contains the antisymmetric third-rank tensor ε_{ijk}, which changes sign under spatial inversions; the term is therefore allowed only in *chiral* nematics.

It is convenient to express the gradient free-energy density as a linear combination of these three independent terms of the form

$$f_{\text{grad}} = \tfrac{1}{4}K_1[(\nabla\times\mathbf{Q})_{ij} + 2q_0 Q_{ij}]^2 + \tfrac{1}{4}K_0[(\nabla\cdot\mathbf{Q})_i]^2 , \tag{4.14}$$

where the tensor $\nabla\times\mathbf{Q}$ and vector $\nabla\cdot\mathbf{Q}$ are defined by

$$(\nabla\times\mathbf{Q})_{ij} = \varepsilon_{ist}\nabla_s Q_{tj}, \quad (\nabla\cdot\mathbf{Q})_i = \nabla_j Q_{ji} . \tag{4.15}$$

The terms in gradients in Eq. (4.14) are identical (except for a harmless integration by parts) to the three independent terms described above. The corresponding three independent parameters are taken to be two elastic constants, K_1 and K_0, and an inverse length q_0, named in anticipation of its identification as the wave vector in Eq. (2.1) that characterizes the helical phase of the chiral nematics. To ensure that the gradient energy is non-negative we have also added to f_{grad} the additional gradient-independent piece $K_1 q_0^2 \text{tr}(Q^2)$—i.e, we have found it convenient to incorporate into f_{grad} a piece borrowed from f_{bulk}.

In the absence of more accurate information about the relative values of K_1 and K_0, it is sometimes convenient to investigate the specific model in which $K_0 = K_1$. This simplification is known as the "one-constant approximation."

If K_1 and K_0 are both positive, then f_{grad} is evidently non-negative and assumes its minimum value (zero) for any order parameter that satisfies the linear condition

$$\nabla\times\mathbf{Q} = -2q_0\mathbf{Q} , \tag{4.16}$$

since the vanishing of $\nabla\cdot\mathbf{Q}$ is a consequence of Eq. (4.16). Since (4.16) is linear, linear combinations of solutions are also solutions; this underlies the method of constructing blue phase structures in the high-chirality limit.

In Appendix C we show that stability of the full (gradient plus bulk) free energy requires K_1 to be positive and K_0 to be greater than $-\frac{1}{2}K_1$. We also show that throughout this range of stability the gradient free energy remains non-negative and minimized by order parameters that satisfy Eq. (4.16).

The condition (4.16) that the order parameter $\mathbf{Q}$ minimize the gradient energy (4.14) is uniquely satisfied (to within an overall rotation) by a structure proportional to

$$\begin{aligned} Q_{ij}^{\text{bh}} &= \text{Re}[(\mathbf{x}-i\mathbf{y})_i(\mathbf{x}-i\mathbf{y})_j e^{2iq_0 z}] \\ &= (\hat{x}_i\hat{x}_j - \hat{y}_i\hat{y}_j)\cos(2q_0 z) \\ &\quad + (\hat{x}_i\hat{y}_j + \hat{y}_i\hat{x}_j)\sin(2q_0 z) , \end{aligned} \tag{4.17}$$

or by linear combinations of such structures. Note that the form (4.17) is identical to the dielectric anisotropy (4.4) in the uniaxial helical phase *except* for the absence of the $k=0$ Fourier component. Like (4.4), Q^{bh} is constant in directions perpendicular to the pitch axis $\mathbf{z}$ and rotates uniformly along $\mathbf{z}$. Point by point, however, it is strikingly different. The eigenvalues of $\mathbf{Q}^{\text{bh}}$ are 1, 0, and -1. It is thus, in a sense, maximally biaxial: while uniaxial structures have two degenerate eigenvalues and maximize $|\text{tr}(\mathbf{Q}^3)|$ for given $\text{tr}(\mathbf{Q}^2)$, the structure $\mathbf{Q}^{\text{bh}}$ minimizes it. Because of this, a single term of the form (4.17) does not take full advantage of the possibilities for minimizing the bulk free energy, as we shall note in some detail in Sec. VI. We refer to the order parameter (4.17) as the "biaxial helix."

E. The full free energy: Some elementary features

To determine the equilibrium structure of a chiral nematic we must minimize the full free energy F, which is the volume integral of the free-energy density

$$\begin{aligned} f &= f_{\text{grad}} + f_{\text{bulk}} \\ &= \tfrac{1}{4}K_1[(\nabla\times\mathbf{Q})_{ij} + 2q_0 Q_{ij}]^2 + \tfrac{1}{4}K_0[(\nabla\cdot\mathbf{Q})_i]^2 \\ &\quad + c\ \text{tr}(\mathbf{Q}^2) - \sqrt{6}b\ \text{tr}(\mathbf{Q}^3) + a[\text{tr}(\mathbf{Q}^2)]^2 . \end{aligned} \tag{4.18}$$

Because the gradient and bulk free energies favor different strucutres, this minimization problem has not been solved. The body of theoretical literature on possible equilibrium blue phase structures offers testimony to its intractability. Two simple solvable limiting cases are worth noting at the outset, however.[14]

1. The nematic limit: Infinite pitch

When $q_0=0$ the gradient free energy (4.14) attains its minimum value of 0 for any constant tensor $\mathbf{Q}$, regardless of its form. Minimizing the bulk free energy (4.5) then requires that form to be uniaxial, and we recover the equilibrium structure for the ordinary (nonchiral) nematic: a homogeneous uniaxial structure.

2. The second-order limit: Vanishing cubic term

When $b=0$ the bulk free energy depends only on $\mathrm{tr}(\mathbf{Q}^2)$, and it is minimized by any $\mathbf{Q}$ with the appropriate value of $\mathrm{tr}(\mathbf{Q}^2)$, regardless of the value of $\mathrm{tr}(\mathbf{Q}^3)$. If $f_{\rm bulk}$ is to be minimized everywhere, then $\mathrm{tr}(\mathbf{Q}^2)$ must be independent of position. As it happens, although the biaxial helical structure (4.17) that minimizes the gradient energy does depend on position, its square does not:

$$[(\mathbf{Q}^{\rm bh})^2]_{ij}=\lambda^2(\hat{x}_i\hat{x}_j+\hat{y}_i\hat{y}_j)\ . \tag{4.19}$$

Thus $\mathrm{tr}(\mathbf{Q}^{\rm bh})^2=2\lambda^2$, so that for $b=0$ $\mathbf{Q}^{\rm bh}$ can minimize the bulk as well as the gradient free energy with a suitable choice of the constant amplitude λ.

It seems likely that the equilibrium order parameter is uniquely of this form (to within a rotation) in the $b=0$ case. A competing structure would have to be a linear combination of $\mathbf{Q}^{\rm bh}$ and its rotations (to minimize $f_{\rm grad}$) that continued to have position-independent $\mathrm{tr}(\mathbf{Q}^2)$ (to minimize $f_{\rm bulk}$). Although no such structure is known to us, we are unaware of a proof that none exists.

With the exception of the "curved-space" solution described in Sec. VIII, these extreme cases exhaust what is known precisely about minima of the full free energy.

F. The coherence length

It is useful to define a coherence length ξ characterizing an ordinary ($q_0=0$) nematic at the temperature at which the first-order transition from the isotropic liquid takes place ($c=c_0$). Suppose we force the amplitude of the order parameter to deviate slightly from the value λ_0 that minimizes the free energy:

$$\mathbf{Q}=\frac{\lambda}{\sqrt{6}}\begin{bmatrix}-1&0&0\\0&-1&0\\0&0&2\end{bmatrix},\quad \lambda=\lambda_0+\delta\lambda\ . \tag{4.20}$$

With this definition of λ the value of the bulk free energy (4.5) is simply given by Eq. (4.8). When $c=c_0$ it follows directly from Eq. (4.10) that to leading order in $\delta\lambda$ the cost in bulk free energy is

$$\delta f_{\rm bulk}=(b^2/4a)(\delta\lambda)^2\ . \tag{4.21}$$

The cost in gradient energy [in the one constant approximation, where $f_{\rm grad}$ becomes simply $(\nabla_i Q_{jk})^2$] is

$$\delta f_{\rm grad}=\tfrac{1}{4}K_1(\nabla\delta\lambda)^2\ . \tag{4.22}$$

If $\delta\lambda$ is constrained to be nonzero in a region, its relaxation back to zero will be governed by the condition for minimizing δf,

$$\nabla^2\delta\lambda=\delta\lambda/\xi^2\ , \tag{4.23}$$

where the coherence length ξ is given by

$$\xi=(aK_1/b^2)^{1/2}\ . \tag{4.24}$$

The length ξ provides an important scale in chiral as well as in ordinary nematics. We shall continue to refer to this particular combination of free-energy parameters as the "coherence length" even when q_0 is nonzero (or when K_0 differs from K_1).

G. The full free energy: Dimensionless variables

It is convenient to rescale the quantities appearing in the free energy (4.18) to focus attention on a small number of important dimensionless parameters. We define a dimensionless free-energy density φ, effective temperature τ, order parameter χ, and length scale r' as follows:

$$\begin{aligned}&\varphi=(a^3/b^4)f,\quad \tau=(a/b^2)c\ ,\\&\chi=(a/b)\mathbf{Q},\quad r'=2q_0r\ .\end{aligned} \tag{4.25}$$

This rescaling is singular in the limits $b\to 0$ and $q_0\to 0$. It is therefore unsuitable for describing the two cases discussed above in which the exact free-energy minima are known. Except for these limits, however, the new variables do provide the natural scales of energy density, temperature, and length for a discussion of the blue phases.

In terms of the dimensionless variables of Eq. (4.25), the dimensionless free-energy density becomes

$$\begin{aligned}&\varphi=\varphi_{\rm grad}+\varphi_{\rm bulk}\ ,\\&\varphi_{\rm grad}=\kappa^2\{[(\nabla\times\chi)_{ij}+\chi_{ij}]^2+\eta[(\nabla\cdot\chi)_i]^2\}\ ,\\&\varphi_{\rm bulk}=\tau\,\mathrm{tr}(\chi^2)-\sqrt{6}\,\mathrm{tr}(\chi^3)+[\mathrm{tr}(\chi^2)]^2\ .\end{aligned} \tag{4.26}$$

Here κ is the positive dimensionless parameter given by

$$\kappa=(aK_1q_0^2/b^2)^{1/2}=q_0\xi=2\pi\xi/p_0\ , \tag{4.27}$$

where p_0 is the pitch [Eq. (2.2)], and η is the ratio of the bending energy coefficients,

$$\eta=K_0/K_1\ . \tag{4.28}$$

[14] In Sec. VIII we shall note a curious maneuver whereby the full problem *can* be solved, but in a space with an unphysical geometry.

We adopt the convention that lengths are to be measured in units of $1/2q_0$, which gives r and r' the same numerical values, permitting us to drop the primes. On this length scale the pitch is given by

$$p_0=2\pi/q_0=4\pi(1/2q_0)=4\pi \ . \tag{4.29}$$

The coherence length ξ is typically on the scale of molecular dimensions (10–50 Å), except near a second-order transition, while the pitch p_0 is typically 10^3 to 10^4 Å. Therefore κ will be small, except in chiral nematics with very short pitch and/or near a transition from the isotropic phase that is only weakly first order.

Following Grebel *et al.* (1983a) we call the dimensionless parameter κ the "chirality." The chirality is the crucial dimensionless parameter in a chiral nematic; typical values are roughly in the range 0.01–0.5 (see Appendix D). The Ginzburg-Landau theory gives blue phases for arbitrarily high chirality, all the way down to chirality that is low (but not arbitrarily low). The theoretical description of these phases takes on instructive but very different forms in these two limits. We therefore examine the two cases separately in Secs. VI and VII, returning to what they have in common in Sec. VIII.

Before doing this, however, we must examine more carefully the helical phase, which is always the stable equilibrium phase favored by the free energy (4.26) sufficiently far below the transition from the isotropic liquid.

V. THE HELICAL PHASE

The uniaxial helical structure (4.4), which is generally taken to be the order parameter in the helical phase of chiral nematics, is never in fact a minimum of the full free energy. We now examine why it fails to give a minimum, and construct the correct helical phase order parameter. In doing this we shall be led rather naturally to the kinds of structures that have been proposed as models for the blue phase order parameters.

A. Instability of the uniaxial helix

We remarked in Sec. I that there was no symmetry-dictated reason why a uniaxial liquid with anisotropic spatial inhomogeneity should not acquire a degree of biaxiality. The uniaxial helical structure is, in fact, unstable against becoming biaxial, and is therefore not a stationary point of the full free energy. This can be seen as follows.

Since $\chi^{\rm uh}$ does minimize the bulk free energy, to linear order the change in free energy induced by a small change $\delta\chi$ can only come from the gradient free energy. Now the structure (4.4) of the uniaxial helical order parameter is a superposition of a position-independent matrix χ^0 and the structure $\chi^{\rm bh}$ that satisfies the stationary condition (4.16) for the gradient free energy (in rescaled form, $\nabla\times\chi=-\chi$). Because χ^0, being constant, has zero curl and divergence, it follows directly from the form (4.26) of the gradient free energy that if $\chi=\chi^{\rm uh}+\delta\chi$, then to linear order in $\delta\chi$,

$$\delta\int\varphi\, d^3r=\delta\int\varphi_{\rm grad}d^3r=2\kappa^2\int{\rm tr}(\chi^0\delta\chi)d^3r \ . \tag{5.1}$$

This can be made negative by choosing $\delta\chi\propto-\chi^0$. Thus $\chi^{\rm uh}$ has a linear instability against a decrease in the relative weight given to the position-independent matrix χ^0 in the superposition (4.4).

The source of this instability is easily understood. In the helical phase the neighborhood of any point is not isotropic in the plane perpendicular to the director $\mathbf{n}$, since $\mathbf{n}$ twists about the pitch axis as one moves from the point in that direction, while remaining unchanged in the perpendicular direction. There is therefore nothing in the symmetry of the local configuration to support the uniaxiality of χ, and relaxation of the order parameter to acquire at least a small degree of biaxiality should be the normal state of affairs.

B. The general helical order parameter

To assess the extent of this instability toward biaxiality, it is useful to consider the family of order parameters given by assigning arbitrary weights to the constant and biaxial components of $\chi^{\rm uh}$:

$$\chi^{(\theta)}=\sqrt{6}\lambda\cos\theta\begin{bmatrix}-\frac{1}{6}&0&0\\0&-\frac{1}{6}&0\\0&0&\frac{1}{3}\end{bmatrix}+(\lambda/\sqrt{2})\sin\theta\begin{bmatrix}\cos z&\sin z&0\\\sin z&-\cos z&0\\0&0&0\end{bmatrix} . \tag{5.2}$$

With $\theta=2\pi/3$, $\chi^{(\theta)}$ has the form of the uniaxial helical order parameter (4.4) (with $\gamma=\sqrt{3/2}\lambda$). The linear instability causes θ to drop below $2\pi/3$. When θ reaches $\pi/2$, then $\chi^{(\theta)}$ becomes proportional to the biaxial helical order parameter (4.17) favored by the gradient energy alone.

With the order parameter (5.2) the total free-energy density (4.26) takes on the form

$$\langle\varphi\rangle=(\tfrac{1}{2}\kappa^2+\tau)\lambda^2+\lambda^4-\lambda^3\cos3\theta+\tfrac{1}{2}\kappa^2\lambda^2\cos2\theta \ . \tag{5.3}$$

Here and elsewhere we shall use angular brackets to denote an average over the entire volume of the liquid:

$$\langle\varphi\rangle\equiv\frac{1}{V}\int_V\varphi\, d^3r \ . \tag{5.4}$$

The last two terms in Eq. (5.3) explicitly display the competition between the biaxial form ($\cos3\theta=0$, $\cos2\theta=-1$) favored by the gradient free energy and the uniaxial form ($\cos3\theta=1$, $\cos2\theta=-\frac{1}{2}$) favored by the cubic term in the bulk free energy.

If θ and λ are chosen to minimize Eq. (5.3), then the order parameter (5.2) can be shown to make the full free

energy (4.26) stationary against arbitrary traceless symmetric variations $\delta\chi$. (We defer this demonstration and other mathematical distractions to Sec. V.C.) Thus allowing the helix to become biaxial completely repairs the linear instability of the uniaxial helix.

The nature of this new helical stationary point depends on the value of the dimensionless parameter $\kappa=q_0\xi$ defined in Eq. (4.27). Some of the most important features of the minimum of (5.3) can be given simple analytical expressions. We give the details of the minimization in Sec. V.C, and present here only the results.

When $\kappa<\frac{3}{2}$ the transition to the helical phase is first order. The transition temperature is

$$\tau_c=\tfrac{1}{8}[1-4\kappa^2+(1+\tfrac{4}{3}\kappa^2)^{3/2}] , \tag{5.5}$$

and the value of the parameter θ at the transition is given by

$$\cos2\theta_c=-\tfrac{1}{2}(1+\tfrac{4}{3}\kappa^2)^{1/2} . \tag{5.6}$$

When $\kappa=0$ we recover the behavior of an ordinary nematic: a first-order transition at $\tau_c=\frac{1}{4}$ to a strictly uniaxial phase ($\cos2\theta=-\frac{1}{2}$, $\cos3\theta=1$). The deviation of $\cos3\theta=\sqrt{6}\,\mathrm{tr}\chi^3/(\mathrm{tr}\chi^2)^{3/2}$ from unity is a direct measure of the extent to which χ deviates from uniaxiality (see Sec. IV.C). For small κ it follows from Eq. (5.6) that, to leading order in κ,

$$\cos3\theta_c=1-\tfrac{1}{6}\kappa^4+O(\kappa^6) , \tag{5.7}$$

so that deviations from uniaxiality are, by this measure, only of fourth order in κ (and with a rather small coefficient). As a result, even when κ is as large as 0.5, we still have $\cos3\theta_c=0.99$, and even $\kappa=0.75$ only reduces $\cos3\theta_c$ to 0.95.

Thus for κ significantly less than unity the order parameter is predominately uniaxial, and the first-order transition is to an essentially uniaxial helical phase, with just a trace of biaxiality induced by the twist of the director. This is consistent with the fact that chiral nematics of large pitch (small κ) enter an essentially uniaxial helical phase directly from the isotropic liquid, without displaying blue phases.

As κ grows toward $\frac{3}{2}$ the transition temperature τ_c drops monotonically, and the value of $\cos2\theta_c$ drops further below the uniaxial value $-\frac{1}{2}$, reaching the value -1 ($\cos3\theta_c=0$) when κ reaches $\frac{3}{2}$. At this point τ_c reaches zero, the transition changes from first to second order, and at the transition the order parameter is a pure biaxial helix. The transition remains second order for κ greater than $\frac{3}{2}$ even though there is a nonzero cubic term in the free energy (Brazovskii and Dmitriev, 1975; Hornreich and Shtrikman, 1979, 1980a, 1980b; Kleinert and Maki, 1981; Grebel *et al.*, 1983a).

Thus the character of the helical phase depends critically on the value of κ. There will be a first-order transition to an order parameter that is very close to the conventional uniaxial helix, provided κ is small compared with $\frac{3}{2}$—i.e., provided the coherence length is small compared with the pitch. Should, however, the coherence length be comparable to the pitch then the degree of biaxiality in the helical phase order parameter can be significant. Above the critical value of $\kappa=\frac{3}{2}$ the transition changes from first to second order, and at the transition the order parameter is the biaxial helix, Eq. (4.17). We shall show in Sec. VI, however, that when κ exceeds $\frac{3}{2}$ this transition to a biaxial helix—the most stable form of the helical phase—has already been overtaken by transitions to phases with much more intricate structures. These are the blue phases.

We conclude this section by filling in some of the omitted mathematical details underlying the above conclusions. Readers interested only in the conclusions themselves can go directly to Sec. VI.

C. Some mathematical details

1. Minimization of the free energy for the helical phase

We parametrize the amplitude λ of the order parameter in the free energy (5.3) by

$$\lambda=\tfrac{1}{6}\kappa^2\sinh\alpha . \tag{5.8}$$

It is easy to show that for any α, the free energy is minimized by taking θ to satisfy

$$\cos\theta=-\tfrac{1}{2}\tanh\tfrac{1}{2}\alpha \tag{5.9}$$

or, equivalently,

$$\cos2\theta=-\tfrac{1}{2}(1+\mathrm{sech}^2\tfrac{1}{2}\alpha) . \tag{5.10}$$

When θ has this minimizing value we express the free energy in terms of

$$u\equiv\sinh^2\tfrac{1}{2}\alpha . \tag{5.11}$$

The result is

$$\varphi=\tfrac{1}{9}\kappa^6[(\tau/\kappa^2)u+(\tau/\kappa^2+\tfrac{1}{9}\kappa^2-\tfrac{1}{4})u^2 +(\tfrac{2}{9}\kappa^2-\tfrac{1}{3})u^3+\tfrac{1}{9}\kappa^2u^4] . \tag{5.12}$$

When κ exceeds $\frac{3}{2}$ the free energy φ is clearly non-negative for positive τ, but can become negative for negative τ and small enough u. There is therefore a second-order transition at $\tau=0$. Since u is zero at the transition, α is also zero, and hence (5.10) gives the condition $\cos2\theta=-1$ that characterizes the biaxial helix.

To explore the first-order transition when κ is less than $\frac{3}{2}$, note that at such a transition there will be a nonzero value u_c at which φ and its first derivative vanish. As it happens, φ' has the simple factorization

$$\varphi'=\tfrac{1}{9}\kappa^6(u+\tfrac{1}{2})[\tfrac{4}{9}\kappa^2u^2+(\tfrac{4}{9}\kappa^2-1)u+2\tau/\kappa^2] . \tag{5.13}$$

Since u is non-negative, the vanishing of φ' gives a quadratic equation for u_c. A second quadratic equation

comes from the fact that, if φ and φ' both vanish at u_c, so does $(\varphi/u)'$. Thus u_c satisfies the pair of quadratic equations

$$\begin{aligned} &\tfrac{4}{9}\kappa^2 u_c^2+(\tfrac{4}{9}\kappa^2-1)u_c+2\tau/\kappa^2=0\ , \\ &\tfrac{1}{3}\kappa^2 u_c^2+(\tfrac{4}{9}\kappa^2-\tfrac{2}{3})u_c+(\tau/\kappa^2+\tfrac{1}{9}\kappa^2-\tfrac{1}{4})=0\ . \end{aligned} \tag{5.14}$$

Eliminating the quadratic term between these two gives

$$u_c=18\tau/\kappa^2-4\kappa^2+\frac{9}{4\kappa^2+3}\ . \tag{5.15}$$

If this value of u_c is substituted back into either of the equations in (5.14), we get the equation for the first-order phase boundary given in (5.5). Using this relation to eliminate τ from Eq. (5.15) gives

$$u_c=\frac{3}{4\kappa^2}[1-\tfrac{4}{3}\kappa^2+(1+\tfrac{4}{3}\kappa^2)^{1/2}]\ . \tag{5.16}$$

With this result, Eqs. (5.9) and (5.11) then lead directly to the expression (5.6) for $\cos 2\theta_c$ in terms of κ.

2. Stationarity of the general helical order parameter

The general helical order parameter $\chi^{(\theta)}$ makes the free energy stationary over all linear combinations of

$$\chi^c=\begin{bmatrix} -1 & 0 & 0 \\ 0 & -1 & 0 \\ 0 & 0 & 2 \end{bmatrix} \quad \text{and} \quad \chi^{\rm bh}=\begin{bmatrix} \cos z & \sin z & 0 \\ \sin z & -\cos z & 0 \\ 0 & 0 & 0 \end{bmatrix}\ . \tag{5.17}$$

Since the stationary condition against general variations $\delta\chi$ is linear in $\delta\chi$, it is easy to show that for $\chi^{(\theta)}$ to satisfy the general stationary condition, it is enough for it to be stationary against traceless $\delta\chi$ that are orthogonal to the space of helical order parameters in the sense that they satisfy

$$\langle \mathrm{tr}(\chi^c\delta\chi)\rangle=\langle \mathrm{tr}(\chi^{\rm bh}\delta\chi)\rangle=0\ . \tag{5.18}$$

Computing the general stationary condition from the explicit form (4.26) of the free energy φ, one easily establishes [as a direct consequence of the fact that $\nabla\times\chi^{(\theta)}$, $\nabla\cdot\chi^{(\theta)}$, and $\chi^{(\theta)2}$ can all be expressed as linear combinations of χ^c, $\chi^{\rm bh}$, and the unit matrix] that when χ is a linear combination of the two forms (5.17), every term in the general stationary condition is proportional either to $\langle \mathrm{tr}(\delta\chi)\rangle$, which vanishes, or to one of the two expressions required by Eq. (5.18) to vanish.

VI. BLUE PHASES: THE HIGH-CHIRALITY LIMIT

If the stationary points given by the helical-phase order parameter (5.2) were the true minima of the free energy, then chiral nematics would behave as follows.

(1) Well below the transition from the isotropic phase the order parameter would be essentially the uniaxial helix that minimizes the bulk free energy, modified by a slight degree of biaxiality induced by the local anisotropy associated with the twisting of the director.

As the temperature rose two cases would be distinguished depending on the value of the chirality κ.

(2a) $\kappa<\frac{3}{2}$. Helical ordering would disappear through a first-order transition back to the isotropic liquid. When the chirality κ was significantly less than one, the degree of biaxiality would still be slight, even at the transition. At larger κ, biaxial corrections to the purely uniaxial helix would become more pronounced as the transition temperature was approached.

(2b) $\kappa>\frac{3}{2}$. Helical ordering would disappear through a second-order transition back to the isotropic liquid. At the transition the order parameter would have the "maximally biaxial" form $\mathbf{Q}^{\rm bh}$ that minimizes the gradient free energy [Eq. (4.17) or (5.17)].

The behavior described in (1) is in fact the observed behavior of chiral nematics. The helical phase is always stable more than a few degrees below the transition from the isotropic liquid (unless, of course, it is preempted by phases with positional ordering, such as smectic or crystalline phases).

The behavior described in (2a) is also the observed behavior of chiral nematics with sufficiently large pitch (low chirality). These liquids undergo first-order transitions directly from the isotropic liquid to the helical phase without passing through any other intermediate structures.

Type (2b) behavior, characteristic of helical phases of short pitch (high chirality), is never observed. When the pitch is short the second-order transition to the ordered phase is always replaced by a series of first-order transitions to a set of intermediate phases—blue phases—that intervene between the isotropic and helical phases. As we shall see, the chirality κ does not have to be very high (or even larger than unity) for this to take place. Two rather different descriptions of blue phase ordering have been put forth, which are best viewed as the natural points of view to take when the chirality is high or low.

(i) The high-chirality behavior is given by a model of the blue phases developed in detail by Hornreich and Shtrikman (1979, 1980a, 1980b, 1981b, 1981c), following a line of attack first developed by Brazovskii and Dmitriev (1975). (See also Grebel, Hornreich, and Shtrikman, 1983a, 1984; Kleinert and Maki, 1981; Wright and Mermin, 1985.) The blue phase structures developed in this model can be viewed as expansions about the relatively simple blue phase order parameters that can be derived in the limit of infinite chirality.

(ii) The low-chirality behavior is described by a model put forth by Meiboom, Sethna, Anderson, and Brinkman (1981), subsequently developed by Meiboom, Sammon, and Brinkman (1983), and Meiboom, Sammon, and Berreman (1983). Although there exists no expansion about zero chirality (where there are no blue phases), their model is best characterized as a low-chirality theory, with the proviso that "low" means low enough for the helical phase to be only weakly biaxial, as is the

case even when κ is close to unity, as noted in Sec. IV.

We describe the high-chirality approach in this section and the low-chirality in the next. We stress at the outset that these are not two competing theories of blue phases, but two methods for extracting blue phase structures from a common theoretical starting point (such as the Ginzburg-Landau theory of Sec. IV), depending on whether or not κ is large. In Sec. VIII we note that although the structures emerging from the two approaches appear to be quite different, upon more careful examination one can find features of each present in the other, in just the forms one would expect in view of the different sizes of κ.

A. General features of the high-chirality limit

In the limit of large κ the free energy (4.26) is dominated by the gradient free energy. As discussed in Sec. IV, the gradient free energy is non-negative and is given its minimum value of zero by the biaxial helix (4.17) or by any linear combination of biaxial helical order parameters differing from one another by translations and/or rotations. This high degree of degeneracy follows from the linearity of the minimization condition (4.16), which in terms of the dimensionless quantities (4.25) has the form

$$\nabla\times\chi=-\chi\ . \tag{6.1}$$

The role of the bulk free energy in the large-κ limit is simply to reduce this degeneracy by selecting the most favorable such linear combination. As $\kappa\rightarrow\infty$, the problem therefore reduces to that of minimizing the bulk free energy in the space of order parameters that are linear combinations of biaxial helices. In this limit the helical-phase order parameter becomes a single biaxial helix. Thus as $\kappa\rightarrow\infty$ the question of whether the chiral nematic can support phases other than the helical phase reduces to the question of whether linear combinations of the biaxial helical order parameter can have lower free energy than a single biaxial helix.

One sees immediately that, for a sufficiently small positive reduced temperature τ, a single biaxial helix cannot in fact be the best choice. This follows directly from the form (5.17) of the biaxial helical order parameter, which implies that $\mathrm{tr}(\chi^{\mathrm{bh}})^3=0$. As a result the bulk free energy (4.26) for positive τ is positive for a biaxial helix of nonzero amplitude. On the other hand, any linear combination of biaxial helices with a nonzero cubic bulk free energy will, with a suitable choice of amplitude, yield a negative free energy for small enough positive τ, since (a) with an amplitude of appropriate sign the cubic term will be negative, (b) with an amplitude sufficiently small the cubic term will dominate the quartic, and (c) with a positive value of τ sufficiently small the cubic term will also dominate the quadratic.

Hence any linear combination of biaxial helices with a nonvanishing cubic bulk free energy gives an order parameter with lower free energy than the isotropic or helical phases for sufficiently small positive τ, and it is among these that we must look for candidates for the blue phases in the high-chirality limit. Before embarking on the search, we note two general points.

(1) Because the gradient energy of a linear combination of biaxial helices vanishes, the argument that there are linear combinations with negative free energy for sufficiently small positive τ is independent of the value of the coefficient κ multiplying the gradient free energy. But we found in Sec. V that when κ exceeded $\frac{3}{2}$, no helical phase could have negative free energy for positive τ, whatever the degree of biaxiality. This already establishes that nonhelical phases will be stable for positive τ, not only as $\kappa\rightarrow\infty$ but for any κ greater than $\frac{3}{2}$. (We shall shortly push the critical value of κ lower than this.)

(2) As the temperature drops and τ becomes more and more negative, the order parameter grows, and eventually the quartic term becomes the dominant term in the bulk free energy. The Schwarz inequality

$$\langle(\mathrm{tr}\chi^2)^2\rangle\geq(\langle\mathrm{tr}\chi^2\rangle)^2 \tag{6.2}$$

gives a lower bound for this term. The quartic free energy can achieve this lower bound with a single biaxial helix, which has a position-independent value of $\mathrm{tr}\chi^2$. The helical phase is therefore the favored form at sufficiently low temperatures in the high-chirality limit.[15] Thus the high-chirality limit provides in a very simple way for the existence of blue phases (phases with a nonvanishing cubic invariant which are therefore not of simple helical symmetry) between the high-temperature isotropic phase and a stable low-temperature helical phase.

B. High-chirality order parameters: O^5, O^8, and hexagonal

In the high-chirality limit the nonhelical phases existing in the neighborhood of the transition will have an order parameter given by a linear combination of biaxial helices of the form [Eq. (4.17)]

$$\chi^{\mathrm{bh}}_{ij}=\mathrm{Re}[(\mathbf{a}-i\mathbf{b})_i(\mathbf{a}-i\mathbf{b})_j e^{i\mathbf{c}\cdot\mathbf{r}}]\ , \tag{6.3}$$

where **a**, **b**, and **c** are any triad of orthonormal vectors obtained by a (proper) rotation of **x**, **y**, and **z**.

Suppose we have found a linear combination of biaxial helices that has a nonzero value of $\langle\mathrm{tr}\chi^3\rangle$ (and is therefore stable for some positive τ). It is useful to scale out the amplitude dependence of the cubic term by expressing it in terms of the value of the quadratic term

$$\gamma^2\equiv\langle\mathrm{tr}\chi^2\rangle \tag{6.4}$$

and defining a cubic invariant β by

$$\beta\gamma^3/\sqrt{6}\equiv\langle\mathrm{tr}\chi^3\rangle\ . \tag{6.5}$$

[15] In the infinite-κ limit, the helical structure will remain biaxial for all τ below the transition. For any finite κ the order parameter will, of course, become predominantly uniaxial for sufficiently negative τ, as discussed in Sec. V.

The $\sqrt{6}$ appears in Eq. (6.5) so that if χ were independent of position the largest possible value of $\langle \mathrm{tr}\chi^3 \rangle$ for given $\langle \mathrm{tr}\chi^2 \rangle$ would be given by $\beta=1$ [see Eq. (4.7)]. Since this maximum value is only achieved by a uniaxial χ, the closeness of the cubic invariant β to unity can be viewed as a measure of the extent to which the tensor χ succeeds in attaining the uniaxial form favored by the bulk free energy.

In a similar way, we define a quartic invariant α by writing the quartic term as

$$\alpha\gamma^4 \equiv \langle (\mathrm{tr}\chi^2)^2 \rangle \ , \tag{6.6}$$

and note that α attains its minimum value of unity for a single biaxial helix, so the extent to which α exceeds unity is a measure of the damage done to the quartic free energy by forming a linear combination of biaxial helices.

The values of α and β depend on the particular linear combination of biaxial helices making up the order parameter χ. Given a particular form, the free energy then depends only on the overall amplitude γ:

$$\langle \varphi \rangle = \langle \varphi \rangle_{\mathrm{bulk}} = \tau\gamma^2 - \beta\gamma^3 + \alpha\gamma^4 \ . \tag{6.7}$$

This can first become negative for some γ when τ drops below the critical value:

$$\tau_c = \beta^2/4\alpha \ . \tag{6.8}$$

The form of the order parameter immediately below the transition from the isotropic phase is therefore the one with the highest value of β^2/α.

A superposition χ of biaxial helical order parameters χ^{bh} of the form (6.3) for many different orthonormal triads **a**, **b**, and **c** will give for $\mathrm{tr}\chi^3$ a sum of terms with spatial dependence proportional to $e^{i(\mathbf{c}+\mathbf{c}'+\mathbf{c}'')\cdot\mathbf{r}}$, where **c**, **c**′, and **c**″ are among the set of wave vectors in the superposition. The spatial average of the cubic term, and hence the cubic invariant β, can only be nonzero if the set of wave vectors appearing in the superposition contains at least one group of three that add up to zero. To maximize the transition temperature τ_c we would therefore like a superposition composed of many trios of wave vectors that sum to zero (to maximize β) but that does not give an excessively large quartic invariant α.

As pointed out by Baym, Bethe, and Pethick (1971) and subsequently rediscovered by Alexander and McTague (1978), an extremely efficient way to achieve many such trios of unit wave vectors is to take a linear combination of twelve $\langle 110 \rangle$ directions, since there are eight distinct trios summing to zero, given by the eight ways of assigning $u=\pm1$, $v=\pm1$, $w=\pm1$ (see Fig. 12) to the trio

$$\frac{1}{\sqrt{2}}(u,v,0), \quad \frac{1}{\sqrt{2}}(-u,0,w), \quad \frac{1}{\sqrt{2}}(0,-v,-w) \ . \tag{6.9}$$

These twelve unit wave vectors point along the twelve nearest-neighbor directions of a face-centered-cubic lattice with conventional cubic cell of side $\sqrt{2}$. The real space structure therefore has the translational symmetry

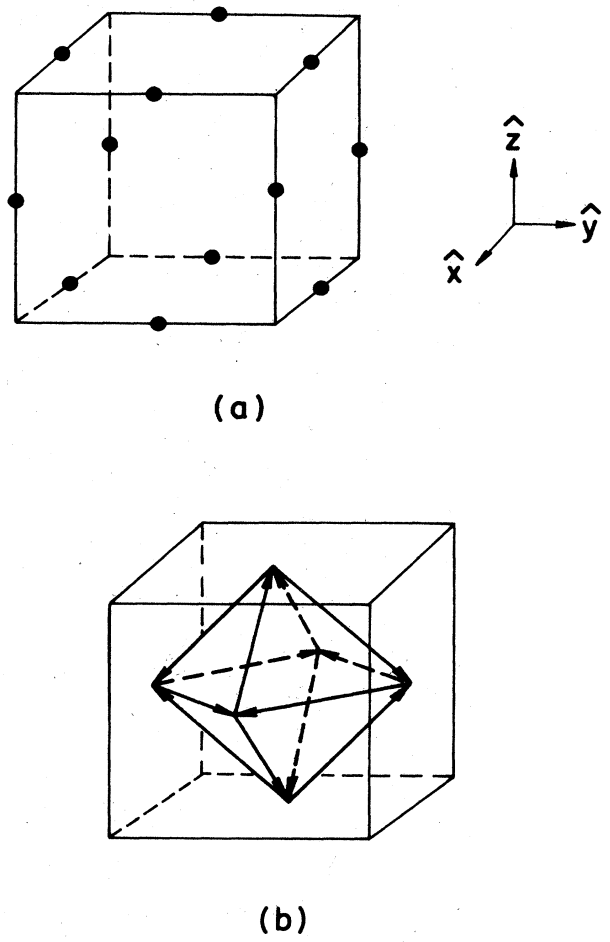

FIG. 12. (a) The set of $\langle 110 \rangle$ wave vectors that generate the bcc O^5 and O^8 structures. (b) These vectors form eight distinct trios that sum to zero, which can contribute to the cubic term in the free energy.

of a body-centered cubic lattice with conventional cubic cell of side $a=4\pi/\sqrt{2}$ (or $a=p_0/\sqrt{2}$ in dimensional units, where $p_0=2\pi/q_0$ is the pitch). Minimizing the bulk free energy over a linear combination of twelve such biaxial helices yields two different sets of amplitudes and phases, both of which give the resulting structure cubic point group symmetry. These two order parameters have the bcc space groups[16] $O^5(I432)$ and $O^8(I4_132)$. We give a detailed description of these two cubic order parameters in the remainder of this section, after remarking on the roles they play in the high-chirality limit of the theory.

The O^5 structure has the largest value of $\tau_c=\beta^2/4\alpha$ of any linear combination of biaxial helices anybody has yet proposed and is believed (though this has not been prov-

[16]For an introduction to space-group notation, see footnote 7 in Sec. III.

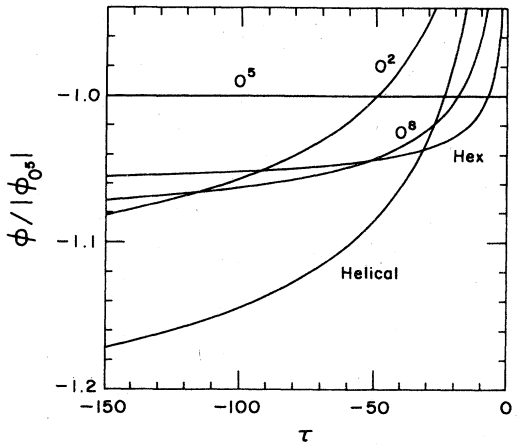

FIG. 13. A plot of the free energies of the O^2, O^5, and O^8, hexagonal, and helical structures for negative τ in the high-chirality limit. Energies are normalized to the magnitude of the energy of the O^5 structure. Values of the transition temperatures are given in Table IV.

en) to give the true form of the ordered state into which the isotropic liquid first condenses in the high-chirality limit. As τ drops below τ_c, however (but before the helical phase has acquired a lower energy than the O^5 structure), the free energy of the O^8 structure drops below that of the O^5. Only at still lower values of τ does the free energy of the helical phase finally become lower than the free energy of either of these cubic phases.

Thus within the restricted family of order parameters with cubic symmetry, the high-chirality limit provides a simple model of two distinct blue phases intervening between the isotropic and helical phases. The O^8 structure, however, is never stable in this limit. With six coplanar wave vectors that are 60° apart one can build a structure with hexagonal symmetry that has a lower free energy than the O^8 structure throughout the region in which the O^8 structure is favored over the O^5. This hexagonal structure remains lower than O^8 throughout the range in which the O^8 structure is lower than the helical phase, eventually itself losing to the helix at still lower temperatures (see Fig. 13).

Although it is never stable in the high-chirality limit, the O^8 structure is still of considerable interest since, starting from both the high and the low chirality limits, theoretical evidence has been presented in favor of a structure with O^8 symmetry at physically accessible values of the chirality (and no physical blue phase structures with O^5 symmetry have been found). We therefore describe all three of these structures below, indicating some of the details that underlie the results we have just described.

C. Structure and energetics of the high-chirality order parameters

The O^5 and O^8 structures are superpositions of twelve terms with unit wave vectors along the twelve [110] directions:

$$\chi=\frac{1}{\sqrt{12}}\sum\chi^{(n)}\ , \tag{6.10}$$

where

$$\chi^{(n)}_{ij}=\tfrac{1}{2}\zeta_n(\mathbf{a}^{(n)}-i\mathbf{b}^{(n)})_i(\mathbf{a}^{(n)}-i\mathbf{b}^{(n)})_j e^{i\mathbf{c}^{(n)}\cdot\mathbf{r}}\ . \tag{6.11}$$

The orthornormal triads consisting of the vectors

$$\mathbf{c}^{(n)},\ \mathbf{a}^{(n)},\ \text{and}\ \mathbf{b}^{(n)}=\mathbf{c}^{(n)}\times\mathbf{a}^{(n)} \tag{6.12}$$

are given in Table II.

The ζ_n are complex numbers characterized by a phase and a real amplitude. Although all amplitudes are the same in the cubic structures, we allow for the possibility of amplitude variation because this permits the properties for the hexagonal structure to be extracted from the same general expressions. Reality of the order parameter χ requires that

$$\zeta_n^*=\zeta_{n+6},\quad n=1,\ldots,6\ . \tag{6.13}$$

The order parameter specified in this way yields the following values for the bulk free-energy terms [Eqs. (6.4)–(6.6)]:

$$\gamma^2=\langle \mathrm{tr}\chi^2\rangle=\tfrac{1}{6}\sum_{n=1}^{6}|\zeta_n|^2\ , \tag{6.14}$$

$$\beta\gamma^3=\sqrt{6}\langle \mathrm{tr}\chi^3\rangle=\frac{\sqrt{2}}{128}\mathrm{Re}(23+5\sqrt{8}i)(\zeta_4\zeta_5\zeta_6+\zeta_2\zeta_3^*\zeta_4^*+\zeta_1^*\zeta_3\zeta_5^*+\zeta_1\zeta_2^*\zeta_6^*)\ , \tag{6.15}$$

$$\alpha\gamma^4=\langle(\mathrm{tr}\chi^2)^2\rangle=\gamma^4+\frac{1}{2304}\left\{41\sum_{m=1}^{6}\sum_{n<m}|\zeta_m|^2|\zeta_n|^2-25(|\zeta_4|^2|\zeta_1|^2+|\zeta_5|^2|\zeta_2|^2+|\zeta_6|^2|\zeta_3|^2)\right.$$
$$\left.+50\,\mathrm{Re}(\zeta_4\zeta_5\zeta_1\zeta_2^*+\zeta_6\zeta_4\zeta_3\zeta_1^*+\zeta_5\zeta_6\zeta_2\zeta_3^*)\right\}\ . \tag{6.16}$$

To construct structures with cubic symmetry we give all the ζ_n the same modulus:

$$|\zeta_n|=\gamma \tag{6.17}$$

[where the value of the modulus is set by Eq. (6.14)]. As we show in Appendix E, the cubic invariant β achieves its maximum when the phases of all the ζ_n are zero. The resulting order parameter (as we shall see below) has the symmetry of the body-centered-cubic space group $O^5(I432)$. This choice, however, is least favorable for

TABLE II. The vectors used in calculating the O^5 and O^8 order parameters.

n	$a^{(n)}$	$\sqrt{2}c^{(n)}$
1	x	y+z
2	y	z+x
3	z	x+y
4	−x	z−y
5	−y	x−z
6	−z	y−x
$12 \geq n > 6$	$\mathbf{a}^{(n-6)}$	$-\mathbf{c}^{(n-6)}$

the quartic invariant α, which from Eq. (6.16) can be shown to be minimized by taking all the phases to be $\pi/2$. With this choice of phase, the resulting structure has the symmetry of the bcc space group $O^8(I4_132)$. (For graphic representations of the structure of the order parameter in the O^8 structure, see Barbet-Massin and Pieranski, 1985.)

The structure with hexagonal symmetry has values of β and α that are each intermediate between the extremes given by the two cubic structures. In the hexagonal structure ζ_1, ζ_2, and ζ_3 are zero. The phase-dependent quartic terms then vanish, and ζ_4, ζ_5, and ζ_6 can be given the phases $(-1+i\sqrt{8})/3$ that maximize the one surviving cubic term in Eq. (6.15).

In Table III we give the values of the cubic and quartic parameters β and α that Eqs. (6.15) and (6.16) give for these three structures, together with the value of the transition temperature from the isotropic phase, $\tau_c=\beta^2/4\alpha$. We also give the corresponding values for the high-chirality form of the helical phase (which corresponds to taking only a single pair of nonzero ζ's).

Of these three structures, O^5 has the highest transition temperature from the isotropic phase. Although nobody has proven that there is no linear combination of biaxial helices with a higher τ_c than the O^5 structure, none has yet been found, and O^5 is therefore the currently accepted model for the structure of blue phase II in the high-chirality limit.

One can compute the free energy of each of these structures as τ drops below t_c by minimizing the free energy (6.7) with respect to the amplitude γ. The result is

$$\langle\varphi\rangle=-(u^2/4\alpha)\psi(\tau/u)\ , \tag{6.18}$$

where

$$u=9\beta^2/8\alpha \tag{6.19}$$

TABLE III. The values of the cubic and quartic parameters β and α, and the transition temperature τ_c from the isotropic phase for the O^5, O^8, hexagonal, and helical structures.

Structure	β	α	$\tau_c=\beta^2/4\alpha$
Cubic (O^5)	$23\sqrt{2}/32=1.0165$	$\frac{499}{384}=1.2995$	0.198 77
Hexagonal	$\frac{27}{32}=0.843\,15$	$\frac{466}{384}=1.2135$	0.146 66
Cubic (O^8)	$\frac{20}{32}=0.625$	$\frac{449}{384}=1.1693$	0.083 52
Helical	0	1	0

TABLE IV. Transition temperatures between various phases in the high-chirality limit. The phase heading each column is stable over the phase given on the left above the indicated temperature and unstable below that temperature.

	Isotropic	Cubic (O^5)	Hexagonal	Cubic (O^8)
Cubic (O^5)	0.198 8			
Hexagonal	0.146 7	−7.3456		
Cubic (O^8)	0.083 52	−18.606	−52.732	
Helical	0	−23.866	−32.032	−27.829

and

$$\psi(z)=z^2-z+\tfrac{1}{6}[1+(1-4z)^{3/2}]\ . \tag{6.20}$$

The corresponding expression for the high-chirality form of the helical phase is simply

$$\langle\varphi\rangle_{\text{helix}}=-\tfrac{1}{4}\tau^2 \tag{6.21}$$

[the $\alpha\to1,\beta\to0$ limit of Eq. (6.18)].

The free energy of a nonhelical structure characterized by particular values of the invariants β and α rises above that of the helical phase when the free energy (6.18) becomes higher than (6.21). This occurs when the temperature drops below

$$\tau_{\text{helix}}=-(\beta^2/8\alpha)[9\alpha-1+(3\alpha+1)^{3/2}]/(\alpha-1)^2\ . \tag{6.22}$$

Note that if the quartic invariant α is close to the theoretical minimum of unity, then such a phase will be stable over the helical phase for a considerable range of negative τ.

In Table IV we give for the three nonhelical phases the values of the transition temperatures (6.22) to the helical phase, as well as the transition temperatures at which their free energies (6.18) cross. The phase heading each column is stable over the phase given on the left above the indicated temperature, and unstable below that temperature (see Fig. 13).

Pending the discovery of still more favorable linear combinations of biaxial helices, the current theoretical description of the high-chirality limit is therefore as follows.

On lowering the reduced temperature τ from the isotropic phase, at $\tau=0.1988$ there is a transition from the isotropic liquid to a blue phase (BP II) with the body-centered-cubic space group O^5. This remains stable until a temperature $\tau=-7.3456$, where there is a transition to a blue phase (BP I) with planar hexagonal structure. The hexagonal structure remains stable until $\tau=-32.032$, at which point the transition to the ordinary helical phase occurs. If only the two cubic phases are considered, the sequence is an isotropic-to-O^5 transition at $\tau=0.1988$, an O^5-to-O^8 transition at $\tau=-18.606$, and an O^8-to-helical transition at $\tau=-27.829$.

D. Icosahedral models of blue phase III

The only suggestion that has been put forth for a high-chirality model of BP III is that it has the transla-

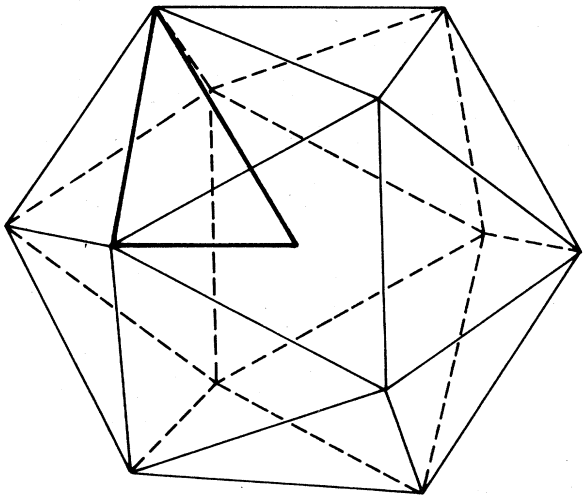

FIG. 14. The wave vectors of the icosahedral edge model. They lie along the light lines in the figure. The additional wave vectors in the edge-vertex model lie along the lines connecting the center of the icosahedron to its 12 vertices. The additional triangles of wave vectors that can be formed as a result of including the vertex vectors consist of two vertex vectors and one edge vector, an example of which is shown in dark lines.

tional symmetry of an icosahedral quasicrystal (Filev, 1986; Hornreich and Shtrikman, 1986a, 1986b, 1987; Rokhsar and Sethna, 1986). The argument for this is that the set of 30 wave vectors directed along 15 twofold axes of an icosahedron contains a great many trios that sum to zero (Fig. 14), giving a cubic bulk free energy that might compete favorably with that of the bcc phases. (This structure is known as an "icosahedral edge model," since the wave vectors are parallel to the edges of an icosahedron.) Calculations analogous to those just described, however, show that the quasicrystalline order parameter always has a higher free energy than one of the above-mentioned crystalline structures in the high-chirality limit.

The bulk energy of this structure can be improved considerably by adding a set of twelve more wave vectors lying along the six fivefold axes of an icosahedron ("vertex" directions), with length chosen to form additional trios that sum to zero with the 30 original wave vectors (see Fig. 14). This leads to a cubic and quartic invariant competitive with the O^5 structure (see Table V). This arrangement requires, however, that the two sets of wave vectors differ in length by 5%, which for large κ imposes a considerable penalty in gradient energy.

The cubic and quartic invariants for these icosahedral structures are shown in Table V. Whether an icosahedral phase might be stable as the chirality drops remains an open question, although Hornreich and Shtrikman (1987) have shown that including up to five sets of wave vectors in the free energy does not stabilize the structure with respect to O^5.

Since no blue phases have been reported with icosahedral symmetry, or with hexagonal symmetry in the absence of external fields, we confine our attention below to cubic structures.

TABLE V. The values of the cubic and quartic parameters β and α for two models having icosahedral symmetry. The "edge" model consists of a single set of wave vectors, which lie along the edges of an icosahedron, while the "edge-vertex" model has in addition to these a set lying along the vertex directions. Since the edge-vertex model has a nonzero gradient free energy, the transition temperature is not given by $\beta^2/4\alpha$. Source: Rokhsar (1987).

Structure	β	α	$\tau_c=\beta^2/4\alpha$
Edge	0.721	1.528	0.0851
Edge-vertex	1.010	1.516	

E. Importance of the high-chirality limit

The high-chirality limit is quite far from the physical range of κ, which is very roughly in the range 0.01–0.5 (see Appendix D). The limit is nevertheless of interest for several reasons:

(1) It provides a rigorous proof (within the Landau-Ginzburg theory) that one or more thermodynamically stable phases with nonhelical symmetry do indeed intervene between the isotropic liquid and the conventional helical phase for appropriate values of κ. We have noted that this proof continues to hold all the way down to the value $\kappa=1.5$, at which the transition from the isotropic to the helical phase changes from second to first order. We can use the high-chirality form of the O^5 structure to extend this critical value of the chirality still lower.

Because a linear combination of biaxial helices with unit wave vector makes the gradient free energy vanish, the free energy of such a structure will have the form (6.7) even for finite values of κ. The high-chirality O^5 structure will therefore continue to be stable at a temperature above that of the helical phase until the first-order transition temperature (5.5) to the helical phase rises above the temperature 0.198 77, at which the O^5 structure first appears. This does not happen until κ drops to 0.469 45, which lies at the high end but within the physical range of values.

(2) The high-chirality limit provides the basis for an expansion in $1/\kappa^2$. The infinite-chirality solutions are all linear combinations of the rotations and displacements of a single form [Eq. (6.3)] with unit wave vector. In the infinite-chirality limit the bulk free energy merely splits the degeneracy of this family of solutions. When it is treated as a perturbation of order $1/\kappa^2$, the bulk free energy also mixes into the order parameter correction terms with nonunit wave vectors that are linear combinations (higher harmonics) of the unit wave vectors that appear in the infinite-chirality form. The correction terms generated in this way will in general differ from the biaxial helical form [Eq. (6.3)] in overall structure, as well as in wave vector.

Nobody has yet systematically carried through this procedure even to first order. Grebel *et al.* (1983a, 1984) have explored a restricted family of order parameters given by adding to the infinite-chirality superposition of biaxial helices, structures that continue to have the biaxial helical form, but with additional wave vectors **c** corresponding to the first three higher harmonics of the unit vectors appearing in the infinite-chirality order parameter. (They also allow for an overall rescaling of the magnitude of the fundamental wave vector.) Their structures can be viewed as trial functions in a variational procedure, and they reduce to about 0.3 the value of κ, above which blue phases can rigorously be shown to intervene between the isotropic and helical phases.

(3) The methods appropriate to the high-chirality limit also suggest other structures that, though clearly not favored at infinite κ, can play an important role at physically relevant values. The most important of these is a structure with the simple cubic space group $O^2(P4_232)$, which we describe in Sec. VI.F below.

(4) The high-chirality forms of the O^5 and O^8 structures have an interesting real-space form, which is highly suggestive of the kinds of structures put forth by Meiboom *et al.*, which can be viewed as approaches to the blue phase from the low-chirality limit. We discuss this in some detail in Sec. VI.G below.

F. The simple cubic O^2 structure

Consider an order parameter of the form

$$\chi=\frac{1}{\sqrt{6}}\sum_{n=1}^{6}\chi^{(n)}\ , \tag{6.23}$$

where the $\chi^{(n)}$ are again as in Eqs. (6.11) and (6.12) but with the six wave vectors $\mathbf{c}^{(n)}$ along the six $\langle 100\rangle$ directions. If all the amplitudes ζ_n have the same magnitude γ, then for suitable choice of origin (depending on the phases) the resulting order parameter can always be put in the form

$$\chi=\frac{1}{\sqrt{6}}(1+R+R^2)\mathrm{Re}[(\mathbf{x}+i\mathbf{y})(\mathbf{x}+i\mathbf{y})e^{iz}]\ , \tag{6.24}$$

where R is a 120° rotation about the [111] direction. This has the real-space form

$$\chi_{zz}=\cos y-\cos x,\quad \chi_{xy}=-\sin z\ , \tag{6.25}$$

the other components being given by cyclic permutations of x,y,z. This structure has space group $O^2(P4_232)$.

Because this structure contains no trios of wave vectors adding to zero, the cubic invariant β vanishes. The quartic invariant α, however, has the remarkably small value of $\frac{13}{12}$, only 8.33% higher than the minimum of unity achieved by the helical order parameter. This should be compared with the quartic invariants for the O^8, hexagonal, and O^5 structures, which exceed the minimum by 16.9%, 21.4%, and 29.9%. As a result, this simple cubic structure will have a lower free energy then either of the bcc forms at low enough temperatures, even though it will always lose out (though not by much) to the helix.

When κ is less than infinity, this very simple O^2 structure acquires additional Fourier components through the process of higher harmonic generation described above. The biaxial helical structure, on the other hand, does not acquire additional wave vectors when perturbatively modified by the bulk free energy. The new Fourier components of the O^2 structure produce a nonvanishing cubic invariant, which makes it more stable than the helical phase at high temperatures and high chiralities (certainly at κ in excess of 1.5, the value at which the helical phase finally acquires a nonvanishing cubic term at its transition temperature).

The small quartic term of the O^2 structure raises the possibility that it might, as the chirality dropped, also become more stable than the O^5, O^8, or hexagonal structures. From the perspective of the high-chirality limit it is these considerations that form the basis for the possibility (supported by the detailed calculations of Grebel *et al.*) that there might be regions of the κ-τ phase diagram where the stable equilibrium nonhelical phase is a descendant of the high-chirality O^2 simple cubic form, rather than any of the forms (bcc or hexagonal) that are stable at infinite chirality.

G. The O^5 and O^8 structures in real space

We can write Eq. (6.10) for the order parameter χ in the equivalent form

$$\chi=\frac{1}{\sqrt{3}}\mathrm{Re}\sum_{n=1}^{6}\chi^{(n)}\ . \tag{6.26}$$

Since the amplitudes ζ_n of the $\chi^{(n)}$ are independent of n for both the O^5 and O^8 structures, the symmetry exhibited by Table II permits us to express Eq. (6.26) as

$$\chi=\frac{1}{\sqrt{3}}\mathrm{Re}(1+R+R^2)(\chi^{(3)}+\chi^{(6)})\ , \tag{6.27}$$

where R is a 120° rotation about the direction $\mathbf{x}+\mathbf{y}+\mathbf{z}$.

The structure $\chi^{(3)}+\chi^{(6)}$ can be read off from Table II:

$$\chi^{(3)}+\chi^{(6)}=\zeta(C_y+iS_y)\{C_x[\mathbf{zz}-\tfrac{1}{2}(\mathbf{xx}+\mathbf{yy})-i(\mathbf{zx}+\mathbf{xz})/\sqrt{2}]-\frac{1}{\sqrt{2}}S_x[\mathbf{y}(\mathbf{z}-i\mathbf{x}/\sqrt{2})+(\mathbf{z}-i\mathbf{x}/\sqrt{2})\mathbf{y}]\}\ , \tag{6.28}$$

where $C_x=\cos(x/\sqrt{2})$, $S_x=\sin(x/\sqrt{2})$, etc. Note that the form of Eq. (6.28) in the O^8 case ($\zeta=i|\gamma|$) differs from the O^5 form ($\zeta=|\gamma|$) only by a factor of i, which has the sole effect of shifting the phase of the factor C_y+iS_y by $\pi/2$, i.e, the O^8 form of Eq. (6.28) can be constructed from the O^5 form by shifting it by a distance $\pi/\sqrt{2}$—a quarter of the conventional cubic cell—along the y axis.

Setting $\zeta=|\gamma|$ and taking the real part of Eq. (6.28), we find for the O^5 structure

$$\chi^{(O^5)}=\frac{1}{\sqrt{3}}\gamma(1+R+R^2)\{C_xC_y[\mathbf{zz}-\tfrac{1}{2}(\mathbf{xx}+\mathbf{yy})] -\tfrac{1}{2}S_xS_y(\mathbf{xy}+\mathbf{yx}) +C_xS_y(\mathbf{zx}+\mathbf{xz})/\sqrt{2} -S_xC_y(\mathbf{yx}+\mathbf{zy})/\sqrt{2}\}. \quad (6.29)$$

The corresponding expression for $\chi^{(O^8)}$ is given by replacing C_y and S_y with $-S_y$ and C_y, respectively. Note that prior to the symmetrization about $\mathbf{x}+\mathbf{y}+\mathbf{z}$, Eq. (6.29) has a fourfold symmetry axis parallel to $\mathbf{z}$ and passing through $x=y=0$, so that the O^8 version has such an axis passing through $x=0$, $y=\pi/\sqrt{2}$. Because of the bcc translational symmetry in the x-y plane, these fourfold axes are repeated in the positions shown in Fig. 15(a) for O^5 and Fig. 16(a) for O^8.

After the symmetrization about $\mathbf{x}+\mathbf{y}+\mathbf{z}$, these axes are distributed as in Figs. 15(b) and 16(b). It is clear from these figures that they remain fourfold axes in the O^5 structure, but in the O^8 structure they are now 4_1 axes; i.e., after rotation through 90° about the axis a translation along the axis of $\frac{1}{4}$ of the cubic cell is required to bring the structure back into self-coincidence. This is the basis for the identification of these structures with $O^5(I432)$ and $O^8(I4_132)$, these being the only two bcc space groups that contain fourfold axes and have no improper elements (a necessary feature for the symmetry groups of structures with a definite chirality).

The explicit symmetrization specified in Eq. (6.29) is easily carried out to find $\chi^{(O^5)}$, and the corresponding explicit form for the O^8 structure can be found directly from the result, provided we keep track of the C's and S's that came, under the symmetrization, from the C_y's and S_y's in Eq. (6.29); we can do this by continuing to keep them on the right in every term. We then have for $\chi^{(O^5)}$

$$\chi^{(O^5)}_{zz}=\frac{1}{\sqrt{12}}\gamma(2C_xC_y-C_yC_z-C_zC_x)\,,$$
$$\chi^{(O^5)}_{xy}=\frac{1}{\sqrt{12}}\gamma(\sqrt{2}C_yS_z-\sqrt{2}S_zC_x-S_xS_y)\,, \quad (6.30)$$

with the remaining matrix elements being given by cyclic permutations of x,y,z.

The corresponding structure for $\chi^{(O^8)}$ is given by replacing the right-hand C or S in each term by $-S$ or C, respectively:

$$\chi^{(O^8)}_{zz}=\frac{1}{\sqrt{12}}\gamma(-2C_xS_y+C_yS_z+C_zS_x)\,,$$
$$\chi^{(O^8)}_{xy}=\frac{1}{\sqrt{12}}\gamma(\sqrt{2}C_yC_z+\sqrt{2}S_zS_x-S_xC_y)\,. \quad (6.31)$$

Note that every matrix element of the O^5 structure vanishes at the origin (and therefore at the bcc lattice of points generated from the origin by the translational symmetry). This is a necessary feature of any order parameter with O^5 symmetry, since the points where three fourfold axes intersect have full cubic symmetry, but

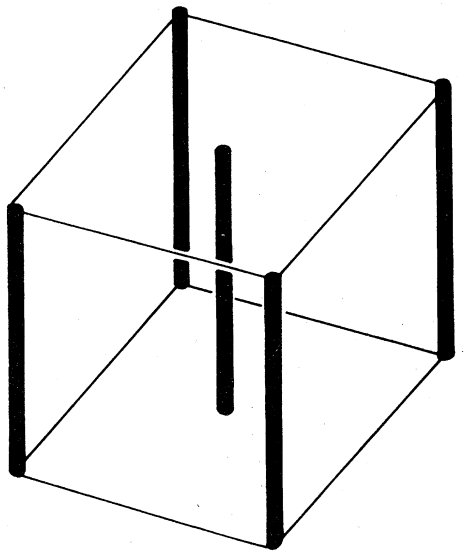

(a)

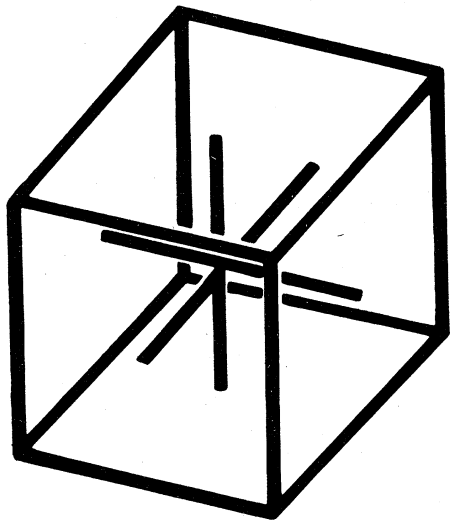

(b)

FIG. 15. Fourfold axes in the O^5 structure in real space. (a) The dark lines are the fourfold symmetry axes of the expression in Eq. (6.29) prior to symmetrizing about $\mathbf{x}+\mathbf{y}+\mathbf{z}$. The light lines indicate the edges of the unit cell, which has lattice constant $4\pi/\sqrt{2}$ in dimensionless units. (b) After symmetrizing about $\mathbf{x}+\mathbf{y}+\mathbf{z}$, the lines in (a) remain fourfold axes.

there is no nonzero traceless symmetric tensor with cubic symmetry. The O^8 structure has no points of full cubic symmetry, and it is easily established that there are no points where all matrix elements vanish.

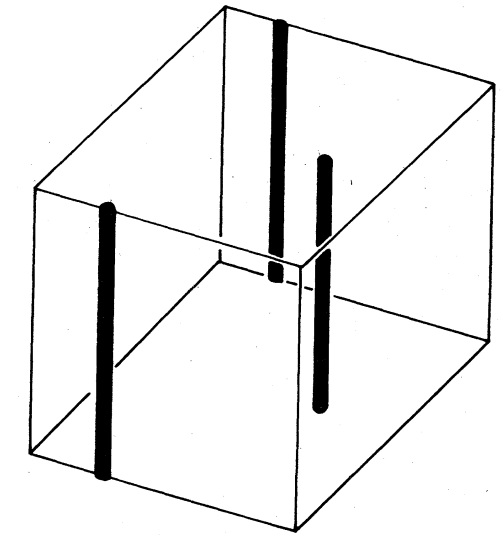

(a)

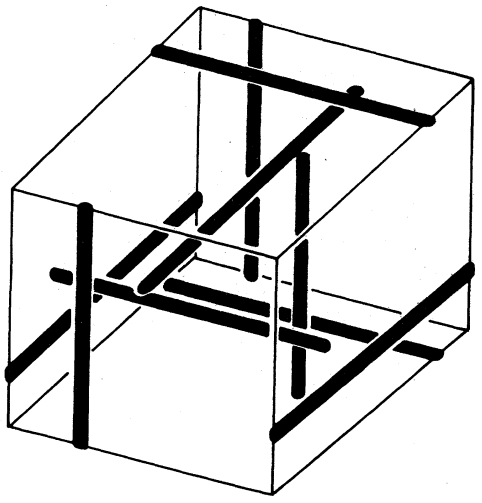

(b)

FIG. 16. Fourfold axes in the O^8 structure in real space. (a) The dark lines are the fourfold symmetry axes of Fig. 15(a) shifted by a quarter of the lattice constant along the **y** direction, as appropriate for the O^8 structure. (b) After symmetrizing about $\mathbf{x}+\mathbf{y}+\mathbf{z}$, the lines in (a) become fourfold screw axes.

Thus from the point of view of the tensor order parameter, the O^5 structure (and any structure with O^5 symmetry) necessarily contains a bcc lattice of point defects—points at which the entire order parameter vanishes—while the O^8 structure is free of defects. This is reflected in the fact that the quartic invariant α, a measure of the mean-square fluctuations of $\mathrm{tr}(\chi^2)$, is 11% larger for the O^5 structure than it is for the O^8. The O^5 structure is still favored at the highest temperatures, because of its more favorable cubic bulk free energy, but as the temperature drops the energetic cost of its point defects becomes prohibitive and it eventually loses out to O^8.

Because the bulk free energy favors a uniaxial order parameter χ with positive $\mathrm{tr}\chi^3$ (see the discussion in Sec. III), it is instructive to look for regions in which the O^5 and O^8 structures have this character. The only regions in which symmetry requires the O^8 structure to be uniaxial are along the four threefold axes. (The fourfold axes in the O^8 structure are screw axes and therefore do not require a uniaxial structure.) Along the line $x=y=z$, it follows from Eq. (6.31) that the diagonal elements of $\chi^{(O^8)}$ vanish, while its off-diagonal elements are given by

$$\chi_{xy}^{(O^8)}=\chi_{yz}^{(O^8)}=\chi_{zx}^{(O^8)}=\frac{1}{\sqrt{12}}(\sqrt{2}-\tfrac{1}{2}\sin\sqrt{2}x)\ . \quad (6.32)$$

As symmetry requires, this is indeed uniaxial with (111) as the preferred direction, and (as symmetry alone does not require) with the cubic invariant positive, as favored by the bulk free energy.

The O^5 structure has both threefold and fourfold axes. Along the threefold axis $x=y=z$ it follows from Eq. (6.30) that the diagonal elements of $\chi^{(O^5)}$ vanish, while the off-diagonal elements are given by

$$\chi_{xy}^{(O^5)}=\chi_{yz}^{(O^5)}=\chi_{zx}^{(O^5)}=-\frac{1}{\sqrt{12}}\gamma S_x^2\ . \quad (6.33)$$

It is interesting to note (we shall return to this point in Sec. VIII) that although this order parameter is indeed uniaxial with (111) as the preferred direction, as symmetry requires, its sign is *opposite* to that favored by the bulk free energy, so that as far as bulk free energy is concerned it has the *worst* possible form (compare the discussion of the bulk free energy in Sec. III). (There are similar disadvantageously uniaxial lines in the O^8 structure, which are somewhat less straightforward to extract: they are very near the fourfold screw axes, spiraling around them.)

The favorably uniaxial lines in the O^5 structure are the fourfold axes. Along the line $x=y=0$, for example, Eq. (6.30) gives

$$\chi_{zz}^{(O^5)}=\frac{2\gamma}{\sqrt{12}}(1-C_z),\quad \chi_{xx}^{(O^5)}=\chi_{yy}^{(O^5)}=-2\chi_{zz}^{(O^5)}\ , \quad (6.34)$$

and the diagonal elements vanish. This is everywhere favorably uniaxial, although the order parameter vanishes at the origin (where the fourfold axes meet) as required by symmetry. The amplitude of $\chi^{(O^5)}$ is largest at the point $z/\sqrt{2}=\pi$, i.e., when z is at the center of the

square surface of the cubic conventional cell.

It is instructive to examine the order parameter at points in the cubic cell near these face center points of most favorable bulk free energy. If x and y are not zero, but small, then to linear order in x, y, and $\delta z = z - \sqrt{2}\pi$, the order parameter at the point (x,y,z) is given by

$$\chi = \begin{bmatrix} 4 & 0 & 2y \\ 0 & -2 & -2x \\ 2y & -2x & -2 \end{bmatrix} . \tag{6.35}$$

As one moves away from the center of the face this structure remains uniaxial to linear order, the local preferred axis being

$$\mathbf{n} = \mathbf{z} + \tfrac{1}{3}(y\mathbf{x} - x\mathbf{y}) \tag{6.36}$$

or, in cylindrical coordinates, to linear order,

$$\mathbf{n} = \mathbf{z}\cos qr - \mathbf{z}\times\mathbf{r}\sin qr \ , \tag{6.37}$$

with $q = \frac{1}{3}$, or, in dimensional units, $q = \frac{2}{3}q_0$.

To summarize, the O^5 structure is the most favorable high-temperature form for a blue phase in the high-chirality limit. In the neighborhood of the points where this structure is favorably uniaxial and with largest amplitude, it is locally uniaxial, with a director of the form (6.37).

The form (6.37) has been called "double twist" by Meiboom *et al.* (1981), and it plays a central role in their model of blue-phase structure in the low-chirality limit, to which we now turn.

VII. BLUE PHASES: THE LOW-CHIRALITY LIMIT

In the high-chirality limit ($\kappa \to \infty$) discussed in Sec. VI, the role of the bulk free energy is only to select the most favorable form out of the large degenerate family of order parameters that minimize the dominant gradient free energy.

This situation is reversed in the low-chirality limit ($\kappa \to 0$), where the bulk free energy dominates. As noted in Sec. IV, the bulk free energy is minimized by taking the order parameter to be uniaxial (with the appropriate overall amplitude). Thus minimizing the dominant term in the free energy again results in a highly degenerate family of possible forms, since the bulk free energy is indifferent to any spatial variation in the direction of the preferred axis $\mathbf{n}$. This degeneracy is now reduced by the gradient free energy.

The analysis of the degeneracy splitting is quite different in the two limits. In the high-chirality limit, a rigorous derivation of which structures are the most favorable has yet to be given, although it is known that the helical phase is not the lowest-energy structure. The current best guesses, described in Sec. VI, lead to two distinct blue phases before the temperature drops to a point where the helical phase is finally stable. These conjectured forms do provide rigorous upper bounds to the critical chirality κ_c above which blue phases *must* intervene between the isotropic liquid and the helical phase. There also exists, at least in principle (it is very cumbersome to execute in practice), a completely systematic expansion in $1/\kappa$ giving the corrections to any infinite-κ structure as the chirality drops.

In the extreme low-chirality limit, on the other hand, the manner in which the degeneracy is split can rigorously be shown to lead uniquely to the helical phase at all temperatures: there are no blue phases when $\kappa = 0$ (consistent with the experimental fact that blue phases are not observed in chiral nematics of large pitch). There is, however, currently no computation of any rigorous nonzero *lower* bound for κ_c. Nor is there a systematic small-κ expansion scheme for computing the structure of blue phase order parameters.

Nevertheless the low-chirality limit enjoys two considerable advantages. Typical rough values of κ seem to be in the range 0.01–0.5 (see Appendix D), which is certainly on the low-chirality side. The low-chirality limit also has the great conceptual advantage of providing a very simple and appealing physical picture of why chiral nematics should prefer blue phases to the helical phase near the transition temperature. This picture forms the basis for a different phenomenological approach to blue phases when the chirality is small, which permits the computation of the stability of various blue phase forms, compared with each other or with the helical phase. The picture even lends insight into the structure and meaning of the blue phase forms that emerge from the analysis appropriate to the high-chirality limit.

A. General features of the low-chirality limit

Underlying the low-chirality analysis is the fact that the bulk free energy, which dominates in the low-chirality limit, favors a uniaxial order parameter. The simplest way to take this into account is to limit the family of possible order parameters to those of the strictly uniaxial form [Eq. (4.3)]:

$$\chi_{ij} = \frac{1}{\sqrt{6}}\lambda(3n_i n_j - \delta_{ij}) \ , \tag{7.1}$$

where both the director $\mathbf{n}(\mathbf{r})$ and the overall amplitude $\lambda(\mathbf{r})$ are allowed to vary with position.

The uniaxial ansatz (7.1) is routinely made in the treatment of nonchiral nematics and in most discussions of the helical phase of chiral nematics ("cholesterics"). As we emphasized in Sec. V, however, the order parameter will not be strictly uniaxial if nonuniformities in the director field $\mathbf{n}(\mathbf{r})$ or the amplitude λ break the local symmetry about the direction of $\mathbf{n}$. When κ is small, however, the degree of biaxiality induced by these nonuniformities will be slight, because of its large cost in bulk free energy. The spirit of the low-chirality limit is simply to ignore this slight biaxiality induced by the nonuniformities, taking as a first approximation an order parameter χ lying within the restricted uniaxial family (7.1). A more refined subsequent calculation could then allow the

structures determined in this way to relax into biaxiality. Except in the cores of the defects that turn out to play an important role in these structures, this refinement will be of minor importance. One is, in any event, assured that the free energies computed under the uniaxial ansatz are upper bounds to the free energies of the forms assumed when relaxation into biaxiality is allowed.

In describing the theory of the low-chirality limit we shall make the simplifying "one-constant approximation," taking the ratio $\eta=K_0/K_1$ [cf. Eqs. (4.28) and (4.26)] to be unity. This makes the analytic structure of the theory considerably more transparent, but as noted in Sec. IV, it has no physical basis (see Appendix F). The simplification is made in the expectation that the physics will be similar in the general case; detailed computations suggest that this is true (Meiboom, Sammon, and Berreman, 1983; Meiboom, Sammon, and Brinkman, 1983), and the conceptual points revealed by this simplified case are certainly more generally applicable.

Within the one-constant approximation the general gradient free-energy density (4.26) has the form

$$\begin{aligned}\varphi_{\rm grad}&=\kappa^2\{[(\nabla\times\chi)_{ij}+\chi_{ij}]^2+[(\nabla\cdot\chi)_i]^2\}\\&=\kappa^2[(\nabla_i\chi_{jk})(\nabla_i\chi_{jk})+2\,{\rm tr}(\chi\nabla\times\chi)+{\rm tr}\chi^2\\&\quad+\nabla_i(\chi_{in}\nabla_j\chi_{jn}-\chi_{jn}\nabla_j\chi_{in})]\ .\end{aligned}\tag{7.2}$$

The last set of terms in the second form is a total derivative, which therefore gives only a surface term when φ is integrated to give the total free energy. In the limit in which surface energies are negligible compared with bulk effects (or for any periodic structure), this term can be ignored. We can therefore take the gradient energy in the one-constant approximation to be simply

$$\varphi_{\rm grad}=\kappa^2[(\nabla_i\chi_{jk})(\nabla_i\chi_{jk})+2\,{\rm tr}(\chi\nabla\times\chi)+{\rm tr}\chi^2]\ .\tag{7.3}$$

If the order parameter has the uniaxial form (7.1), then the gradient free-energy density (7.3) can be expressed in either of the equivalent forms

$$\begin{aligned}\varphi_{\rm grad}=\kappa^2((\nabla\lambda)^2+\tfrac{1}{4}\lambda^2+3\lambda^2\nabla\cdot[(\mathbf{n}\cdot\nabla)\mathbf{n}-\mathbf{n}(\nabla\cdot\mathbf{n})]\\+3\lambda^2\{(\nabla\cdot\mathbf{n})^2+[\mathbf{n}\times(\nabla\times\mathbf{n})]^2+(\mathbf{n}\cdot\nabla\times\mathbf{n}+\tfrac{1}{2})^2\})\end{aligned}\tag{7.4}$$

or

$$\varphi_{\rm grad}=\kappa^2[(\nabla\lambda)^2-\tfrac{1}{2}\lambda^2+3\lambda^2(\nabla_i n_j+\tfrac{1}{2}\varepsilon_{ijk}\mathbf{n}_k)^2]\ .\tag{7.5}$$

The accompanying bulk free-energy density [Eq. (4.26)], when the order parameter has the uniaxial form (7.1), is just

$$\varphi_{\rm bulk}=\tau\lambda^2-\lambda^3+\lambda^4\ .\tag{7.6}$$

As $\kappa\to0$, the bulk free-energy density (7.6) dominates the total free energy. The amplitude λ is thus required everywhere to have the fixed amplitude λ_0 that minimizes Eq. (7.6). If λ is constant, the first two terms of the gradient free-energy density (7.4) give a constant. The third term becomes a total derivative, which can be converted to an unimportant surface term when the system is large. The structure of $\mathbf{n}$ is therefore entirely determined by the remaining expression in curly brackets. This is the sum of three nonnegative terms, which are just the splay, bend, and twist terms in the Frank free energy that underlies the familiar elasticity theory of "cholesterics." This set of terms, and thus the entire gradient free energy, is minimized by the uniaxial helical phase: for the second (bend) term to vanish, $\nabla\times\mathbf{n}$ must be parallel to $\mathbf{n}$; for the third (twist) term also to vanish, the amplitude of $\nabla\times\mathbf{n}$ must be $-\frac{1}{2}$. The vanishing of both terms thus requires $\mathbf{n}$ to satisfy

$$\nabla\times\mathbf{n}=-\tfrac{1}{2}\mathbf{n}\ ,\tag{7.7}$$

which also causes the first (splay) term to vanish. Our dimensionless length scale is such that $2q_0$ is the unit of the wave vector [cf. Eq. (4.25)], so that in dimensional units Eq. (7.7) becomes

$$\nabla\times\mathbf{n}=-q_0\mathbf{n}\ .\tag{7.8}$$

This condition is satisfied by the director field (2.1) of the uniaxial helical phase:

$$\mathbf{n}(\mathbf{r})=\mathbf{x}\cos q_0z+\mathbf{y}\sin q_0z\ .\tag{7.9}$$

It can be shown (Wright, 1983) that Eq. (7.9) gives the unique minimum to the Frank free energy to within an overall rotation.

There are thus no blue phases when $\kappa=0$. When κ is small but nonzero, the phenomenological theory of the low-chirality limit continues to take the free-energy density to have the uniaxial form (7.4) [or the equivalent Eq. (7.5)] and (7.6) under the assumption that relaxation into biaxiality will give only small corrections that can be computed at a later stage.

How, then, can the free energy of such uniaxial structures be reduced below that of the helical phase? The only obvious clue provided by Eq. (7.4) is that any such structure *must* have a nonuniform amplitude λ, since the proof that the helical phase gives the minimum when $\kappa=0$ uses only the uniformity of λ in that limit. [Indeed, Eq. (7.4) demonstrates that among uniaxial phases with uniform λ, the helical phase is the most favorable whatever the value of κ.] Since any reduction in energy below the helical phase can only come from the third term in Eq. (7.4), it follows from integrating that term by parts that any phase more stable than the helical must contain regions in which $(\mathbf{n}\cdot\nabla)\mathbf{n}-\mathbf{n}(\nabla\cdot\mathbf{n})$ is directed along the gradient of the amplitude λ. Meiboom *et al.* (1981) and Sethna (1985) give an interesting and important interpretation of this condition, which we return to at the end of this section, after considering a much more direct hint of how uniaxial structures can acquire a free energy lower than the helical phase, provided by the alternative form (7.5) of the free energy.

B. Local order in the low-chirality limit: Double twist

According to Eq. (7.5) the *local* gradient free-energy density is everywhere bounded below by the value $-\frac{1}{2}\kappa^2\lambda_0^2$, a value that is lower than the value $\frac{1}{4}\kappa^2\lambda_0^2$ assumed at every point in the uniaxial helical phase. This lower value is attained at points where $\nabla\lambda$ vanishes and where the director field satisfies the condition

$$\nabla_i n_j + \tfrac{1}{2}\varepsilon_{ijk} n_k = 0 \ . \tag{7.10}$$

We can conclude at once that no unit vector field can satisfy the condition (7.10) throughout all of space, for if there *were* such a vector field, we could pick the amplitude λ to have the constant value λ_0 and arrive at an integrated *total* free energy lower than the helical phase, contradicting the fact that the helical phase has the lowest free energy among uniaxial structures with constant amplitudes.

This conclusion can also be reached more directly. The question of whether the local vector field specified by Eq. (7.10) can be defined throughout a region of space is just the question of whether the differential equation (7.10) can be integrated to give a nonsingular vector field $\mathbf{n}(\mathbf{r})$ throughout the region. If Eq. (7.10) did hold in a region, then we could take a second derivative to get

$$\nabla_s \nabla_i n_j + \tfrac{1}{2}\varepsilon_{ijk} \nabla_s n_k = 0 \ . \tag{7.11}$$

But using Eq. (7.10) to evaluate the second term in (7.11) gives

$$\nabla_s \nabla_i n_j = \tfrac{1}{4}(\delta_{js} n_i - \delta_{is} n_j) \ , \tag{7.12}$$

which is inconsistent with the integrability conditions that $\nabla_s \nabla_i n_j$ should be symmetric in i and s.

One can, however, satisfy the condition (7.10) along lines, and by continuity the local bulk free-energy density will then be lower than that of the helical phase in some neighborhood of those lines as well. A particularly simple way to do this, with a clear and plausible physical motivation, has been given by Meiboom *et al.* (1981), and forms the basis for all models of blue phases in the low-chirality limit. Consider the director field given in cylindrical coordinates by

$$\mathbf{n} = \mathbf{z}\cos\tfrac{1}{2}r - \boldsymbol{\phi}\sin\tfrac{1}{2}r \ . \tag{7.13}$$

One easily calculates that

$$(\nabla_i n_j + \tfrac{1}{2}\varepsilon_{ijk} n_k)^2 = \tfrac{1}{4} + (\sin\tfrac{1}{2}r/r)^2 - \sin r/2r \ , \tag{7.14}$$

which does indeed vanish on the axis of the cylinder ($r=0$), but not in its immediate neighborhood.

Thus if $\nabla\lambda$ is small, in the neighborhood of $r=0$ the structure (7.13) has a more favorable free-energy density than the helical structure (7.9). At large r, where $\boldsymbol{\phi}$ varies slowly with position, the director field (7.13) locally approaches the helical one, and it can be viewed as the result of wrapping the planes of constant $\mathbf{n}$ in the helical structure (7.9) into cylinders.

Meiboom *et al.* characterize the configuration (7.13) of the director near the axis of the cylinder, $r=0$, as one of *double twist* (Fig. 17). Their terminology refers to the fact that near $r=0$, $\mathbf{n}$ twists along all directions perpendicular to itself (and in particular it rotates along *both* of a pair of orthogonal directions—thus "double twist"), in contrast to the helical structure in which $\mathbf{n}$ twists only about a single direction, the pitch axis, and is uniform along directions perpendicular to the pitch axis.

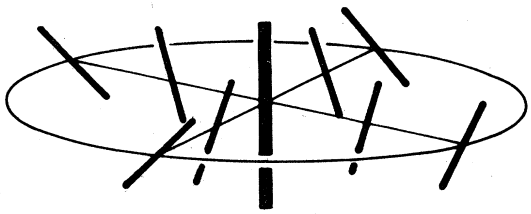

FIG. 17. The dark lines show the orientation of the director field of "double twist" given by Eq. (7.13). The configuration is cylindrically symmetric around $r=0$, which is at the center of the figure.

If one thinks of the constituents of a chiral nematic as being screwlike objects and asks for the most efficient way to pack a group of such "screws" about a central one, the *local* arrangement that takes maximal advantage of the helical symmetry of the screws is clearly one of double twist. This is preferable to a "helical" arrangement in which the axes of the neighboring screws twist only in one direction, remaining parallel to the central screw in the other.

As we have seen analytically, however, and as is evident when contemplating a collection of screws, double twist cannot be extended to fill a region of space. As a result, if we attempt to build a structure consisting of local regions of approximate double twist, the interpolating regions must necessarily be less favorably aligned. It is therefore possible that the locally less favorable helical arrangement may still turn out to give the best overall configuration.[17] Whether a structure with local regions of double twist can be stable with respect to the helical phase is thus a question of whether the free-energy gain over the helical phase from the local double-twist regions more than offsets this increase in free energy outside of the regions of double twist. The contribution to the gradient energy of such unfavorable regions can be reduced by decreasing λ in these regions, which is why λ is necessarily nonuniform in such structures. Variations in λ, however, force one to pay a price in bulk free energy, which penalizes any deviation from $\lambda=\lambda_0$. Since the energetics are dominated by the bulk free energy as $\kappa\to 0$, there will be a threshold value of κ below which such variations are too costly and no blue phases are possible.

[17] As we shall see in Sec. VIII, this is indeed true for chiral ferromagnets, in which the locally ordered state always loses to the helical phase.

Even if such locally ordered nonhelical structures are stable in some parameter range, as the temperature drops, the cost in bulk energy of the regions between the double twist will increase and the helical phase will become favored. We would therefore expect these nonhelical phases to exist only near the transition to the isotropic phase. This is just the behavior of the blue phases.

C. The energetics of double-twist cylinders

To sharpen this intuitive picture of the blue phase structures in the low-chirality limit, we must specify the shape of the local regions of double twist used to build these structures. A particularly simple region can be formed by noting that although perfect double twist cannot exist in a region, the director field (7.13) has a favorable free energy in a significant neighborhood of $r=0$. Thus nearly perfect double twist can clearly be extended along the z axis to form an extended cylinder with perfect double twist along the entire axis, and a very favorable free energy near the axis. The specific proposals that have been made for blue phase structures consist of cunning arrangements of such "double-twist cylinders" in periodic arrays.[18]

We therefore consider cylinders consisting of the double-twist director field (7.13), with amplitude λ constant out to some radius R, and zero beyond. To estimate the radial extent of a double-twist cylinder we compare its local free energy with that of a helical order parameter at points that are not on the axis of perfect double twist. The double-twist (dt) configuration (with the constant amplitude λ_0 that minimizes the bulk free energy) will have a lower free-energy density than the uniaxial helix (uh) wherever the gradient free-energy density [Eq. (7.5)] is lower than the uniform value $\frac{1}{4}\lambda_0^2$ assumed by the uniaxial helical order parameter. The difference between these free-energy densities is just (Fig. 18).

$$\varphi^{\rm dt}(r)-\varphi^{\rm uh}=3\lambda_0^2[(\nabla_i n_j+\tfrac{1}{2}\varepsilon_{ijk}n_k)^2-\tfrac{1}{4}]$$
$$=\tfrac{3}{4}\lambda_0^2[(\sin\tfrac{1}{2}r/\tfrac{1}{2}r)^2-2\sin r/r]\ . \qquad (7.15)$$

Thus the local free energy of the double-twist cylinder lies below that of the uniaxial helix until $\tan\frac{1}{2}r$ becomes equal to r, i.e., until the distance from the axis has grown to $r=2.331$ or, in dimensional units, $q_0 r=1.166$. At this distance the director has rotated over 60° (66.78°) from the cylinder axis. If the one-constant approximation is not made (i.e., if η is not equal to unity), an additional term $\frac{3}{2}\lambda_0^2(\eta-1)\sin^4(\frac{1}{2}r)/r^2$ must be added to Eq. (7.15). For $\eta=3$, the radius at which $\varphi^{\rm dt}$ equals $\varphi^{\rm uh}$ is reduced to $q_0 r=0.8180$, at which point the director has rotated to nearly 47° (see Fig. 18). Physical values of η seem to fall roughly in the range 1–3 (Appendix F).

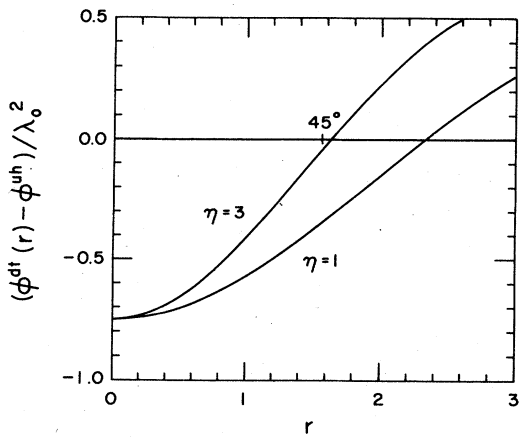

FIG. 18. A comparison of the gradient free-energy density of a double-twist configuration ($\varphi^{\rm dt}$) and the uniform helical structure ($\varphi^{\rm uh}$) for two values of η, the ratio of elastic constants. The point $r=0$ is the center of the double-twist pattern.

D. Stable structures in the low-chirality limit

Equation (7.15) for the energy difference demonstrates that imperfect local double twist is preferable to the helical phase out to a significant distance from the axis of perfect double twist, but it also confirms the general result that in the absence of variations in the amplitude λ the helical phase must have the lowest total free energy for a sufficiently large sample. To see this, note that the difference in total free energy per unit length in a cylinder of radius R is given by

$$\tfrac{3}{2}\pi\lambda_0^2\int_0^R r\,dr[(\sin\tfrac{1}{2}r/\tfrac{1}{2}r)^2-2\sin r/r]\ . \qquad (7.16)$$

The first term in the integrand is everywhere positive and gives a contribution that diverges logarithmically with large R. The second term, which is responsible for double twist being favored locally for small r, gives a bounded oscillatory contribution with increasing R, and therefore for large enough R the free-energy difference becomes positive, and the helical phase is indeed favored over a single double-twist cylinder.

Can this relative stability be reversed by diminishing the amplitude λ of the doubly twisting order parameter with increasing distance R from the axis? Since the helical phase is locally favored over the double-twist cylinder beyond a certain distance, this can be achieved with a single cylinder only if the amplitude becomes vanishingly small at large R, and only if the isotropic phase (which is what a zero-amplitude order parameter describes) has lower free energy than the helical phase. Hornreich, Kugler, and Shtrikman (1982) have answered this ques-

[18]Cladis, Garel, and Pieranski (1986) consider distortions of the blue phases in an electric field, and interpret their results as evidence against the model of BP I consisting of such cylinders. Finn and Cladis (1982) have proposed an emulsion model of the blue phases based on spheres of local ordering, although there have been no detailed studies of the energetics of such structures.

tion, showing for a range of κ that at temperatures just above the isotropic-helical transition a single double-twist cylinder of variable amplitude can become stable: the fact that its local free energy is significantly lower than the helical phase near the cylinder axis is enough to give a structure of lower total free energy than the isotropic phase, even after paying the free-energy cost of a nonuniform amplitude that falls to zero away from the axis.[19]

One can then construct stable structures out of many such cylinders, floating apart from each other in a sea of isotropic phase. A collection of such double-twist cylinders that does not possess a periodic structure is an appealing model for the amorphous BP III (Marcus, 1981; Hornreich, Kugler, and Shtrikman, 1982; Kleman, 1982). If the cylinders are arranged periodically, the existence of stable isolated cylinders can form the basis for a kind of "tight-binding" blue phase model. With appropriately oriented cylinders, the amplitude λ would not have to drop to zero in regions where the director field matched smoothly between nearby cylinders. This would reduce both the bulk free-energy cost of these regions and the surface energy of the cylinders, thereby further stabilizing the structure. Nobody has attempted directly to build such a "tight-binding" model into a computational scheme, but it provides an intuitive picture of the general strategy pursued in constructing low-chirality blue phase models: the idea is to arrange double-twist cylinders in ways that minimize the unfavorably aligned regions between the cylinders.

Since the local free energy in a double-twist cylinder still compares favorably with that of the helical phase, even when the director has turned as much as 45°–60° from the cylinder axis, the diameters of the constituent cylinders can be of the order of the cholesteric pitch, which is indeed the scale of characteristic blue phase lattice constants. The extensive range of angles the director can make with the axis within the radius of favorable free energy leaves room for considerable imagination in inventing efficient packings of such cylinders.

E. The O^2, O^{8-}, and O^{8+} structures

The first such arrangement was proposed by Meiboom *et al.* (1981) (this was prior to the demonstration by Hornreich *et al.* that a single cylinder could be stable and was the first suggestion that local double twist is the key to understanding blue phases). Their structure illustrates most of the pertinent features of subsequently proposed competing configurations. Consider three families of cylinders with mutually orthogonal axes in which the director in each cylinder double twists out to an angle of 45° with its axis. Such cylinders can be woven into a periodic array with simple cubic translational symmetry and the space group $O^2(P4_232)$, as shown in Fig. 19.

This arrangement succeeds in filling at least 58.9% $(3\pi/16)$ of space with regions whose free-energy density is lower than that of the helical phase. Furthermore, the directors match at the points of contact between cylinders, thereby doing no violence to the gradient free energy. One pays a price for this admirable arrangement in the interstitial regions about the $\langle 111 \rangle$ directions, and a rather extensive numerical computation is required to determine whether there are values of κ for which this strategem will succeed in making a simple cubic blue phase stable over the helical phase.

Independent of such a calculation, however, one striking feature of the arrangement stands out. In the vicinity of four of the eight body diagonals emerging from the center of the cubic cell [the dark lines in Fig. 20(b)] there is no way to interpolate uniaxial material without resulting in a singularity in the director field. This is easily verified by attaching "arrowheads" to the directors, keeping track of their orientations as one encircles such a line, and noticing that when one returns to the starting point the direction of the "arrow" is reversed. This is the topological signature of a (stable) π-disclination line (Fig. 4). (The other four body diagonals also lie in regions of unfavorably oriented material, but the arrows come back to their original positions, so the field is not singular.)

For this particular structure, a nonuniform amplitude λ is necessary not only to do better than the helical phase, but also to avoid an infinite free energy, for within the restricted family of locally uniaxial order parameters it is impossible to avoid a divergent gradient energy at the core of a π disclination, unless the amplitude is allowed to vanish, giving a nonsingular core of isotropic liquid.

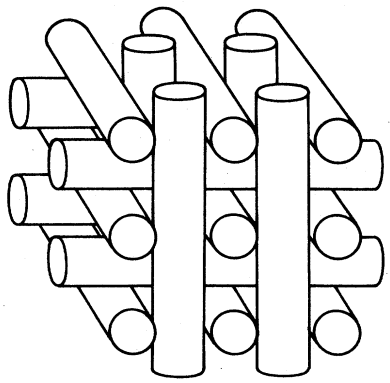

FIG. 19. The arrangement of double-twist cylinders in the O^2 structure. The director at the surface of each cylinder makes an angle of 45° with the cylinder axis.

[19]Using a strictly uniaxial double-twist cylinder, they find that for $\kappa > 0.39$ there is a range of temperatures in which isolated cylinders are stable when the helical phase is also restricted to be purely uniaxial. When the helical phase is allowed to become biaxial, the range shrinks to $0.5 < \kappa < 1.49$. Allowing the double-twist cylinder to acquire biaxiality would extend this range.

Other proposed weavings of cylinders of double twist into cubic structures contain similar unavoidable networks of line defects. For example the cylinders can again be arranged with mutually orthogonal axes and with the director twisting out to 45°, but woven into the body-centered-cubic array with space group $O^8(I4_132)$ (see Fig. 21) (Meiboom, Sammon, and Berreman, 1983). (This structure has been called "O^{8-}" to distinguish it from another structure having O^8 symmetry, described below.) Now the highly favorable regions of doubly twisted structure fill only 29.45% of space ($3\pi/32$). Perhaps more advantageously, however, the defect lines are now well separated [see Fig. 22(b)], lacking the network of nodes [at the center and corners of the cubic cell of Fig. 20(b)] characterizing the O^2 structure.

Because threefold axes in different directions do not intersect in the O^8 structure, one can entertain a second possibility with O^8 symmetry (called "O^{8+}"), in which the double-twist cylinders are along ⟨111⟩ directions, and the defect lines lie along the ⟨100⟩ directions (see Fig. 22) (Hornreich and Shtrikman, 1981a, 1981b). This differs from O^{8-} by interchanging the position of the double-twist cylinders and the defect lines. This possibility appears attractive since the cylinders fill more than two-thirds ($68\% = \pi\sqrt{3}/8$) of the liquid. The director in each cylinder double twists to an angle of 54.7°

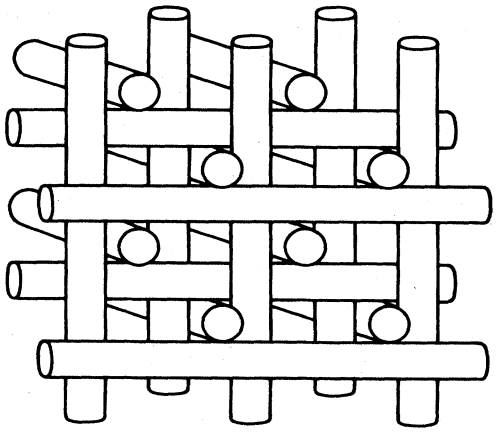

FIG. 21. The arrangement of double-twist cylinders in the O^{8-} structure. As in the O^2 structure (Fig. 19), the director twists out to 45° at the cylinder surfaces.

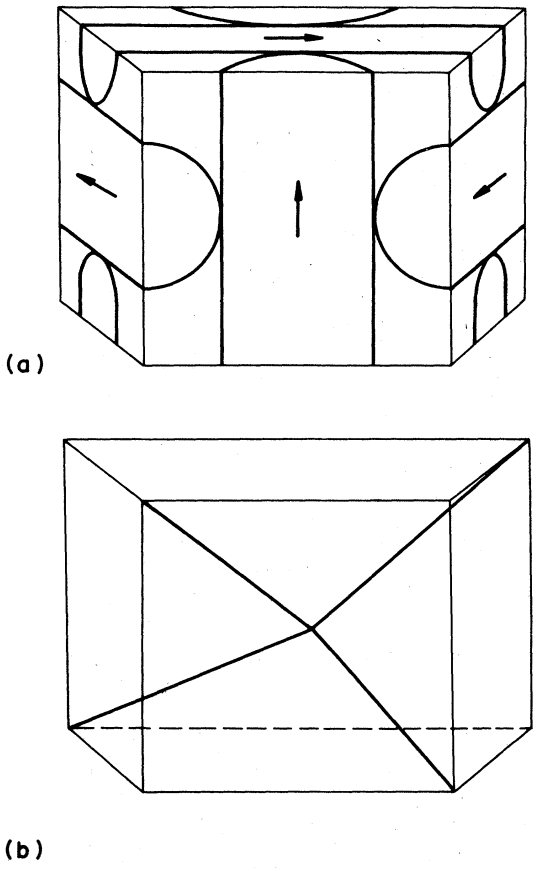

FIG. 20. (a) The cubic unit cell of the O^2 structure in a distorted view that allows the sides to be seen. The parts of the double-twist cylinders contained in the unit cell are shown. By attaching "arrow heads" to the director as shown and keeping track of the orientation as one traverses a path surrounding one of the ⟨111⟩ lines, one finds that four of the eight such directions are π disclinations, which are shown as the cube diagonals in (b).

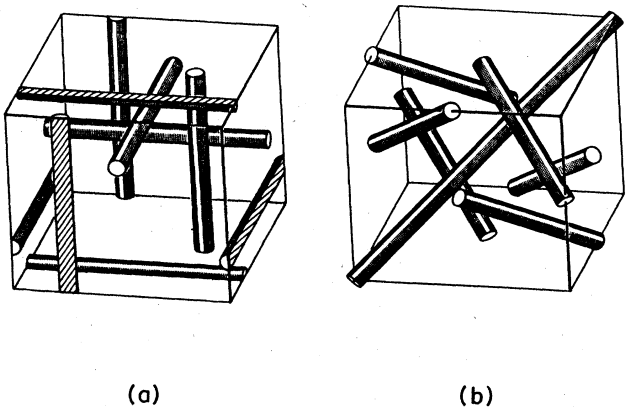

FIG. 22. The unit cells of the O^8 structures. For O^{8-}, the positions of the double-twist cylinders are shown in (a) (cf. Fig. 21), with the positions of the resulting defect lines shown in (b). Interchanging the positions of the cylinders and defects gives O^{8+}. The arrangement of double-twist cylinders in O^{8+} is shown in (b), with the arrangement of defects shown in (a). In this structure the director at the surface of each cylinder makes an angle of 54.7° with the cylinder axis. Reproduced from Meiboom, Sammon, and Berreman, 1983.

$[\frac{1}{2}\cos^{-1}(-\frac{1}{3})]$ at the surface of the cylinder, which is less than the angle of 68.78° at which the local free-energy density of double twist (for $\eta=1$) ceases to lie below that of the helical phase.

F. A calculation of energies of uniaxial structures

Meiboom, Sammon, and co-workers (Sammon, 1982; Meiboom, Sammon, and Berreman, 1983; Meiboom, Sammon, and Brinkman, 1983) have carried out detailed computer calculations to determine the free energies of these structures in the uniaxial limit over a temperature range of a degree below the transition to the isotropic phase. In these calculations, they consider a vector field that is constrained to have the symmetry of one of the structures described above, and numerically relax the configuration to minimize the gradient energy (7.4). The vector field is taken to have a constant amplitude that drops abruptly from unity in the ordered regions to zero in the defect cores. The cost of a defect is estimated from experimental quantities: the bulk free-energy cost of the disordered core is estimated from typical measured values of the entropy of transition of nematic compounds, and the gradient energy at the interface between the defect core and the ordered region is estimated from measured values for the surface tension. The values of the measured quantities they use are consistent with a value of κ in the physical range. Their calculations are carried out for $\eta=1$ and 3.

Sufficiently near the transition to the isotropic phase, their calculations show that all of the structures mentioned above, as well as a uniaxial structure they consider with O^5 symmetry, become stable with respect to the helical phase. As expected from the energetics of double-twist cylinders (Fig. 18), the free energies of the structures are considerably lower for $\eta=1$ than for $\eta=3$.

For both values of η, the O^5 structure has the least favorable energy of the four structures they consider. For $\eta=1$, their calculations show that the O^{8-} and O^2 structures are very close in energy near the transition, with the O^{8+} structure 10–20 % higher in energy. For temperatures more than about 0.5 °C below the transition from the isotropic, the O^{8-} structures appears unambiguously to be the lowest-energy phase. For $\eta=3$, O^2 and O^{8+} are found to be very close in energy over the range calculated, with O^{8-} somewhat lower in energy. These findings are in agreement with the observed structures described above in Sec. III.F. Note that the energetic preference of O^{8-} over O^{8+} provides a warning that considering merely the packing fraction of double-twist cylinders may not be a good indicator of relative energies of structures. The unfavorably aligned regions between cylinders are apparently much more costly in O^{8+} than in O^{8-}.

The calculation of Meiboom *et al.* strongly suggests that models of the type discussed can indeed be stable with respect to the helical phase over some range of temperature near the transition to the disordered phase. However, because of the way the calculation estimates the cost of defect cores, its detailed results for the relative stability of the structures should be viewed with some caution (for example, cf. Gerber, 1984). Moreover, the details of which structures appear in a physical system may depend on the physical parameters of the system. There is, of course, no guarantee that the most favorable structure is among those investigated to date.

All of these locally uniaxial models for the blue phases are characterized by interweaving cylinders of double twisting material threaded by networks of line defects. Meiboom *et al.* (1981) and Sethna (1985) argue that such networks are an inherent feature of blue phases, being driven by the free-energy term [cf. Eq. (7.4)]

$$3\kappa^2\int\lambda^2\nabla\cdot[(\mathbf{n}\cdot\nabla)\mathbf{n}-\mathbf{n}(\nabla\cdot\mathbf{n})] = -3\kappa^2\int\nabla\lambda^2\cdot[(\mathbf{n}\cdot\nabla)\mathbf{n}-\mathbf{n}(\nabla\cdot\mathbf{n})]\ , \quad (7.17)$$

which, as noted above, is the only one that can stabilize blue phases over the helical phase. This term does indeed give a negative contribution in regions containing the appropriate kind of line singularities. Consider a line defining the z axis in the neighborhood of which the director has the form

$$\mathbf{n}=\mathbf{x}\cos\phi+\mathbf{y}\sin\phi\ , \quad (7.18)$$

where ϕ is a function only of the polar coordinate θ. One easily verifies that $(\mathbf{n}\cdot\nabla)\mathbf{n}-\mathbf{n}(\nabla\cdot\mathbf{n})$ is along the radial direction with amplitude $-(1/r)d\phi/d\theta$. It follows that a $-\pi$ disclination, in which $\phi=-\theta/2$ and λ grows with r from zero on the singular line to its bulk value, will make a negative contribution to Eq. (7.17). If the chirality is low enough that bulk free energy dominates, it is reasonable to expect the region of reduced λ to be confined to the core of such a line singularity rather than distributed more widely (at lower cost in gradient energy). Meiboom *et al.* (1981) treat λ as constant and equal to its uniform bulk value except for a cylindrical core region about the defect lines which is excluded from the integration, its contribution being replaced by a term giving a phenomenological estimate of the positive core energy. The integral in Eq. (7.17) then becomes an integral over the surface of the cylinder and contributes a negative energy $-3\kappa^2\lambda^2\pi$ per unit length to the line defects. The combined contribution of these two terms can be viewed as an effective energy per unit length for the defect lines, which, if negative, can stabilize such a network over the helical phase.

Although blue phases can be stable at moderately low chirality, it cannot be too low. Thus this argument, while suggestive that the nonuniformity in λ required to stabilize a blue phase might be concentrated into line defects (as it would have to be at zero chirality), does not establish that it must be. Sethna (1985) has developed a systematic approach to low-chirality chiral nematics based on a model elastic energy for which the *only* way to exploit the extra term in Eq. (7.4) is through line defects. In this model the interesting complementarity in the pa-

per of Meiboom *et al.* (1981) can be made rigorous: blue phases can be viewed either as networks of disclination lines (which necessarily imply regions of double twist) or interwoven double-twist cylinders (which necessarily imply disclination lines).

In terms of the order parameter we use here, however, we are aware of no general topological proof that line defects should necessarily accompany double-twist cylinders, or vice versa.[20] There are, however, several theoretical indications in addition to the original argument by Meiboom *et al.* (1981) and Sethna (1985) that the appearance of singular lines is more than just an artifact of the particular structures so far proposed. These considerations are not special to the low-chirality limit, and we examine them in our concluding section.

VIII. BLUE PHASES: SOME GENERAL THEORETICAL FEATURES

In this concluding section we examine three aspects of the blue phase structures which, while of some interest in themselves, also provide evidence that the line singularities that emerge in the low-chirality models of the blue phase may indeed be expected on more general grounds.

A. Can chiral ferromagnets have blue phases?

Consider a chiral anisotropic liquid in which the order parameter is not a traceless symmetric tensor, but a vector, as in a ferromagnet. This is a conceptually interesting case, because the major difference between a vector order parameter and the traceless uniaxial tensor order parameter that prevails in the low-chirality limit is that in the vector case there are no stable line defects. The π disclinations appearing in the low-chirality models of the blue phases cannot be constructed with a vector order parameter without introducing singular *planes* across which the directions of the arrows reverse. Thus the packing of double-twist cylinders described above cannot be realized for a vector order parameter, without such energetically expensive structures. On the other hand, any structure without π disclinations that can be made out of a director can be mimicked with a vector.

It is therefore interesting to note that at the phenomenological level of the Landau theory, in which our whole treatment of chiral nematics has been framed, one can prove in the analogous theory of chiral ferromagnets that the equilibrium phase is always the helical one. Double-twist cylinders are, of course, locally just as advantageous in the chiral ferromagnet as they are in the chiral nematic. But it follows on rather general grounds that there is no way at all to weave a network of such cylinders that does not cost more in the interstitial regions than is gained in the regions of double twist.

The chiral ferromagnetic order parameter is simply a vector σ, which we can decompose into an amplitude λ and a unit vector $\mathbf{n}$, analogous to the corresponding quantities for the uniaxial chiral nematic:

$$\sigma=\lambda\mathbf{n} \ . \tag{8.1}$$

The gradient energy analogous to Eq. (7.3) for the tensor order parameter (in the corresponding one-constant approximation) is simply

$$\varphi_{\rm grad}=\kappa^2[(\nabla_i\sigma_j)(\nabla_i\sigma_j)+\sigma\cdot\nabla\times\sigma+\tfrac{1}{2}\sigma^2] \ . \tag{8.2}$$

With σ given by Eq. (8.1) we have

$$\varphi_{\rm grad}^{\rm "fm"}=\kappa^2[\lambda^2(\nabla_i n_j+\tfrac{1}{2}\varepsilon_{ijk}n_k)^2+(\nabla\lambda)^2] \ . \tag{8.3}$$

We have added the superscript "fm" for purposes of comparing this gradient energy for the vector ferromagnet with the corresponding two terms from the gradient energy (7.5) for the tensor order parameter of a chiral nematic in the uniaxial limit [the $-\frac{1}{2}\lambda^2$ appearing in Eq. (7.5) can be absorbed in the quadratic term of the bulk free energy]:

$$\varphi_{\rm grad}^{\rm nem}=3\kappa^2[\lambda^2(\nabla_i n_j+\tfrac{1}{2}\varepsilon_{ijk}n_k)^2+\tfrac{1}{3}(\nabla\lambda)^2] \ . \tag{8.4}$$

In both cases the full free energy consists of $\varphi_{\rm grad}$ plus terms in λ without gradients which can be associated with the bulk free-energy density. This bulk free-energy density alone will be minimized by picking the appropriate (constant) value for the amplitude λ. In the case of the tensor order parameter we found that the gradient free energy was not necessarily minimized by a structure with constant λ—a fact essential for the possible stability of blue phases. In the case of the vector order parameter, we can reach quite a different conclusion.

We can examine both the tensor and vector cases together by considering a gradient energy of the form

$$\varphi_{\rm grad}=\kappa_1^2\lambda^2(\nabla_i n_j+\tfrac{1}{2}\varepsilon_{ijk}n_k)^2+\kappa_2^2(\nabla\lambda)^2 \ , \tag{8.5}$$

with

$$\begin{aligned}&\kappa_2^2=\kappa_1^2, \ \text{ferromagnet} \ ,\\ &\kappa_2^2=\tfrac{1}{3}\kappa_1^2, \ \text{nematic} \ .\end{aligned} \tag{8.6}$$

The two cases differ only in the relative weight assigned to the first term, which favors double twist, and the second, which penalizes amplitude variations. Amplitude variations are three times as costly, on the scale of double-twist energies, for the ferromagnet as they are for the nematic. Remarkably, this is just enough additional cost to demonstrate that chiral ferromagnets cannot have blue phases. This conclusion follows from the easily established identity

[20] Very recently, Hornreich and Shtrikman (1988b) have given a topological argument that such defects are inherent to structures with space groups O^5 and O^2, but that they are not required in structures with space group O^8.

$$\kappa_1^2\lambda^2(\nabla_i n_j+\tfrac{1}{2}\varepsilon_{ijk}n_k)^2+\kappa_2^2(\nabla\lambda)^2$$
$$=\kappa_1^2\lambda^2\{(\nabla\cdot\mathbf{n}+\mathbf{n}\cdot\nabla\lambda/\lambda)^2+(\mathbf{n}\cdot\nabla\times\mathbf{n}+\tfrac{1}{2})^2$$
$$+[\mathbf{n}\times(\nabla\times\mathbf{n})+\nabla\lambda-\mathbf{n}(\mathbf{n}\cdot\nabla)\lambda]^2\}$$
$$+\tfrac{1}{4}\kappa_1^2\lambda^2+(\kappa_2^2-\kappa_1^2)(\nabla\lambda)^2 . \qquad (8.7)$$

The term in large square brackets is a sum of three nonnegative terms, each of which vanishes in the helical phase if λ is uniform. In the nematic the coefficient of the term in $(\nabla\lambda)^2$ is *negative,* leaving open the possibility of a nonhelical phase with nonuniform amplitude. But in the ferromagnet the coefficient of the term in $(\nabla\lambda)^2$ is *zero.* Thus the uniform helical phase minimizes the gradient as well as the bulk free energy, and blue phases can never do better, even though double-twist cylinders continue to be locally favorable, as is clear from Eq. (8.3).

It is a remarkable fact that the *energetics* of the Landau theory of the chiral ferromagnet reflect the *topological* constraints on the order parameter by permitting a proof that in this system, which cannot support π disclinations, blue phases are never favored over the helical one. We are unaware of any deep reason why this should work as neatly as it does.

B. The residue of line defects in the high-chirality limit

In the low-chirality limit the order parameter χ is taken to be a traceless symmetric *uniaxial* tensor. The local order parameter is thus completely specified by the three numbers that specify the preferred axis $\mathbf{n}$ and the overall amplitude λ (which will be positive or negative depending on the sign of the cubic invariant in the free energy). More generally, and especially in the high-chirality limit, the traceless symmetric order parameter χ is not constrained to be uniaxial, and one requires the full five numbers (six for a symmetric tensor minus one for the constraint of zero trace) to specify its local value. The geometric spaces representing the possible values of the order parameter in these two cases—the "order-parameter spaces"—have very different topological properties, with important implications for the kinds of line defects that can exist in either case.[21]

A region contains a line defect if the only way to maintain continuity of the order parameter on a closed path encircling the region as the path shrinks to a point is by allowing the order parameter to go to zero somewhere on the surface swept out by the shrinking path. Therefore, if we do not allow the order parameter to vanish, i.e., if we exclude the value zero from the order-parameter space, then a path encircles a defect if it is *impossible* to maintain continuity of the order parameter on the path as it shrinks to a point.

This criterion can be expressed in terms of the topology of the order-parameter space: a system has no topologically stable line defects if and only if any closed path in the order-parameter space can be continuously shrunk to a point. (Such a space is called "simply connected.")

The order-parameter space for a uniaxial tensor consists of a three-dimensional space excluding the origin, with every point identified with its inversion through the origin: the configuration represented by amplitude λ and direction $\mathbf{n}$ can be represented by the point $\mathbf{r}=\lambda\mathbf{n}$ in the order-parameter space, and since $\mathbf{n}$ and $-\mathbf{n}$ specify the same tensor, $\mathbf{r}$ and $-\mathbf{r}$ must be identified. Such a space has precisely one class of closed paths that cannot be shrunk to a point—namely, those connecting any point $\mathbf{r}_0$ with its negative $-\mathbf{r}_0$. (Such a path is closed because $\mathbf{r}_0$ and $-\mathbf{r}_0$ represent the same value of the order parameter; in contrast, closed paths connecting any point $\mathbf{r}_0$ to itself can be shrunk to a point.) If the values of the order parameter on a closed path in the nematic form such a path in the order-parameter space, then the path in real space must encircle a π disclination.

On the other hand, the order-parameter space for a general traceless symmetric nonzero tensor consists of all of a five-dimensional space (to specify each of the five independent components of the tensor) except for the origin (which would represent the zero tensor). Every point in this space corresponds to a distinct tensor order parameter. As a result, the only closed paths connect a point to itself, and since the absence of the origin clearly cannot prevent these from being shrunk to a point in more than two dimensions, there are no line defects.

We illustrate this with a simple example. Write a biaxial tensor $\mathbf{Q}$ as a sum of uniaxial tensors

$$Q_{ij}=\lambda[(n_in_j-\tfrac{1}{3}\delta_{ij})+\varepsilon(m_im_j-\tfrac{1}{3}\delta_{ij})] , \qquad (8.8)$$

where $\mathbf{m}$ and $\mathbf{n}$ are orthogonal vector fields in the x-y plane. If the vector field $\mathbf{n}$ has a stable singularity at a point P, and $\mathbf{Q}$ is restricted to be uniaxial ($\varepsilon=0$), then gradients of $\mathbf{Q}$ will diverge at P unless the amplitude λ of $\mathbf{Q}$ vanishes at that point. But if ε is allowed to grow to unity in the neighborhood of P, $\mathbf{Q}$ will have the form

$$Q_{ij}=\lambda(\tfrac{1}{3}\delta_{ij}-z_iz_j) \qquad (8.9)$$

near P (since $\delta_{ij}=m_im_j+n_in_j+z_iz_j$), which is constant and therefore has a vanishing gradient. Thus allowing $\mathbf{Q}$ to become biaxial can remove the singularity without requiring the amplitude λ to vanish.

How can one relate the view of blue phases in the low-chirality limit—uniaxial structures permeated by a network of line defects—to the more general picture of a tensor order parameter incapable of supporting such defects? If one takes the view that uniaxiality is the normal state of affairs, i.e., that low chirality is the physically pertinent limit, then the two points of view are reconciled when one takes into account the relaxation into biaxiality

[21]The discussion that follows is not intended to serve as a careful introduction to the topological theory of defects, but to remind readers acquainted with that subject of some of the relevant ideas, and to try to convey to unacquainted readers some rough indication of what is at stake here. For an introduction to the topological theory of defects, see Mermin (1979).

induced by spatial nonuniformities in the director $\mathbf{n}$.

We noted in Sec. V that if $\mathbf{n}(\mathbf{r})$ varies in the neighborhood of a point $\mathbf{r}_0$ in a way that breaks the local rotational symmetry about $\mathbf{n}(\mathbf{r}_0)$, then the order parameter at $\mathbf{r}_0$ will be unstable against acquiring a certain degree of biaxiality. In the low-chirality limit this relaxation into biaxiality will be negligibly small, except in regions where the spatial variation of $\mathbf{n}$ is very large (Meiboom, Sammon, and Brinkman, 1983). As the cores of line defects are approached in a strictly uniaxial phase, the gradients of $\mathbf{n}$ become arbitrarily large, so relaxation into biaxiality will occur in the cores no matter how low the chirality. Indeed, this is a far better solution to the core problem than remaining uniaxial with a vanishing amplitude, since a biaxial core, though it has a higher bulk free-energy density than a uniaxial phase of nonzero amplitude λ, is still energetically favored over an isotropic ($\lambda=0$) core, which makes no attempt at all to lower the bulk free energy by ordering.

It is important to note that one can identify the network of line defects characteristic of the low-chirality limit even in structures that are not nearly everywhere uniaxial. Corresponding networks can be found in the significantly biaxial order parameters characteristic of the high-chirality limit, notwithstanding the fact that a biaxial order parameter supports no line defects. The trick is simply knowing what to look for.

From the general point of view the order parameter is a real traceless symmetric tensor χ. It therefore has real eigenvalues and three orthonormal eigenvectors, and since χ is nonzero but has zero trace, at least one of these eigenvectors is associated with a positive eigenvalue. If the largest positive eigenvalue is not degenerate, then it belongs to a unique eigenvector, which we call $\mathbf{n}$ in anticipation of its identification below with the usual director in the uniaxial low chirality limit. Because $\chi(\mathbf{r})$ has no line singularities, neither can the vector field $\mathbf{n}(\mathbf{r})$ *unless* there are lines along which the largest eigenvalue of χ is degenerate. In the neighborhood of such lines, a small change in χ can change which eigenvalue is the largest, and therefore induce a large change in $\mathbf{n}$.

But if the largest eigenvalue of χ is degenerate, then the three eigenvalues are in the ratio $1:1:-2$. Thus χ is uniaxial, *but with the wrong (negative) sign for* $\mathrm{tr}(\chi^3)$. (Recall from Sec. IV that for given $\mathrm{tr}\chi^2$ the bulk free energy assumes its extreme values for a uniaxial χ, being minimum or maximum according to whether $\mathrm{tr}\chi^3$ is positive or negative.) Thus the lines along which $\mathbf{n}$ becomes singular are lines of maximally *unfavorable* bulk free energy, for the given value of $\mathrm{tr}\chi^2$.

We can thus associate with a biaxial tensor order parameter which is entirely free of line singularities a directorlike unit vector field $\mathbf{n}(\mathbf{r})$, which can have line singularities, along which the (well-behaved) tensor order parameter is uniaxial.

These unfavorably uniaxial lines in the high-chirality form of the order parameter are nothing but the residues of the cores of the line singularities that can exist undisguised in the low-chirality limit. To see this, imagine a uniaxial configuration supporting a conventional stable disclination such as one might find in a low-chirality nematic (a π disclination). As noted above, in the immediate vicinity of the core of the disclination a nonsingular biaxial core will be preferable to a completely disordered core of isotropic fluid. Far from the core the order parameter (being a uniaxial tensor with the favored sign for the cubic invariant) will indeed have a unique largest eigenvalue belonging to an eigenvector that is just the ordinary director $\mathbf{n}(\mathbf{r})$. Since the core lies within a π disclination, but the tensor order parameter is not singular in the core, we know from the above argument that within the core there must be a line along which the fluid is uniaxial with the unfavorable sign for the cubic invariant.

Now imagine turning up the chirality and letting the nematic adjust its configuration. As long as the largest eigenvalue remains nondegenerate in a region, the director field will evolve continuously into the field of the eigenvector belonging to that largest eigenvalue. Because the evolution is continuous, that field will continue to have a π disclination, and therefore at its core there must continue to be a line of unfavorably uniaxial material.

Thus if blue phases are characterized by a network of disclinations, as suggested by considerations appropriate to the low-chirality limit, one might expect to find similar structures even in the high-chirality limit, in the form of lines of unfavorably uniaxial material. In Sec. VI we noted precisely this behavior in the most favorable (body-centered-cubic O^5) structure currently known for the *infinite*-chirality limit. The O^5 structure has favorably uniaxial lines along $\langle 100 \rangle$ directions, but unfavorably uniaxial lines along $\langle 111 \rangle$ directions. The latter lines we now recognize as the signature in the nonsingular biaxial structure of what would become, with decreasing κ, the biaxial cores of uniaxial disclination lines.

Furthermore, in the vicinity of the favorably uniaxial lines in the high-chirality O^5 structure, one finds [see Eqs. (6.34)–(6.37)] that the structure of the order parameter is precisely that found in the vicinity of the axis of the double-twist cylinders that are locally favored in the low-chirality limit [though with a local pitch that is 50% larger ($q=\frac{2}{3}q_0$)].

Thus the two most characteristic structures of the low-chirality models—double-twist cylinders and π disclinations—can be unambiguously identified in the more systematic, but physically less pertinent high-chirality limit. This suggests that the defects that turn up in the structures guessed for the low-chirality limit may be inherent in the problem.[22] It also suggests that even though κ is not large, the structures emerging in the

[22]Hornreich and Shtrikman (1988b) argue that such defects are topologically necessary in the O^5 and O^2 structures, but not in the O^8 structure.

high-chirality limit already embody much of the pertinent physics and can serve as alternative starting points for more accurate investigations.

C. Exact minimization of the free energy in a curved space

One can also gain some insight into the role of defects in the blue phases by looking at them from a rather different point of view, as examples of "geometric frustration" (Meiboom *et al.*, 1981; Kleman, 1982; Sethna, 1983, 1985, 1987; Sethna, Wright, and Mermin, 1983; Dubois-Violette and Pansu, 1988).[23] A simple prototype of this phenomenon arises when one attempts to tile the plane with regular pentagons. In contrast to what happens with regular hexagons, if one starts trying to tile with pentagons one quickly runs into trouble: one can surround the first one with five adjoining neighbors, but already gaps are opened up between the neighbors, leading to even worse irregularities in the next layer [Fig. 23(a)]. The impossibility, for purely geometric reasons, of extending the preferred local ordering throughout a large region is reminiscent of the impossibility of extending perfect double twist through a region, as noted in Sec. VII.

The resemblance goes farther than this. The tiling problem with pentagons is solved if one moves it from a plane to the surface of a sphere of the appropriate radius: a regular dodecahedron can be viewed as a perfect tiling of the sphere with regular pentagons on its curved surface [Fig. 23(b)]. Interestingly, the corresponding problem for blue phases can also be solved in an appropriate curved space, but because the blue phase structure is inherently three-dimensional, the space required is the three-dimensional surface of a four-dimensional sphere (Sethna, Wright, and Mermin, 1983). For the appropriate choice of radius, perfect double twist can be extended over the whole surface, and in doing so one succeeds in minimizing the full free energy $\varphi=\varphi_{\rm grad}+\varphi_{\rm bulk}$.

To show this we rewrite the gradient free-energy density once again, this time casting Eq. (7.3) into the form

$$\varphi_{\rm grad}=\kappa^2(\chi_{ij;k}+\tfrac{1}{2}\varepsilon_{iks}\chi_{sj}+\tfrac{1}{2}\varepsilon_{jks}\chi_{si})^2 \ . \qquad (8.10)$$

[This differs from Eq. (7.3) by an extra $\frac{1}{2}{\rm tr}\chi^2$, which can be absorbed into a redefined $\varphi_{\rm bulk}$. One can also relax the one-constant approximation by adding to Eq. (8.10) a term $\kappa_0^2(\chi_{ij;j})^2$ without altering the curved-space solution described below.] We have changed the notation for gradients in Eq. (8.10), replacing $\nabla_k\chi_{ij}$ with $\chi_{ij;k}$ [defined explicitly in Eq. (8.15) below], in anticipation of the fact that in a curved space both the components of a tensor *and* the basis vectors must in general vary with position, making it necessary to distinguish between the gradient of the components and the components of the gradient. [The relation between the two is given in Eq. (8.16) below.]

We wish to minimize Eq. (8.10) not in ordinary three-dimensional Euclidean space, but in the curved three-dimensional surface S_3 of a sphere of radius a in four dimensions. We introduce ordinary Cartesian coordinates in the four-dimensional space, so that S_3 consists of the set of points (x_0,x_1,x_2,x_3) with $x_\mu x_\mu=a^2$. (Our summation convention is that repeated greek indices are summed from 0 to 3, and repeated roman indices from 1 to 3.)

For each point (x_0,x_1,x_2,x_3) on S_3 we define the unit radius vector

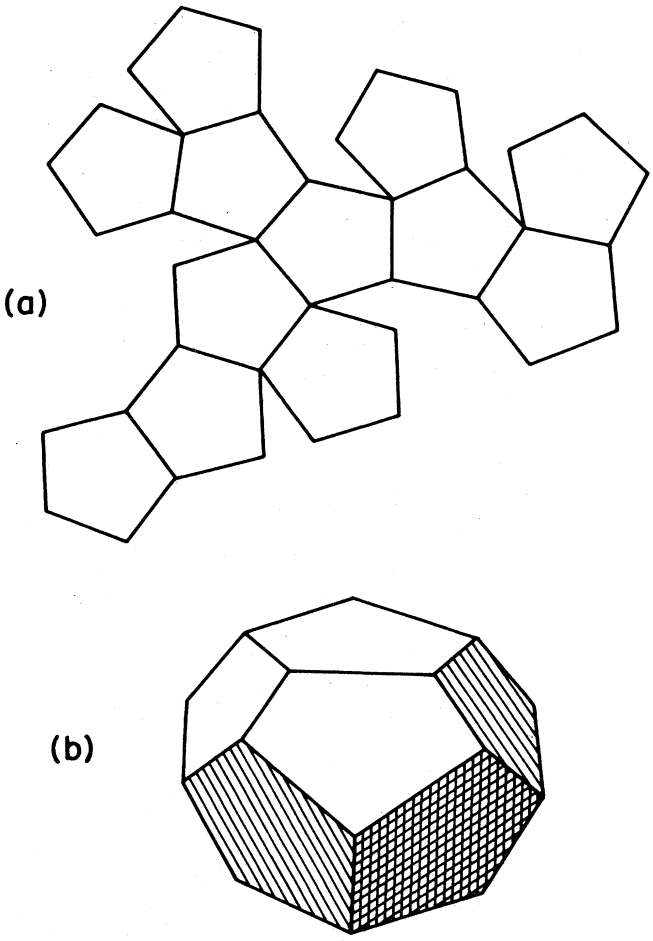

FIG. 23. (a) An example of geometric frustration in flat, two-dimensional space. If we consider the pentagonal tiles to represent some preferred local order with pentagonal symmetry, then the observation that pentagons cannot tile a plane illustrates the fact that local pentagonal order cannot be extended throughout a region without introducing defects. (b) By working in an appropriately curved space, the incompatibility between local and global order can be removed.

[23]For studies of geometric frustration in other systems, see for example Frank (1952), Frank and Kasper (1958, 1959), Kleman and Sadoc (1979), Sadoc (1980), Kleman (1981, 1983, 1985), Steinhardt, Nelson, and Ronchetti (1981, 1983), Sadoc and Mosseri (1982, 1984), Nelson (1982, 1983a, 1983b), Renn and Lubensky (1988).

$$\mathbf{e}^{(0)}=(1/a)(x_0,x_1,x_2,x_3) \tag{8.11}$$

and introduce three additional orthonormal vectors $\mathbf{e}^{(1)}$, $\mathbf{e}^{(2)}$, and $\mathbf{e}^{(3)}$ tangent to S_3—i.e., orthogonal to the radius vector $\mathbf{e}^{(0)}$:

$$\begin{aligned}\mathbf{e}^{(1)}&=(1/a)(-x_1,x_0,x_3,-x_2)\ ,\\ \mathbf{e}^{(2)}&=(1/a)(-x_2,-x_3,x_0,x_1)\ ,\\ \mathbf{e}^{(3)}&=(1/a)(-x_3,x_2,-x_1,x_0)\ ,\end{aligned} \tag{8.12}$$

satisfying

$$\mathbf{e}^{(\mu)}\cdot\mathbf{e}^{(\nu)}=e_\alpha^{(\mu)}e_\alpha^{(\nu)}=\delta_{\mu\nu}\ . \tag{8.13}$$

The three $\mathbf{e}^{(i)}$ at any point form an orthonormal basis for the local 3-space tangent to S_3.

We define a field of traceless symmetric 3-tensors $\chi_{\mu\nu}$ on S_3 by giving the components of such tensors in the orthonormal 3-basis for the local tangent space, $\mathbf{e}^{(i)}$:

$$\chi_{\mu\nu}=\chi_{ij}e_\mu^{(i)}e_\nu^{(j)}\ . \tag{8.14}$$

The gradient of χ in S_3 at any point is given by simply projecting the four-dimensional gradient into the tangent 3-space at the point

$$\chi_{ij;k}=e_\mu^{(i)}e_\nu^{(j)}e_\alpha^{(k)}\nabla_\alpha\chi_{\mu\nu}\ . \tag{8.15}$$

Substituting in Eq. (8.14) and writing $\nabla_k=e_\alpha^{(k)}\nabla_\alpha$, we have, with the aid of Eq. (8.13),

$$\chi_{ij;k}=\nabla_k\chi_{ij}+(e_\mu^{(i)}\nabla_k e_\mu^{(s)})\chi_{sj}+(e_\mu^{(j)}\nabla_k e_\mu^{(s)})\chi_{is}\ . \tag{8.16}$$

Note that in addition to the first term that gives the derivatives of the components of χ familiar from flat-space calculations with a position-independent set of basis vectors $\mathbf{e}^{(i)}$, there are two additional terms ("connection coefficients") in Eq. (8.16) as a result of the fact that variations in χ can also be produced by variations in the local 3-basis (Aris, 1962; Misner *et al.*, 1971; Schutz, 1980). The reason the full free energy can be explicitly minimized in the appropriately curved space is that it is possible to curve the 3-space so that these additional terms in Eq. (8.16) precisely cancel the two terms containing ε in Eq. (8.10), as we shall show.

This cancellation is most expeditiously established by working with the three Pauli matrices σ^i, about which it is only necessary to know that they are 2×2 traceless Hermitian matrices satisfying

$$\sigma^i\sigma^j=\delta_{ij}+i\varepsilon_{ijk}\sigma^k\ . \tag{8.17}$$

We then define a set of four matrices τ^μ by

$$\tau^0=1,\quad \tau^i=i\sigma^i,\quad i=1,\ldots,3\ , \tag{8.18}$$

and note that it follows from Eq. (8.17) and the tracelessness and Hermiticity of the Pauli matrices that

$$\tfrac{1}{2}\mathrm{tr}(\tau^\mu)^\dagger\tau^\nu=\delta_{\mu\nu}\ . \tag{8.19}$$

With this apparatus at hand, the basis vectors $\mathbf{e}^{(\alpha)}$ can be written as

$$e_\mu^{(\alpha)}\tau^\mu=\tau^\alpha x_\nu\tau^\nu/a\ . \tag{8.20}$$

Since $\tau^0=1$, it follows directly that $\mathbf{e}^{(0)}$ is indeed the radial unit vector $(1/a)\,(x_0,x_1,x_2,x_3)$. Using the multiplication rule (8.17) for the Pauli matrices one can easily verify that Eq. (8.20) gives the explicit forms (8.12) for the other $\mathbf{e}^{(i)}$. All of the pertinent properties of the $\mathbf{e}^{(\alpha)}$ can be established directly from Eq. (8.20). Note first that it follows from Eq. (8.19) that

$$e_\mu^{(\alpha)}e_\mu^{(\beta)}=\tfrac{1}{2}\mathrm{tr}(e_\mu^{(\alpha)}\tau^\mu)^\dagger(e_\nu^{(\beta)}\tau^\nu) \tag{8.21}$$

and hence, from Eq. (8.20), that

$$e_\mu^{(\alpha)}e_\mu^{(\beta)}=(1/a^2)\tfrac{1}{2}\mathrm{tr}(\tau^\alpha)^\dagger\tau^\beta(x_\mu\tau^\mu)(x_\nu\tau^\nu)^\dagger\ . \tag{8.22}$$

But

$$\begin{aligned}(x_\mu\tau^\mu)(x_\nu\tau^\nu)^\dagger&=(x_0+ix_j\sigma^j)(x_0-ix_k\sigma^k)\\ &=x_0^2+x_ix_i=a^2\ ,\end{aligned} \tag{8.23}$$

and therefore

$$e_\mu^{(\alpha)}e_\mu^{(\beta)}=\tfrac{1}{2}\mathrm{tr}(\tau^\alpha)^\dagger\tau^\beta=\delta_{\alpha\beta}\ , \tag{8.24}$$

as required.

To evaluate Eq. (8.16) we also require the form for $e_\mu^{(i)}\nabla_k e_\mu^{(j)}$, which we can easily work out more generally:

$$\begin{aligned}e_\mu^{(\alpha)}e_\nu^{(\beta)}\nabla_\nu e_\mu^{(\gamma)}&=(1/2)\mathrm{tr}(e_\mu^{(\alpha)}\tau^\mu)^\dagger(e_\nu^{(\beta)}\nabla_\nu)(e_\lambda^{(\gamma)}\tau^\lambda)\\ &=(1/2a)\mathrm{tr}(e_\mu^{(\alpha)}\tau^\mu)^\dagger\tau^\gamma(e_\nu^{(\beta)}\tau^\nu)=(1/2a)\mathrm{tr}\tau^\gamma(e_\nu^{(\beta)}\tau^\nu)(e_\mu^{(\alpha)}\tau^\mu)^\dagger\\ &=(1/2a)\mathrm{tr}\tau^\gamma\tau^\beta(x_\rho\tau^\rho)(x_\sigma\tau^\sigma)^\dagger(\tau^\alpha)^\dagger/a^2=(1/2a)\mathrm{tr}\tau^\gamma\tau^\beta(\tau^\alpha)^\dagger\ .\end{aligned} \tag{8.25}$$

Specializing this to the three vectors in the tangent space, we have

$$\begin{aligned}e_\mu^{(i)}e_\nu^{(j)}\nabla_\nu e_\mu^{(k)}&=(1/2a)i\ \mathrm{tr}\sigma^k\sigma^j\sigma^i\\ &=(1/a)\varepsilon_{kji}=-(1/a)\varepsilon_{ijk}\ .\end{aligned} \tag{8.26}$$

Evaluating the gradient free energy (8.10) with Eqs. (8.26) and (8.16) we find that if we pick the radius of S_3 to be $a=2$ (or, in dimensional units, $a=1/q_0$), then we have simply

$$\varphi_{\mathrm{grad}}=\kappa^2(\nabla_i\chi_{jk})^2\ . \tag{8.27}$$

This is evidently minimized simply by taking the χ_{ij} to be (arbitrary) constants. [Note that this conclusion is not altered if the one-constant approximation is relaxed to in-

clude the additional term $\kappa_0^2(\chi_{ij;j})^2$, since Eqs. (8.26) and (8.16) give $\chi_{ij;j}=\nabla_j\chi_{ij}$.] Since the bulk free energy is entirely local, it is unaffected by the move to a curved space and continues to be minimized by a uniaxial tensor of the appropriate overall amplitude. We conclude that the full free energy $\varphi=\varphi_{\rm grad}+\varphi_{\rm bulk}$ is minimized by any tensor χ whose components in the basis of the $\mathbf{e}^{(i)}$ are of the form

$$\chi_{ij}=\frac{\lambda}{\sqrt{6}}(3n_in_j-\delta_{ij})\ , \tag{8.28}$$

for arbitrary constant n_i and constant amplitude λ (with the magnitude that minimizes the bulk free energy).

It follows from Eq. (8.26) that the gradients of the vector field $\mathbf{n}$ satisfy the double-twist condition (7.10) *everywhere* on S_3, for we have

$$n_{i;j}=\nabla_i n_j+e_\mu^{(i)}\nabla_j e_\mu^{(k)}n_k=-\tfrac{1}{2}\epsilon_{ijk}n_k\ . \tag{8.29}$$

Since real chiral nematics are not found on the surfaces of four-dimensional spheres of radius $1/q_0=p/2\pi$, these facts are of more conceptual than practical interest. Real chiral nematics can be viewed as systems that are frustrated by the misfortune of having to exist in a space incompatible with their energetic demands, which favor double twist at all points. The disclinations that show up in both the low and (properly interpreted) high-chirality models of the blue phases can then be viewed as the inevitable consequences of having to tear apart the ideal curved-space structure if it is to be flattened into ordinary space (Kleman and Sadoc, 1979; Sadoc and Mosseri, 1982; Kleman, 1983; Sethna, 1983, 1985, 1987). They are thus as natural to blue phases as the disclinations that arise from flattening out a dodecahedron are to doomed attempts to tile a plane perfectly with pentagons.

Although the curved-space model is highly suggestive that double twist is the natural state of the chiral nematic, it does not without further (difficult) analysis shed any light on whether or not the traumatic consequences of flattening will preserve anything of the local double twist in the ensuing flat-space structures. Just as pentagons in flat space always have the option of settling into a regular periodic array that makes no attempt to optimize the local energy, so chiral nematics in flat space can always settle for the helical phase.

The chiral ferromagnet serves here as a cautionary demonstration that the most favorable flat-space configuration may make no attempt to reproduce the ideal curved-space structure, for the fields $\mathbf{e}^{(i)}$ are globally well defined on S_3 and can therefore define a vector as well as a tensor order parameter. The equilibrium state of the chiral ferromagnet on S_3 is therefore also a state of perfect double twist, but the result established in Sec. VIII.A above shows that none of the double twist survives in the flattened state, which achieves its equilibrium in the conventional singly twisting helical form.

It seems appropriate to conclude on this abstract four-dimensional note our exposition of the current theoretical understanding of blue phases, those "tangible examples of topological oddities" that "help to bring topology into the public domain of science."

ACKNOWLEDGMENTS

We are indebted to Jim Sethna for several years of stimulating and instructive conversations about blue phases, and for his extended program of advanced advertising for this pedagogical review. Dan Rokhsar's insights and his enthusiasm for the blue phase have been continual inspirations, and the experimental section has benefited from the comments of Pete Crooker and Paul Keyes. Sandra Troian has helped in our efforts to clarify some of the mathematical treatments of blue phases, and our efforts to keep our prose under control have benefited from the astute criticism of Lisbeth Gronlund. We are grateful to John Wilkins for disagreeing on the occasions when we decided we had not gone too far to abandon the project, and we would like to thank Henry Hall for explaining to us the difference between a spiral and a helix. This work was supported by the National Science Foundation through Grant No. DMR-86-13368 and through the Cornell Materials Science Center, Grant No. DMR-85-16616.

APPENDIX A: THE PARAMETERS OF HORNREICH AND SHTRIKMAN

Our definitions of the parameters of the Ginzburg-Landau theory differ in some cases from those used by Hornreich, Shtrikman, and co-workers. We give here the relation between these two sets.

	Hornreich-Shtrikman	Wright-Mermin
Elastic constants	c_1	$\frac{1}{2}K_1$
	c_2	$\frac{1}{2}(K_0-K_1)$
Bulk free-energy constants	a	$2c$
	β	$\sqrt{6}b$
	γ	a
Chirality	$\kappa_{\rm (HS)}$	$2\kappa_{\rm (WM)}$
Inverse helical pitch	$\frac{1}{2}q_c=d/(2c_1)$	$q_0=2\pi/p_0$
Coherence length	ξ_R	ξ
Reduced temperature	$\frac{1}{4}t$	$\tau+\kappa^2_{\rm (WM)}$

APPENDIX B: TRACE RELATIONS

Given an $n\times n$ matrix $\mathbf{Q}$, one can construct only n independent scalars from $\mathbf{Q}$. In particular, $\mathrm{tr}(\mathbf{Q}^s)$ for all $s>n$ can be expressed in terms of those $\mathrm{tr}(\mathbf{Q}^s)$ with $s\le n$. We give here a general method of determining these relations.

We start by generating the trace relations when the $n\times n$ matrix $\mathbf{M}$ is Hermitian. Begin with the identity

$$\det(1-\lambda\mathbf{M})=e^{\mathrm{tr}\ln(1-\lambda\mathbf{M})} \tag{B1}$$

for $\lambda<1/m_{\max}$, where $m_{\max}$ is the largest eigenvalue of $\mathbf{M}$. Expanding the logarithm, we get

$$\det(1-\lambda\mathbf{M})=\exp\left[-\sum_{s=1}^{\infty}\frac{\lambda^s}{s}\mathrm{tr}(\mathbf{M}^s)\right]$$
$$=\sum_{t=0}^{\infty}\frac{(-1)^t}{t!}\left[\sum_{s=1}^{\infty}\frac{\lambda^s}{s}\mathrm{tr}(\mathbf{M}^s)\right]^t . \tag{B2}$$

The left-hand side is an nth-order polynomial in λ, and hence the coefficients of λ^s for $s>n$ on the right-hand side must vanish term by term. These conditions give the desired relations.

To show that these relations hold for an arbitrary $n\times n$ matrix $\mathbf{Q}$, let

$$\mathbf{M}=\left[\frac{\mathbf{Q}+\mathbf{Q}^\dagger}{2}\right]+\mu\left[\frac{\mathbf{Q}-\mathbf{Q}^\dagger}{2i}\right] , \tag{B3}$$

so that $\mathbf{M}$ is Hermitian when μ is real. The trace relations (B2) now hold identically as polynomials in the real variable μ. (The trace relations are homogeneous, so the restriction on the largest eigenvalue is no longer important.) Since polynomials are analytic functions, however, the trace relations also hold for $\mu=i$, for which $\mathbf{M}=\mathbf{Q}$.

For example, if $\mathbf{M}$ is 3×3, the vanishing of the coefficient of λ^4 in Eq. (B2) gives

$$0=-\tfrac{1}{4}\mathrm{tr}(\mathbf{M}^4)+\tfrac{1}{8}(\mathrm{tr}\mathbf{M})^2+\tfrac{1}{3}\mathrm{tr}\mathbf{M}\,\mathrm{tr}(\mathbf{M}^3)$$
$$-\tfrac{1}{4}(\mathrm{tr}\mathbf{M})^2\mathrm{tr}(\mathbf{M})^2+\tfrac{1}{24}(\mathrm{tr}\mathbf{M})^4 , \tag{B4}$$

which for $\mathrm{tr}\mathbf{M}=0$ gives

$$\mathrm{tr}(\mathbf{M}^4)=\tfrac{1}{2}[\mathrm{tr}(\mathbf{M}^2)]^2 . \tag{B5}$$

APPENDIX C: STABILITY OF THE GRADIENT ENERGY

We shall show that the gradient free energy

$$F_g=\int d\mathbf{r}[\tfrac{1}{4}K_1(\nabla\times\mathbf{Q}+2q_0\mathbf{Q})^2+\tfrac{1}{4}K_0(\nabla\cdot\mathbf{Q})^2] \tag{C1}$$

is non-negative throughout its region of stability and is minimized by $F_g=0$. To do this, we Fourier-transform $\mathbf{Q}$,

$$\mathbf{Q}(\mathbf{r})=\frac{1}{V}\sum_{\mathbf{k}}e^{i\mathbf{k}\cdot\mathbf{r}}\mathbf{Q}(\mathbf{k}) , \tag{C2}$$

where $\mathbf{Q}(-\mathbf{k})=\mathbf{Q}(\mathbf{k})^*$ since $\mathbf{Q}(\mathbf{r})$ is real, and recast Eq. (C1) in the form

$$F_g=\int d\mathbf{r}\,f_g=\frac{1}{16V}\sum_{\mathbf{k}}\{|Q_- -2iQ_{xy}|^2K_1(k+2q_0)^2+|Q_-+2iQ_{xy}|^2K_1(k-2q_0)^2$$
$$+2|Q_+|^2[(K_1+2K_0)k^2+12K_1q_0^2]+|Q_{xz}-iQ_{yz}|^2[K_1(k+4q_0)^2+(K_1+2K_0)k^2]$$
$$+|Q_{xz}+iQ_{yz}|^2[K_1(k-4q_0)^2+(K_1+2K_0)k^2]\} , \tag{C3}$$

where $Q_\pm=Q_{xx}\pm Q_{yy}$, and in each term of the summation the z axis is taken along $\mathbf{k}$.

From Eq. (C3) it is obvious that F_g is non-negative as long as

$$K_1\geq0 \quad\text{and}\quad K_1+2K_0\geq0 , \tag{C4}$$

while if either of these conditions is violated, F_g becomes unbounded below. We emphasize that this instability is an instability against gaining unbounded gradients, and is not a trivial amplitude instability which would be cured by including a bulk free energy.

One can also determine from Eq. (C3) the unique (to within rotations) structure that minimizes F_g. To make F_g vanish, we must set $k=\pm2q_0$, $Q_-=\pm2iQ_{xy}$, and $Q_+=Q_{xz}=Q_{yz}=0$ in (C3). This gives the Fourier components of the biaxial helical structure given in Eq. (4.17).

APPENDIX D: ESTIMATING PHYSICAL VALUES OF κ

Equation (4.27) gives the chirality κ in terms of physical quantities as

$$\kappa=(K_1q_0^2a/b^2)^{1/2} , \tag{D1}$$

where a and b are the quartic and cubic terms in the bulk free energy, K_1 is the elastic coefficient in the gradient free energy, and q_0 is 2π over the helical phase pitch. Typical values of the pitch of chiral nematics that show blue phases are in the range 1000–6000 Å, giving q_0 roughly in the range 10^5–10^6 cm^{-1}. Various groups have measured elastic constants for nematics (see Appendix F). From these, one finds that typical values of K_1 lie in the range 10^{-14}–10^{-13} J/cm.

While measurements of the bulk free-energy parameters a and b are not available for chiral nematics, we can use values measured for ordinary nematics to estimate κ. To compare Eq. (4.5) for the bulk free energy with experiment, we insert a uniaxial form for the order parameter

$$Q_{ij}=\lambda(n_in_j-\tfrac{1}{3}\delta_{ij}) , \tag{D2}$$

yielding

$$f_{\mathrm{bulk}}=\tfrac{2}{3}c\lambda^2-\tfrac{2}{9}\sqrt{6}b\lambda^3+\tfrac{4}{9}a\lambda^4 . \tag{D3}$$

The bulk coefficients have been determined by Stinson and Litster (1970) for the nematic compound MBBA, and by Poggi, Filippini, and Aleonard (1976) for the two compounds MBBA and HBN. From these, one finds that

$a/b^2 \simeq 5.3\ \mathrm{J^{-1}cm^3}$ for MBBA and $a/b^2 \simeq 2.0\ \mathrm{J^{-1}cm^3}$ for HBN.

Combining these ranges of values of a, b, K_1, and q_0 gives values of κ roughly in the range 0.01–0.5.

APPENDIX E: MAXIMIZING THE CUBIC INVARIANT

In this appendix, we show that the cubic invariant β in Eq. (6.15) is maximized by taking all the coefficients ζ_n to be real. This requires maximizing the function

$$g = \cos\alpha + \cos\beta + \cos\gamma + \cos\delta \tag{E1}$$

subject to the constraint

$$\alpha + \beta + \gamma + \delta = 4\varphi + 2\pi n \ , \tag{E2}$$

where φ is the phase of $(23 + 5\sqrt{8}i)$. This leads to the condition

$$\sin\alpha = \sin\beta = \sin\gamma = \sin\delta = \lambda \ , \tag{E3}$$

where λ is a Lagrange multiplier.

Note that given a set of values of α, β, γ, and δ satisfying the stationary condition (E3) and constraint (E2), the values $\pi-\alpha$, $\pi-\beta$, $\pi-\gamma$, and $\pi-\delta$ also satisfy the stationary condition and constraint but change the sign of g. We therefore need consider only $g \geq 0$.

To within permutations of α, β, γ, and δ, there are only three possible solutions to Eq. (E3):

$$\begin{aligned} &\text{(a)}\ \ \alpha=\beta=\gamma=\delta \Longrightarrow g = 4|\cos\alpha| \ , \\ &\text{(b)}\ \ \alpha=\beta=\gamma,\ \ \delta=\pi-\alpha \Longrightarrow g = 2|\cos\alpha| \ , \\ &\text{(c)}\ \ \alpha=\beta,\ \ \gamma=\delta=\pi-\alpha \Longrightarrow g = 0 \ . \end{aligned} \tag{E4}$$

For case (a), Eq. (E2) requires $\alpha = \varphi + (\pi/2)n$, so that $|\cos\alpha| = \cos\varphi$ (for n even) or $|\cos\alpha| = \sin\varphi$ (for n odd). Since $\cos\varphi > \sin\varphi > 0$, the maximum value is given by $g = 4\cos\varphi$.

For case (b), Eq. (E2) gives $\alpha = 2\varphi - \pi/2 + \pi n$, so that $|\cos\alpha| = \sin 2\varphi$. This leads to $g = 2\sin 2\varphi = 4\cos\varphi\sin\varphi$, which is less than $4\cos\varphi$.

Thus g is maximized by $\alpha=\beta=\gamma=\delta=\varphi$, which requires that the products of ζ_n's in Eq. (6.15) be real. This can be achieved by taking all the ζ_n's to be real.

APPENDIX F: ELASTIC CONSTANTS IN THE UNIAXIAL LIMIT

The usual Frank free energy used to describe chiral nematics has the form

$$\tfrac{1}{2}k_s(\nabla\cdot\mathbf{n})^2 + \tfrac{1}{2}k_t(\mathbf{n}\cdot\nabla\times\mathbf{n} + q_0)^2 + \tfrac{1}{2}k_b[\mathbf{n}\times(\nabla\times\mathbf{n})]^2 \ , \tag{F1}$$

where the terms correspond to the free-energy cost of splay, twist, and bend distortions of the director field $\mathbf{n}$, respectively. (The elastic constants for these terms are frequently written as k_{11}, k_{22}, and k_{33}.) This form can be recovered (to within a surface term) from the gradient free energy [Eq. (4.14)] for the full tensor order parameter by taking $\mathbf{Q}$ to be uniaxial with a constant amplitude:

$$Q_{ij} \propto (n_i n_j - \tfrac{1}{3}\delta_{ij}) \ . \tag{F2}$$

Comparing the resulting equation to Eq. (F1), one finds

$$\begin{aligned} k_t &= K_1 \ , \\ k_s &= k_b = \tfrac{1}{2}(K_1 + K_0) \ , \end{aligned} \tag{F3}$$

where K_1 and K_0 are the elastic constants appearing in Eq. (4.14).

As expected, the one-constant approximation $\eta \equiv K_0/K_1 = 1$ corresponds to the case $k_s = k_t = k_b$. Notice that deriving the free energy (F1) from Landau theory with a tensor order parameter and quadratic gradient energy does not lead to three independent elastic constants, since it imposes the condition $k_s = k_b$. Thus the measured values of the elastic constants can test the validity of the simplest Landau theory as well as the one-constant approximation.

While measurements of the elastic constants of chiral nematics are difficult to come by, we note the results of measurements of k_s, k_t, and k_b in a number of ordinary (nonchiral) nematics, but of course there is no guarantee that the values of k_t will be similar in the two systems.

In the nematic compounds measured, the elastic constants typically have values in the range 10^{-14}–10^{-13} J/cm. In the compound MBBA, k_b/k_s is in the range 1.1–1.3 (Haller, 1972; Greulich *et al.*, 1975; Langevin *et al.*, 1975; Poggi *et al.*, 1975; Usui *et al.*, 1979; Miraldi *et al.*, 1981, 1982), and k_t/k_s is in the range 0.6–0.7 (Langevin *et al.*, 1975; Usui *et al.*, 1979; Miraldi *et al.*, 1981, 1982). In members of the series *n*CB and *n*OCB ($n = 5,6,7$), Bradshaw *et al.* (1985) found $k_b/k_s \simeq 1.0$–1.5, while for *n*CB ($n = 5,6,7$) Karat and Madhusudana (1977, 1978) found $k_b/k_s \simeq 1.6$–2.0 and $k_t/k_s \simeq 0.4$–0.5. In PAA, Gruler (1973) found $k_b/k_s \simeq 1.7$–2.1 and $k_t/k_s \simeq 0.5$–0.6.

The observation that k_b/k_t is greater than unity could be accounted for in Landau theory by keeping terms in the gradient free-energy expansion of higher than quadratic order. We expect, however, that this would have little effect on the general features predicted by the model. We note that k_t in all of these systems is considerably smaller than k_s and k_b. This may indicate that in actual systems η is greater than unity ($\eta = 3$ corresponds to the case $k_s = k_b = 2k_t$).

REFERENCES

Alexander, S., 1981, in *Symmetry and Broken Symmetry in Condensed Matter Physics*, edited by N. Boccara (IDSET, Paris), p. 141.

Alexander, S., R. M. Hornreich, and S. Shtrikman, 1981, in *Symmetry and Broken Symmetry in Condensed Matter Physics*, edited by N. Boccara (IDSET, Paris), p. 379.

Alexander, S., and J. McTague, 1978, Phys. Rev. Lett. **41**, 702.
Aris, R., 1962, *Vectors, Tensors and the Basic Equations of Fluid Mechanics* (Prentice-Hall, New Jersey), p. 166.
Armitage, D., and R. J. Cox, 1980, Mol. Cryst. Liq. Cryst. Lett. **64**, 41.
Armitage, D., and F. P. Price, 1975, J. Phys. (Paris) Colloq. **36**, C1-133.
Armitage, D., and F. P. Price, 1976, J. Appl. Phys. **47**, 2735.
Armitage, D., and F. P. Price, 1977, J. Chem. Phys. **66**, 3414.
Arnold, H., and P. Roediger, 1968, Z. Phys. Chem. **239**, 283.
Ashcroft, N. W., and N. D. Mermin, 1976, *Solid State Physics* (Holt, Rinehart and Winston, New York).
Barbet-Massin, R., P. E. Cladis, and P. Pieranski, 1984a, Recherche **15**, 548.
Barbet-Massin, R., P. E. Cladis, and P. Pieranski, 1984b, Phys. Rev. A **30**, 1161.
Barbet-Massin, R., and P. Pieranski, 1984, J. Phys. (Paris) Lett. **45**, L-799.
Barbet-Massin, R., and P. Pieranski, 1985, J. Phys. (Paris) Colloq. **46**, C3-61.
Barrall, E. M., R. S. Porter, and J. F. Johnson, 1967, Mol. Cryst. **3**, 103.
Bartolino, R., T. Chiaranza, M. Meuti, and R. Compagnoni, 1982, Phys. Rev. A **26**, 1116.
Baym, G., H. A. Bethe, and C. Pethick, 1971, Nucl. Phys. A **175**, 225.
Beevers, M. S., D. A. Elliott, and G. Williams, 1982, Mol. Cryst. Liq. Cryst. **80**, 135.
Belyakov, V. A., and V. E. Dmitrienko, 1985, Usp. Fiz. Nauk **146**, 369 [Sov. Phys. Usp. **28**, 535 (1985)].
Belyakov, V. A., V. E. Dmitrienko, and S. M. Osadchii, 1982, Zh. Eksp. Teor. Fiz. **83**, 585 [Sov. Phys. JETP **56**, 322 (1982)].
Bensimon, D., E. Domany, and S. Shtrikman, 1983, Phys. Rev. A **28**, 427.
Bergmann, K., P. Pollman, G. Scherer, and H. Stegemeyer, 1979, Z. Naturforsch. **34a**, 253.
Bergmann, K., and H. Stegemeyer, 1978, Ber. Bunsenges. Phys. Chem. **82**, 1309.
Bergmann, K., and H. Stegemeyer, 1979a, Z. Naturforsch. **34a**, 251.
Bergmann, K., and H. Stegemeyer, 1979b, Z. Naturforsch. **34a**, 1031.
Berreman, D. W., 1984, in *Liquid Crystals and Ordered Fluids, Vol. 4,* edited by A. C. Griffin and J. F. Johnson (Plenum, New York), p. 925.
Berreman, D. W., and S. Meiboom, 1984, Phys. Rev. A **30**, 1955.
Berreman, D. W., and S. Meiboom, J. A. Zasadzinski, and M. J. Sammon, 1986, Phys. Rev. Lett. **57**, 1737.
Blümel, Th., P. J. Collings, H. Onusseit, and H. Stegemeyer, 1985, Chem. Phys. Lett. **116**, 529.
Blümel, Th., and H. Stegemeyer, 1984a, J. Cryst. Growth **66**, 163.
Blümel, Th., and H. Stegemeyer, 1984b, Phys. Lett. A **104**, 277.
Blümel, Th., and H. Stegemeyer, 1985, Z. Naturforsch. **40a**, 260.
Blümel, Th., and H. Stegemeyer, 1988, Liq. Cryst. **3**, 195.
Bradshaw, M. J., E. P. Raines, J. D. Bunning, and T. E. Faber, 1985, J. Phys. (Paris) **46**, 1513.
Brazovskii, S. A., 1975, Zh. Eksp. Teor. Fiz. **68**, 175 [Sov. Phys. JETP **41**, 85 (1975)].
Brazovskii, S. A., and S. G. Dmitriev, 1975, Zh. Eksp. Teor. Fiz. **69**, 979 [Sov. Phys. JETP **42**, 497 (1975)].
Brazovskii, S. A., and V. M. Filev, 1978, Zh. Eksp. Teor. Fiz. **75**, 1140 [Sov. Phys. JETP **48**, 573 (1979)].
Brinkman, W. F., and P. E. Cladis, 1982, Phys. Today **35**, 48.
Brog, T. K., and P. J. Collings, 1980, Mol. Cryst. Liq. Cryst. **60**, 65.
Burzlaff, H., and H. Zimmerman, 1987, *International Tables for Crystallography* (Reidel, Boston), p. 793.
Chandrasekhar, S., 1977, *Liquid Crystals* (Cambridge University, Cambridge, England).
Chanishvili, A. G., G. S. Chilaya, Z. M. Elashvili, S. P. Ivchenko, D. G. Khoshtaria, and K. D. Vinokur, 1986, Mol. Cryst. Liq. Cryst. Lett. **3**, 91.
Chidichimo, G., Z. Yaniv, N. A. P. Vaz, and J. W. Doane, 1982, Phys. Rev. A **25**, 1077.
Chistyakov, I. G., and L. A. Gusakova, 1969, Kristallografiya **14**, 153 [Sov. Phys. Crystallogr. **14**, 132 (1969)].
Cladis, P. E., 1987, in *Theory and Applications of Liquid Crystals,* edited by J. L. Ericksen and D. Kinderlehrer (Springer, New York), p. 73.
Cladis, P. E., T. Garel, and P. Pieranski, 1986, Phys. Rev. Lett. **57**, 2841.
Cladis, P. E., P. Pieranski, and M. Joanicot, 1984, Phys. Rev. Lett. **52**, 542.
Clark, N. A., S. T. Vohra, and M. A. Handschy, 1984, Phys. Rev. Lett. **52**, 57.
Coates, D., and G. W. Gray, 1973, Phys. Lett. A **45**, 115.
Coates, D., and G. W. Gray, 1975, Phys. Lett. A **51**, 335.
Coates, D., K. J. Harrison, and G. W. Gray, 1973, Mol. Cryst. Liq. Cryst. **22**, 99.
Collings, P. J., 1984a, Mol. Cryst. Liq. Cryst. **113**, 277.
Collings, P. J., 1984b, Phys. Rev. A **30**, 1990.
Collings, P. J., 1986, Phys. Rev. A **33**, 2153.
Collings, P. J., and J. R. McColl, 1978, J. Chem. Phys. **69**, 3371.
Collings, P. J., T. J. McKee, and J. R. McColl, 1976, J. Chem. Phys. **65**, 3520.
Costello, M. J., S. Meiboom, and M. Sammon, 1984, Phys. Rev. A **29**, 2957.
Crooker, P. P., 1983, Mol. Cryst. Liq. Cryst. **98**, 31.
Crooker, P. P., 1985, Phys. Rev. A **31**, 1010.
Crooker, P. P., 1989, Liq. Cryst. (in press).
Dandoloff, R., and R. Mosseri, 1987, Europhys. Lett. **3**, 1193.
de Gennes, P. G., 1971, Mol. Cryst. Liq. Cryst. **12**, 193.
de Gennes, P. G., 1974, *Physics of Liquid Crystals* (Oxford University, London).
Demikhov, E. I., and V. K. Dolganov, 1983, Pis'ma Zh. Eksp. Teor. Fiz. **38**, 368 [JETP Lett. **38**, 445 (1983)].
Demikhov, E. I., V. K. Dolganov, and S. P. Krylova, 1985, Pis'ma Zh. Eksp. Teor. Fiz. **42**, 15 [JETP Lett. **42**, 16 (1985)].
Demus, D., H.-G. Hahn, and F. Kuschel, 1978, Mol. Cryst. Liq. Cryst. **44**, 61.
Demus, D., and L. Richter, 1978, *Textures of Liquid Crystals* (Weinheim, New York).
Dreher, R., G. Meier, and A. Saupe, 1971, Mol. Cryst. Liq. Cryst. **13**, 17.
Dubois-Violette, E., and B. Pansu, 1988, Mol. Cryst. Liq. Cryst. **165**, 151.
Elser, W., 1966, Mol. Cryst. **2**, 1.
Elser, W., J. L. W. Pohlmann, and P. R. Boyd, 1973, Mol. Cryst. Liq. Cryst. **20**, 77.
Feldman, A. I., P. P. Crooker, and L. M. Goh, 1987, Phys. Rev. A **35**, 842.
Fergason, J., N. Goldberg, and R. Nadalin, 1966, Mol. Cryst. **1**, 309.
Filev, V. M., 1986, Pis'ma Zh. Eksp. Teor. Fiz. **43**, 523 [JETP Lett. **43**, 677 (1986)].

Finn, P. L., and P. E. Cladis, 1981, Mol. Cryst. Liq. Cryst. Lett. **72**, 107.
Finn, P. L., and P. E. Cladis, 1982, Mol. Cryst. Liq. Cryst. **84**, 159.
Flack, J. H., and P. P. Crooker, 1981a, Mol. Cryst. Liq. Cryst. **69**, 281.
Flack, J. H., and P. P. Crooker, 1981b, Phys. Lett. A **82**, 247.
Flack, J. H., P. P. Crooker, D. L. Johnson, and S. Long, 1984, in *Liquid Crystals and Ordered Fluids, Vol. 4,* edited by A. C. Griffin and J. F. Johnson (Plenum, New York), p. 901.
Flack, J. H., P. P. Crooker, and R. C. Svoboda, 1982, Phys. Rev. A **26**, 723.
Frank, F. C., 1952, Proc. R. Soc. London, Ser. A **215**, 43.
Frank, F. C., 1958, Discuss. Faraday Soc. **25**, 19.
Frank, F. C., 1983, Philos. Trans. R. Soc. London, Ser. A **309**, 71.
Frank, F. C., and J. S. Kasper, 1958, Acta Crystallogr. **11**, 184.
Frank, F. C., and J. S. Kasper, 1959, Acta Crystallogr. **12**, 483.
Freiser, M. J., 1970, Phys. Rev. Lett. **24**, 1041.
Friedel, G., 1922, Ann. Phys. (Paris) **18**, 273.
Gerber, P. R., 1984, Mol. Cryst. Liq. Cryst. **111**, 267.
Gerber, P. R., 1985, Mol. Cryst. Liq. Cryst. **116**, 197.
Gleeson, H., R. Simon, and H. J. Coles, 1985, Mol. Cryst. Liq. Cryst. **129**, 37.
Gorman, J. W., Jr., and P. P. Crooker, 1985, Phys. Rev. A **31**, 910.
Gray, G. W., 1956, J. Chem. Soc. 3733.
Gray, G. W., 1962, *Molecular Structure and the Properties of Liquid Crystals* (Academic, New York).
Gray, G. W., and P. A. Winsor, 1974, Eds., *Liquid Crystals and Plastic Crystals* (Ellis Horwood, Chichester), pp. 12 and 16.
Grebel, H., R. M. Hornreich, and S. Shtrikman, 1983a, Phys. Rev. A **28**, 1114; **28**, 3669(E).
Grebel, H., R. M. Hornreich, and S. Shtrikman, 1983b, Phys. Rev. A **28**, 2544.
Grebel, H., R. M. Hornreich, and S. Shtrikman, 1984, Phys. Rev. A **30**, 3264.
Greulich, M., G. Heppke, and F. Schneider, 1975, Z. Naturforsch. **30a**, 515.
Gruler, H., 1973, Z. Naturforsch. **28a**, 474.
Hahn, Th., and A. Vos, 1987, *International Tables for Crystallography* (Riedel, Boston). p. 11.
Haller, I., 1972, J. Chem. Phys. **57**, 1400.
Haller, I., and J. D. Lister, 1970, Phys. Rev. Lett. **25**, 1550.
Heppke, G., H.-S. Kitzerow, and M. Krumrey, 1985a, Mol. Cryst. Liq. Cryst. Lett. **2**, 59.
Heppke, G., H.-S. Kitzerow, and M. Krumrey, 1985b, Mol. Cryst. Liq. Cryst. Lett. **2**, 117.
Heppke, G., H.-S. Kitzerow, and M. Krumrey, 1987, Mol. Cryst. Liq. Cryst. **150b**, 265.
Heppke, G., M. Krumrey, and F. Oestreicher, 1983, Mol. Cryst. Liq. Cryst. **99**, 99.
Her, J., B. B. Rao, and J. T. Ho, 1981, Phys. Rev. A **24**, 3272.
Hornreich, R. M., M. Kugler, and S. Shtrikman, 1982, Phys. Rev. Lett. **48**, 1404.
Hornreich, R. M., M. Kugler, and S. Shtrikman, 1985a, Phys. Rev. Lett. **54**, 2099.
Hornreich, R. M., M. Kugler, and S. Shtrikman, 1985b, J. Phys. (Paris) Colloq. **46**, C3-47.
Hornreich, R. M., and S. Shtrikman, 1979, Bull. Isr. Phys. Soc. **25**, 46.
Hornreich, R. M., and S. Shtrikman, 1980a, in *Liquid Crystals of One and Two Dimensional Order,* edited by W. Helfrich and G. Heppke (Springer, Berlin), p. 185.
Hornreich, R. M., and S. Shtrikman, 1980b, J. Phys. (Paris) **41**, 335; **42**, 367(E) (1981).
Hornreich, R. M., and S. Shtrikman, 1981a, Phys. Lett. A **82**, 345.
Hornreich, R. M., and S. Shtrikman, 1981b, Phys. Lett. A **84**, 20.
Hornreich, R. M., and S. Shtrikman, 1981c, Phys. Rev. A **24**, 635.
Hornreich, R. M., and S. Shtrikman, 1983, Phys. Rev. A **28**, 1791; **28**, 3669(E).
Hornreich, R. M., and S. Shtrikman, 1984, Phys. Rev. A **29**, 3444.
Hornreich, R. M., and S. Shtrikman, 1986a, Phys. Rev. Lett. **56**, 1723.
Hornreich, R. M., and S. Shtrikman, 1986b, Phys. Rev. Lett. A **115**, 451.
Hornreich, R. M., and S. Shtrikman, 1987, Z. Phys. B **68**, 369.
Hornreich, R. M., and S. Shtrikman, 1988a, Mol. Cryst. Liq. Cryst. **165**, 183.
Hornreich, R. M., and S. Shtrikman, 1988b, unpublished.
Jabarin, S. A., and R. S. Stein, 1973, J. Phys. Chem. **77**, 399.
Jerome, B., P. Pieranski, V. Godec, G. Haran, and C. Germain, 1988, J. Phys. (Paris) **49**, 837.
Johnson, D. L., J. H. Flack, and P. P. Crooker, 1980, Phys. Rev. Lett. **45**, 641.
Karat, P. P., and N. V. Madhusudana, 1977, Mol. Cryst. Liq. Cryst. **40**, 239.
Karat, P. P., and N. V. Madhusudana, 1978, Mol. Cryst. Liq. Cryst. **47**, 21.
Keyes, P. H., 1987, Phys. Rev. Lett. **59**, 83.
Keyes, P. H., and D. B. Ajgaonkar, 1977, Phys. Lett. A **64**, 298.
Keyes, P. H., and A. J. Nicastro, 1981, Mol. Cryst. Liq. Cryst. **67**, 715.
Keyes, P. H., A. J. Nicastro, and E. M. McKinnon, 1981, Mol. Cryst. Liq. Cryst. **67**, 59.
Kizel', V. A., and V. V. Prokhorov, 1983, Pis'ma Zh. Eksp. Teor. Fiz. **38**, 283 [JETP Lett. **38**, 337 (1983)].
Kizel', V. A., and V. V. Prokhorov, 1984, Zh. Eksp. Teor. Fiz. **87**, 450 [Sov. Phys. JETP **60**, 257 (1984)].
Kleinert, H., 1981, Phys. Lett. A **81**, 141.
Kleinert, H., and K. Maki, 1981, Fortschr. Phys. **29**, 219.
Kleiman, R. N., D. J. Bishop, R. Pindack, and P. Taborek, 1984, Phys. Rev. Lett. **53**, 2137.
Kleman, M., 1981, in *Continuum Models of Discrete Systems,* edited by O. Brulin and R. K. T. Hsieh (North-Holland, Amsterdam), p. 287.
Kleman, M., 1982, J. Phys. (Paris) **43**, 1389.
Kleman, M., 1983, J. Phys. (Paris) Lett. **44**, L295.
Kleman, M., 1985, J. Phys. (Paris) **46**, 1193.
Kleman, M., and J. F. Sadoc, 1979, J. Phys. (Paris) Lett. **40**, L569. Kuczynski, W., 1985a, Phys. Lett. A **110**, 405.
Kuczynski, W., 1985b, Mol. Cryst. Liq. Cryst. **130**, 1.
Kuczynski, W., K. Bergmann, and H. Stegemeyer, 1980, Mol. Cryst. Liq. Cryst. Lett. **56**, 283.
Kuczynski, W., and H. Stegemeyer, 1980, Naturwissenschaften **67**, 310.
Langevin, D., and M. A. Bouchiat, 1975, J. Phys. (Paris) **36**, C1-197.
Lehmann, O., 1906, Z. Phys. Chem. **56**, 750.
Lubin, D., and R. M. Hornreich, 1987, Phys. Rev. A **36**, 849.
Marcus, M., 1981, J. Phys. (Paris) **42**, 61.
Marcus, M., 1982a, Mol. Cryst. Liq. Cryst. Lett. **82**, 33.
Marcus, M., 1982b, Phys. Rev. A **25**, 2272.
Marcus, M., 1982c, Phys. Rev. A **25**, 2276.

Marcus, M., 1982d, Mol. Cryst. Liq. Cryst. Lett. **82**, 167.
Marcus, M., 1984, Phys. Rev. A **30**, 1109.
Marcus, M., 1985, Mol. Cryst. Liq. Cryst. **122**, 131.
Marcus, M., and J. W. Goodby, 1982, Mol. Cryst. Liq. Cryst. Lett. **72**, 297.
Meiboom, S., and M. Sammon, 1980, Phys. Rev. Lett. **44**, 882.
Meiboom, S., and M. Sammon, 1981, Phys. Rev. A **24**, 468.
Meiboom, S., M. Sammon, and D. W. Berreman, 1983, Phys. Rev. A **28**, 3553.
Meiboom, S., M. Sammon, and W. F. Brinkman, 1983, Phys. Rev. A **27**, 438.
Meiboom, S., J. P. Sethna, P. W. Anderson, and W. F. Brinkman, 1981, Phys. Rev. Lett. **46**, 1216.
Mermin, N. D., 1979, Rev. Mod. Phys. **51**, 591.
Miller, J. D., P. R. Battle, P. J. Collings, D. K. Yang, and P. P. Crooker, 1987, Phys. Rev. A **35**, 3959.
Miraldi, E., C. Oldano, P. Taverna Valabrega, and L. Trossi, 1982, Mol. Cryst. Liq. Cryst. Lett. **82**, 231.
Miraldi, E., L. Trossi, and P. Taverna Valabrega, 1981, Nuovo Cimento **66**, 179.
Misner, C. W., K. S. Thorne, and J. A. Wheeler, 1971, *Gravitation* (Freeman, San Francisco), p. 209.
Nelson, D. R., 1982, Phys. Rev. Lett. **50**, 982.
Nelson, D. R., 1983a, Phys. Rev. B **28**, 5515.
Nelson, D. R., 1983b, in *Topological Disorder in Condensed Matter,* edited by F. Yonezawa and T. Ninomiya (Springer, Berlin), p. 163.
Nicastro, A. J., and P. H. Keyes, 1983, Phys. Rev. A **27**, 431.
Onusseit, H., and H. Stegemeyer, 1981, Z. Naturforsch. **36a**, 1083.
Onusseit, H., and H. Stegemeyer, 1982, Chem. Phys. Lett. **89**, 95.
Onusseit, H., and H. Stegemeyer, 1983a, Chem. Phys. Lett. **94**, 417.
Onusseit, H., and H. Stegemeyer, 1983b, J. Cryst. Growth **61**, 409.
Onusseit, H., and H. Stegemeyer, 1984, Z. Naturforsch. **39a**, 658.
Pelzl, G., and H. Sackman, 1973, Z. Phys. Chem. **254**, 354.
Pieranski, P., R. Barbet-Massin, and P. E. Cladis, 1985, Phys. Rev. A **31**, 3912.
Pieranski, P., and P. E. Cladis, 1986, Chem. Phys. Lett. **130**, 368.
Pieranski, P., and P. E. Cladis, 1987, Phys. Rev. A **35**, 355.
Pieranski, P., and P. E. Cladis, 1988, Liq. Cryst. **3**, 397.
Pieranski, P., P. E. Cladis, and R. Barbet-Massin, 1985, J. Phys. (Paris) Lett. **46**, L973.
Pieranski, P., P. E. Cladis, and R. Barbet-Massin, 1986, J. Phys. (Paris) **47**, 129.
Pieranski, P., P. E. Cladis, T. Garel, and R. Barbet-Massin, 1986, J. Phys. (Paris) **47**, 139.
Poggi, Y., J. Robert, and J. Borel, 1975, Mol. Cryst. Liq. Cryst. **29**, 311.
Poggi, Y., P. Atten, and J. C. Filippini, 1976, Mol. Cryst. Liq. Cryst. **37**, 1.
Poggi, Y., J. C. Filippini, and R. Aleonard, 1976, Phys. Lett. A **57**, 53.
Pollman, P., and G. Scherer, 1979, Z. Naturforsch. **34a**, 255.
Pollman, P., and G. Scherer, 1980, High Temp. High Pressures **12**, 103.
Porsch, F., and H. Stegemeyer, 1986, Chem. Phys. Lett. **125**, 319.
Porsch, F., and H. Stegemeyer, 1987, Liq. Cryst. **2**, 395.
Porsch, F., H. Stegemeyer, and K. Hiltrop, 1984, Z. Naturforsch. **39a**, 475.
Price, F. P., and J. H. Wendorf, 1971, J. Phys. Chem. **75**, 2839.
Price, F. P., and J. H. Wendorf, 1972, J. Phys. Chem. **76**, 276.
Priest, R. G., and T. C. Lubensky, 1974, Phys. Rev. A **9**, 893.
Reinitzer, F., 1888, Monatsh. Chem. **9**, 421.
Renn, S., and T. C. Lubensky, 1988, Phys. Rev. A **38**, 2132.
Robinson, C., J. C. Ward, and R. B. Beevers, 1958, Discuss. Faraday Soc. **25**, 29.
Rokhsar, D. S., 1987, private communication.
Rokhsar, D. S., and J. P. Sethna, 1986, Phys. Rev. Lett. **56**, 1727.
Sadoc, J., 1980, J. Phys. (Paris) Colloq. **41**, C8-326.
Sadoc, J., and R. Mosseri, 1982, Philos. Mag. B **45**, 467.
Sadoc, J., and R. Mosseri, 1984, J. Phys. (Paris) **45**, 1025.
Sammon, M. J., 1982, Mol. Cryst. Liq. Cryst. **89**, 305.
Samulski, E. T., and Z. Luz, 1980, J. Chem. Phys. **73**, 142.
Sands, D., 1969, *Introduction to Crystallography* (Benjamin, New York).
Saupe, A., 1969, Mol. Cryst. Liq. Cryst. **7**, 59.
Schröder, H., 1980, in *Liquid Crystals of One and Two Dimensional Order,* edited by W. Helfich and G. Heppke (Springer, Berlin), p. 196.
Schutz, B. F., 1980, *Geometric Methods of Mathematical Physics* (Cambridge University, Cambridge, England), p. 205.
Sethna, J. P., 1983, Phys. Rev. Lett. **51**, 2198.
Sethna, J. P., 1985, Phys. Rev. B **31**, 6278.
Sethna, J. P., 1987, in *Theory and Applications of Liquid Crystals,* edited by J. L. Ericksen and D. Kinderlehrer (Springer, New York), p. 305.
Sethna, J. P., and M. Kleman, 1982, Phys. Rev. A **26**, 3037.
Sethna, J. P., D. C. Wright, and N. D. Mermin, 1983, Phys. Rev. Lett. **51**, 467.
Shivaprakash, N. C., and J. Shashidhara Prasad, 1982, J. Chem. Phys. **76**, 1209.
Stegemeyer, H., 1980, Phys. Lett. A **79**, 425.
Stegemeyer, H., and K. Bergmann, 1980, in *Liquid Crystals of One and Two Dimensional Order,* edited by W. Helfrich and G. Heppke (Springer, Berlin), p. 161.
Stegemeyer, H., Th. Blümel, K. Hiltrop, H. Onusseit, and F. Porsch, 1986, Liq. Cryst. **1**, 3.
Stegemeyer, H., Th. Blümel, and H. Onusseit, 1988, Liq. Cryst. **3**, 399.
Stegemeyer, H., and P. Pollman, 1982, Mol. Cryst. Liq. Cryst. Lett. **82**, 123.
Stegemeyer, H., and F. Porsch, 1984, Phys. Rev. A **30**, 3369.
Stegemeyer, H., and B. Spier, 1987, Chem. Phys. Lett. **133**, 176.
Steinhardt, P. J., D. R. Nelson, and M. Ronchetti, 1981, Phys. Rev. Lett. **47**, 1297.
Steinhardt, P. J., D. R. Nelson, and M. Ronchetti, 1983, Phys. Rev. B **28**, 784.
Stephen, M. J., and J. P. Straley, 1974, Rev. Mod. Phys. **46**, 617.
Stinson, T. W., and J. D. Litster, 1970, Phys. Rev. Lett. **25**, 503.
Stumpf, F., 1911, doctoral thesis (University of Goettingen).
Taborek, P., J. W. Goodby, and P. E. Cladis, 1989, Liq. Cryst. **4**, 21.
Tanimoto, K., and P. P. Crooker, 1984, Phys. Rev. A **29**, 1566.
Tanimoto, K., P. P. Crooker, and G. C. Koch, 1985, Phys. Rev. A **32**, 1893.
Thoen, J., 1988, Phys. Rev. A **37**, 1754.
Tius, M. A., X. Gu, J. W. Truesdell, S. Savariar, D. K. Yang, and P. P. Crooker, 1987, Mold. Cryst. Liq. Cryst. **150b**, 247.
Usui, H., H. Takezoi, A. Fukuda, and E. Kuze, 1979, Jpn. J. Appl. Phys. **18**, 1599.
van der Meer, B. M., and G. Vertogen, 1976, Phys. Lett. A **59**,

279.
Vertogen, G., 1983, Physica A **117**, 227.
Wright, D. C., 1983, Ph.D. thesis (Cornell University).
Wright, D. C., and N. D. Mermin, 1985, Phys. Rev. A **31**, 3498.
Wulf, A., 1973, J. Chem. Phys. **59**, 1487.
Würz, U., G. Klar, and S.-K. Chan, 1979, J. Phys. (Paris) Colloq. **40**, C3-404.
Yamada, T., and E. Fukada, 1973, Jpn. J. Appl. Phys. **12**, 68.
Yang, D. K., and P. P. Crooker, 1987, Phys. Rev. A **35**, 4419.
Yang, D. K., and P. P. Crooker, 1988, Phys. Rev. A **37**, 4001.
Yang, D. K., P. P. Crooker, and K. Tanimoto, 1988, Phys. Rev. Lett. **61**, 2685.
Yaniv, Z., G. Chidichimo, and J. W. Doane, 1983, Phys. Rev. A **28**, 3012.
Yaniv, Z., M. E. Neubert, and J. W. Doane, 1983, in *Liquid Crystals and Ordered Fluids, Vol. 4,* edited by A. G. Griffin and J. Johnson (Plenum, New York), p. 551.
Yaniv, Z., N. A. P. Vaz, G. Chidichimo, and J. W. Doane, 1981, Phys. Rev. Lett. **47**, 46.
Yu, L. J., and A. Saupe, 1980, Phys. Rev. Lett. **45**, 1000.
Zasadzinski, J. A., S. Meiboom, M. J. Sammon, and D. W. Berreman, 1986, Phys. Rev. Lett. **57**, 364.
Ziolo, J., J. Chrapec, S. J. Rozoska, and W. Pyzuk, 1986, Mol. Cryst. Liq. Cryst. Lett. **3**, 183.

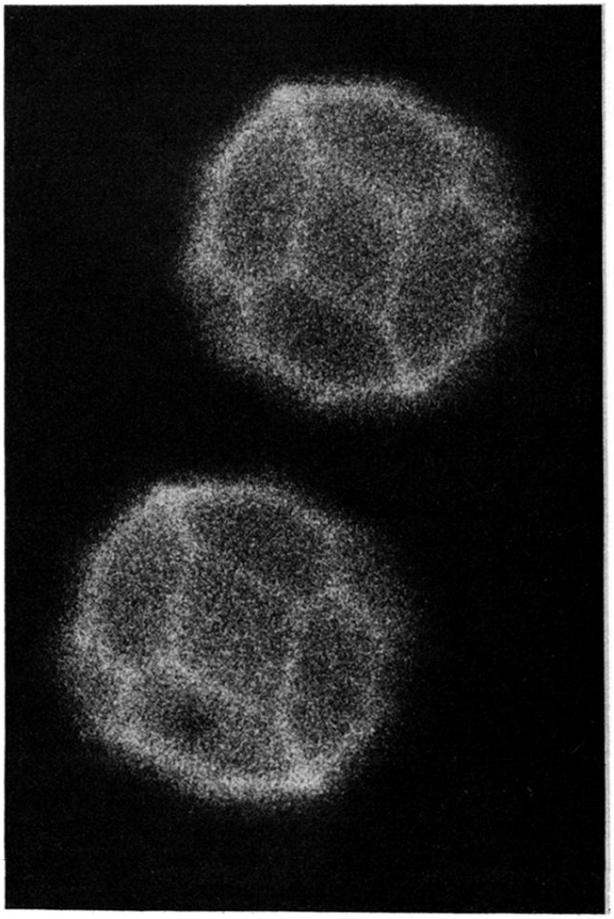

FIG. 10. Single crystals of BP I, showing well-defined facets (cf. Fig. 11) (from Cladis, Pieranski, and Joanicot, 1984). Single crystals up to 0.1–0.2 mm have been grown.